

## **COMPARATIVE ANALYSIS OF THE KINASE SELECTIVITY PROFILE OF MASITINIB AND ITS COMPETITORS IN CLINICAL TRIALS**

### **SUMMARY**

The knowledge of the selectivity of protein kinase inhibitors (PKIs) is a critical point for the development of optimal safe and well tolerated compounds in human health, particularly for the treatment of non-lethal inflammatory diseases. Two complementary studies, recently published in *Nature Biotechnology*, investigated the selectivity of all the kinase inhibitors approved or under clinical development, as well as various investigational ones (Anastassiadis, Deacon et al.; Davis, Hunt et al.). From these studies, it appears that the PKI with the higher kinase selectivity is masitinib from AB Science. Indeed, during clinical trials masitinib has thus far shown an excellent safety record, permitting its clinical development in both oncology and inflammatory diseases.

## INTRODUCTION

The human kinome (Manning, Whyte et al. 2002), which comprises 518 protein kinases, is among the most important pools of therapeutic targets since 150 of them have been shown, or were proposed, to be involved in the etiology and/or the progression of various human diseases including: cancer, inflammatory, metabolic, cardiovascular, or neurodegenerative diseases. Small molecule kinase inhibitors are of considerable therapeutic interest and during the last decade a growing number of therapeutic agents targeting one single kinase (targeted therapy) or several kinases (multi-targeted, polypharmacology) were developed with an impressive success. This is illustrated by the imatinib (Gleevec) story, the first tyrosine kinase inhibitor ever developed, which provided the proof-of-principle that kinase inhibitors can be efficient drugs in human health. To date tens of kinase inhibitors are under clinical development, with the great majority of them targeting the kinase ATP-binding site. Since there are more than 500 different kinases and thousands of ATP-binding proteins, ATP site-targeted compounds have a great potential for cross-reactivity. Indeed, clinical trials have demonstrated that kinase inhibitors are responsible for numerous adverse events, in particular cardiac dysfunctions. It is now well recognized that selectivity is a critical issue for the safety of PKIs and the knowledge of *off-target* interactions and the assessment of molecular specificity of this class of compound is a key feature for development of the safest drugs.

### Masitinib, AB Science

Masitinib (AB1010), developed by AB Science, is a new, orally available, tyrosine kinase inhibitor that primarily targets the proto-oncogene c-Kit and several others kinases. The inhibition of c-Kit permits the development of masitinib both in oncology, by direct inhibition of the activated oncogene, and in inflammatory diseases by the reduction of c-Kit-dependent mast cells, key players of inflammatory processes. In human health, masitinib is currently evaluated in eight phase III clinical trials in both oncology and inflammatory disease fields (Table 1). In most of these indications, masitinib is being evaluated against competitors. In animal health, masitinib (Masivet® in Europe; Kinavet® in USA) was the first veterinary anti-cancer targeted drug approved by EMA in 2008 followed by the FDA in 2010, for treatment of canine mast cell tumors (MCT), a common cutaneous malignant neoplasm in dogs.

**Table 1: Clinical development of masitinib in human and veterinary medicine and status of its competitors**

SPONSOR	COMPOUND	INDICATION	STATUS
<b>Human Medicine</b>			
AB Science	Masitinib	Smoldering Systemic, Indolent Systemic and Cutaneous Mastocytosis with Handicap	Phase III
AB Science	Masitinib	Gastrointestinal Stromal Tumors	Phase III
Novartis	Imatinib		Approved
Pfizer	Sunitinib		Approved
Novartis	Nilotinib		Phase III
AB Science	Masitinib	Rheumatoid Arthritis	Phase III
AstraZeneca	Fostamatinib		Phase III
Pfizer	Tofacitinib		Phase III
AB Science	Masitinib	Melanoma Carrying a Mutation in the Juxta Membrane Domain of c-Kit	Phase III
Novartis	Nilotinib		Phase III
AB Science	Masitinib	Advanced/Metastatic Pancreatic Cancer in Combination with Gemcitabine	Phase III
OSI Pharmaceuticals	Erlotinib, Tarceva		FDA Approved
AB Science	Masitinib	Multiple Myeloma	Phase III
AB Science	Masitinib	Severe Persistent Asthma	Phase III
AB Science	Masitinib	Primary Progressive, Secondary Progressive or Relapse Free Multiple Sclerosis	Phase III
<b>Veterinary medicine</b>			
AB Science	Masitinib	Mast cell tumors	Approved
Pfizer	Toceranib, Palladia		Approved

## **Masitinib's competitors under clinical development (Phase III) or already approved**

### **Human medicine**

In rheumatoid arthritis, masitinib had two competitors: Fostamatinib (R406), from Rigel Pharmaceuticals and tofacitinib (CP-690550) from Pfizer. Fostamatinib is an orally available compound with potential anti-inflammatory and immunomodulating activities currently developed as an inhibitor of Syk tyrosine kinase. Tofacitinib is developed as a JAK2/JAK3 inhibitor in inflammatory diseases (rheumatoid arthritis but also ulcerative colitis and psoriasis). It acts as a potent immuno-suppressor by suppression of the JAK-STAT signaling pathway. On 16<sup>th</sup> November 2011, Jakafi® (ruxolitinib, INCB18424) from Incyte Corporation was approved by the FDA for treatment of patients with intermediate or high-risk myelofibrosis (MF), including primary MF, post-polycythemia vera MF and post-essential thrombocythemia MF. Jakafi is an oral JAK1 and JAK2 inhibitor with a mechanism of action similar to that of tofacitinib. This compound is not a direct masitinib competitor but, as a JAKs inhibitor evaluated in inflammatory diseases (psoriasis Phase II), it was included to the comparative analysis of kinase selectivity profiles.

In oncology, masitinib is being developed in GIST, melanoma with c-Kit mutation and pancreatic carcinoma. In these indications masitinib's competitors are imatinib, sunitinib and nilotinib; nilotinib; and erlotinib, respectively (see table 1).

Nilotinib (Tasigna™) is developed by Novartis as a second generation BCR-ABL inhibitor, the key cause and driver of Ph+ CML, either in patients with newly diagnosed Ph+ CML or in pretreated imatinib-resistant or -intolerant patients. Because nilotinib equally inhibits c-Kit, this activity had lead Novartis to develop it in c-Kit driven-malignancies, for example, GIST and melanoma with mutated c-Kit.

Sunitinib (Pfizer) is a multitargeted tyrosine kinase inhibitor that inhibits primarily VEGFRs 1/2/3 but also numerous RTKs such as platelet derived growth factor receptor (PDGFR), c-Kit, FLT3 or RET. This compound was approved by FDA as antiangiogenic compound (anti VEGFRs) for the treatment of renal cell carcinoma (RCC) and for GIST resistant or intolerant to Gleevec.

Erlotinib specifically targets the epidermal growth factor receptor (EGFR) tyrosine kinase, which is highly expressed and occasionally mutated in various forms of cancer. In 2004, the FDA approved erlotinib for treatment of patients with locally advanced or metastatic non-small cell lung cancer after failure of at least one prior chemotherapy regimen. In 2005, the FDA approved erlotinib in combination with gemcitabine for treatment of locally advanced, unresectable, or metastatic pancreatic cancer.

### **Veterinary Medicine**

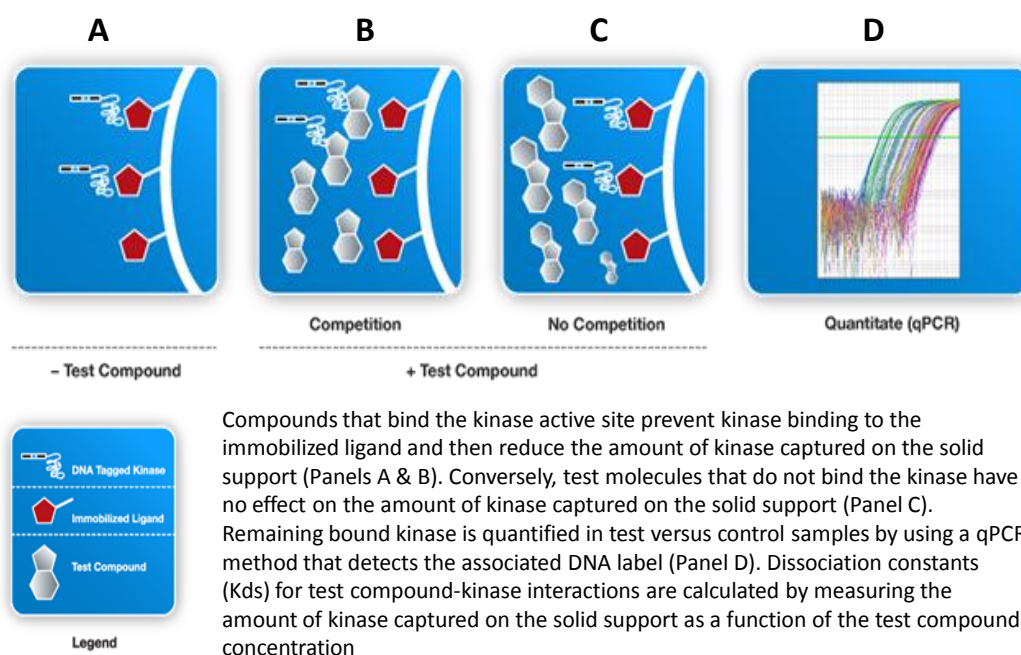
In the treatment of dog mast cell tumors, masitinib has one competitor, toceranib (Pfizer), a sister molecule of sunitinib with which it has identical properties. Toceranib is a multitargeted tyrosine kinase inhibitor that inhibits primarily VEGFRs 1/2/3 but also numerous RTKs including c-Kit.

## METHODS

For several years, the analysis and the quantification of PKIs selectivity was extensively investigated by different complementary *in vitro* technologies known as chemical proteomics (Kim and Sim 2010; Rix and Superti-Furga 2009). These experimental approaches can be divided in two groups: functional assays and competition assays. The functional assays measure the remaining kinase enzymatic activity in presence of an inhibitory compound, a specific substrate and ATP. The competition assays measure the ability for a compound to compete with an ATP-site specific ligand in absence of ATP and substrate. Several others experimental approaches can be used such as thermal enzyme stabilization by inhibitor binding (thermal shift assays).

*Davis et al.* performed a competition study using the technology developed by Ambit Bioscience (Fabian, Biggs et al. 2005) and known as the KINOMEscan screening platform, which permits the measurement of the binding affinity ( $K_d$ ) between PKI and a particular kinase. They have extended their previous study of the interaction of 38 PKIs with 317 kinases (Karaman, Herrgard et al. 2008) by including 34 additional inhibitors and 125 additional kinases. The kinase panel comprises most of the human protein kinases and their disease relevant mutants but also lipid kinases and kinases from human pathogens. Briefly, *E. coli* or mammalian cell-expressed kinases labeled with DNA tag for real-time polymerase chain reaction (qPCR) readout were mixed with the test compound and a known active site binding ligand immobilized on a solid support. Once the binding equilibrium was reached the solid support was washed, in order to remove unbound kinase, and the remaining DNA-tagged bound kinase was quantified by qPCR and compared to control as illustrated in Figure 1.

**Figure 1: Schematic representation of the binding study method developed by Ambit Biosciences**



In their study, *Anastassiadis et al.* performed a classical functional phospho-transfer enzymatic assay to quantify the inhibitory effect of 178 commercially available PKIs against 300 recombinant kinases. They have quantified the remaining activity of the kinases at given compound and ATP concentrations (0.5  $\mu$ M and 10  $\mu$ M, respectively).

It is interesting to note that there is an excellent correlation between the results of the *in vitro* assays used in the *Anastassiadis et al.* and in the *Davis et al.* studies by comparison to the direct proteomic approach based on the LC-MS/MS analysis of PKIs protein ligands in whole cell extracts. Most of the previously unsuspected interactions that were detected by one technology were

confirmed by the other one. For example, the identification of LCK or DDR1 as imatinib targets or TEC kinases as dasatinib targets (Bantscheff, Eberhard et al. 2007; Hantschel, Rix et al. 2007; Rix, Hantschel et al. 2007) and GAK as an erlotinib target (Brehmer, Greff et al. 2005), were all detected independently either by *in vitro* quantitative binding or enzymatic assays or by proteomic technologies (Karaman, Herrgard et al. 2008).

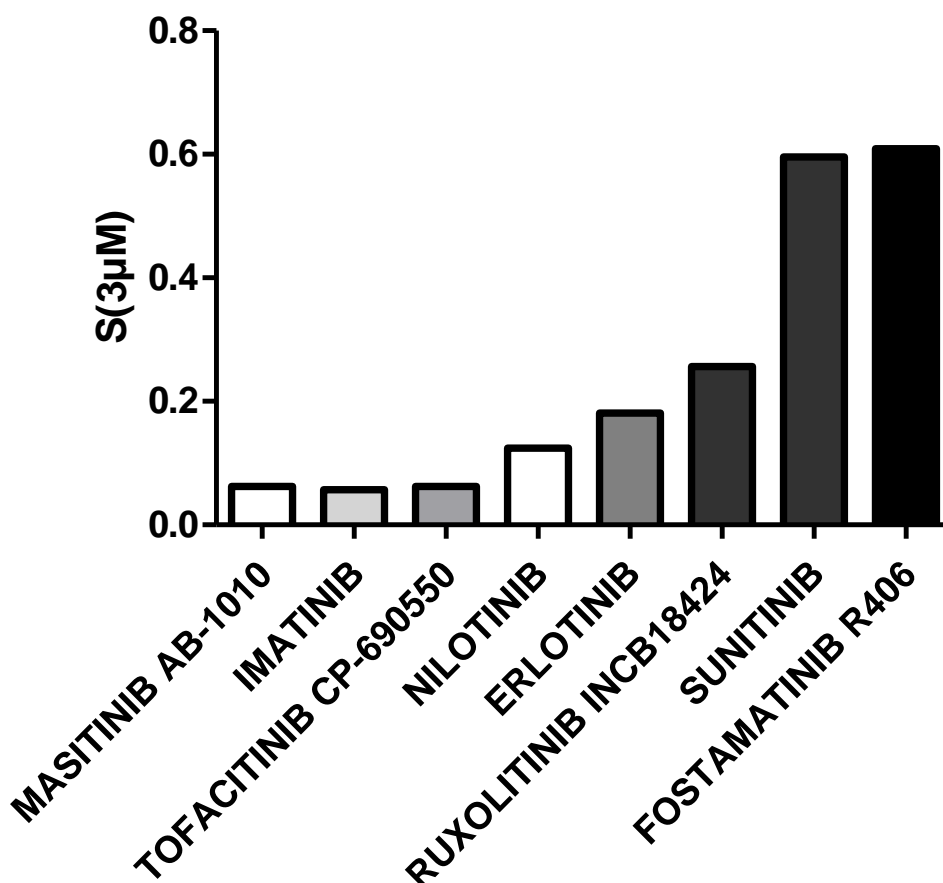
## RESULTS

« **Comprehensive analysis of kinase inhibitor selectivity** », Davis MI, Hunt JP, Herrgard S, Ciceri P, Wodicka LM, Pallares G, Hocker M, Treiber DK, Zarrinkar PP. *Nat Biotechnol.* 2011 Oct 30;29(11):1046-51.

Based on the determination of the  $K_d$  values, *Davis et al.* have determined an absolute selectivity scores: the selectivity score for the binding interactions with  $K_d < 3 \mu\text{M}$ , i.e.  $S(3 \mu\text{M})$ , that was calculated as follows:

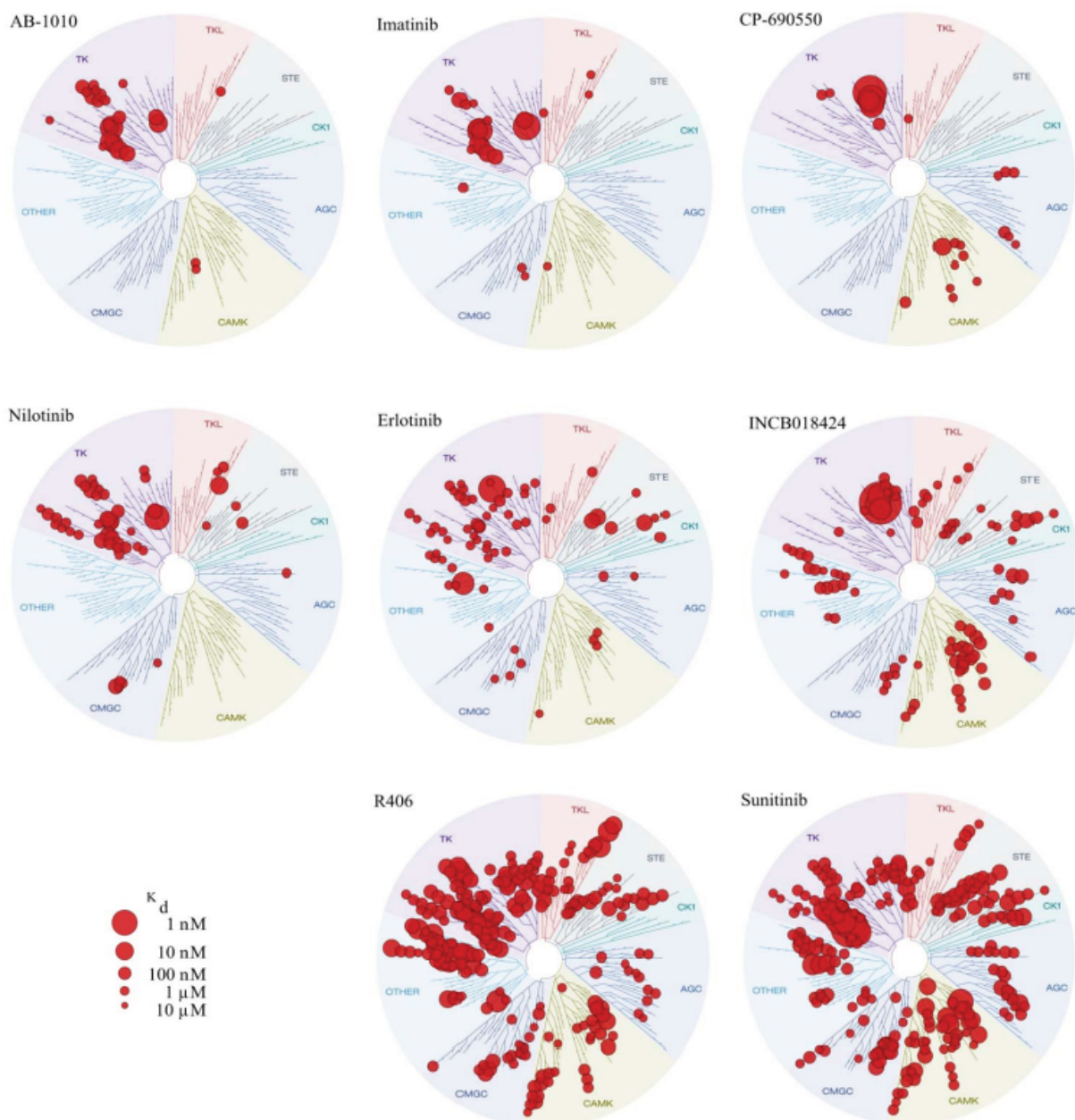
$$S(3\mu\text{M}) = \text{number of interaction with } K_d < 3 \mu\text{M} / \text{number kinases tested}$$

Figure 2: Selectivity scores of masitinib and of its competitors in clinical trials



The graphical representation of  $S(3\mu\text{M})$  (Figure 2) show clearly that masitinib has an equivalent selectivity to that of imatinib and tofacitinib. All others compounds are less selective. This is strikingly illustrated in Figure 3, which represents the kinome interaction map of each of the nine compounds compared here.

**Figure 3: Kinome interaction maps for masitinib and its competitors in clinical development**



AB1010 = masitinib; CP-690550 = tofacitinib; INCB18424 = ruxolitinib; R406 = fostamatinib.

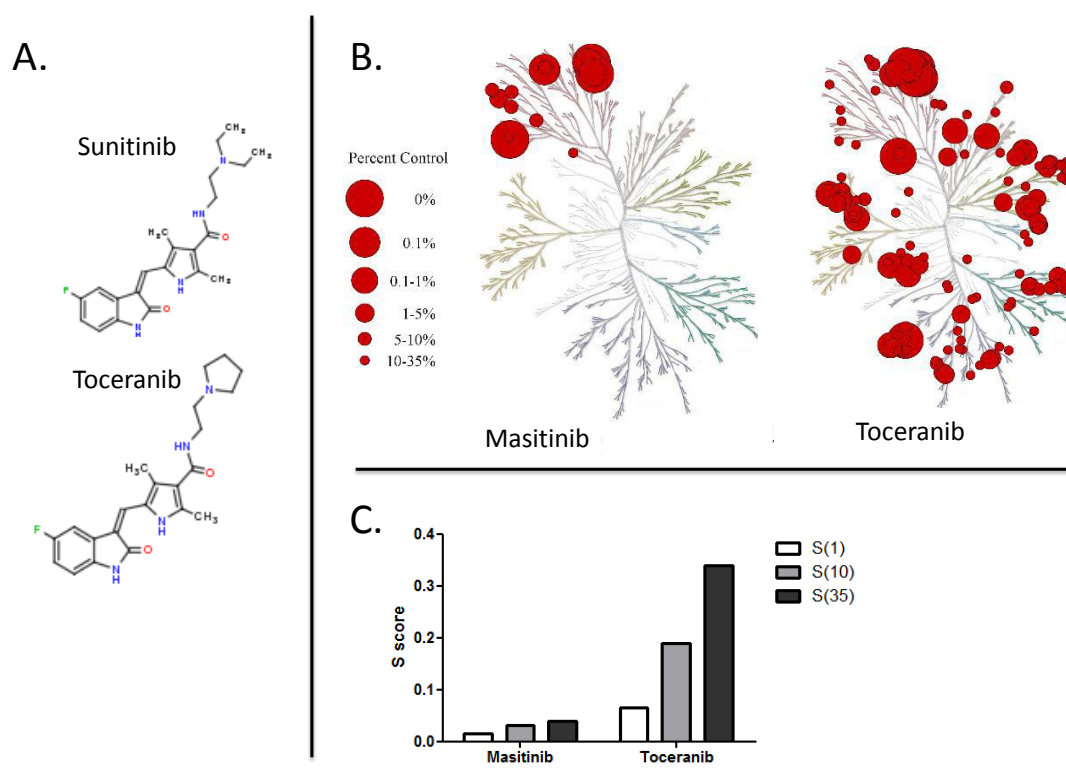
Toceranib was not directly evaluated in this study but it can be considered that toceranib is absolutely equivalent to sunitinib. The comparison of the chemical structures of sunitinib and toceranib represented in Figure 4A show that they differ only by one chemical motif (N-diethyl versus pyrrolidine). This minor difference has no impact on their kinase selectivity profile. Indeed, the comparative KINOMEScan analysis of masitinib and toceranib performed at 1  $\mu$ M concentration (Figure 4B), respectively reveals a pattern identical to that of that of masitinib and sunitinib kinome interaction maps shown in Figure 3.

The selectivity scores S(1), S(10) and S(35), used in this case, were calculated using the proportion of control (%Ctrl) as a potency threshold. These selectivity scores are defined as follow:

$S(35) = (\text{number of non-mutant kinases with \%Ctrl} < 35) / (\text{number of non-mutant kinases tested});$   
 $S(10) = (\text{number of non-mutant kinases with \%Ctrl} < 10) / (\text{number of non-mutant kinases tested});$   
 $S(1) = (\text{number of non-mutant kinases with \%Ctrl} < 1) / (\text{number of non-mutant kinases tested}).$

As for the previously defined  $K_d$  values, they provide a quantitative method to describe the selectivity of the two compounds.

**Figure 4: Comparative kinome interaction maps for masitinib and toceranib, its competitor in veterinary medicine**



A comparison of the selectivity scores demonstrates without any doubt that masitinib is more selective than toceranib (Figure 4C).

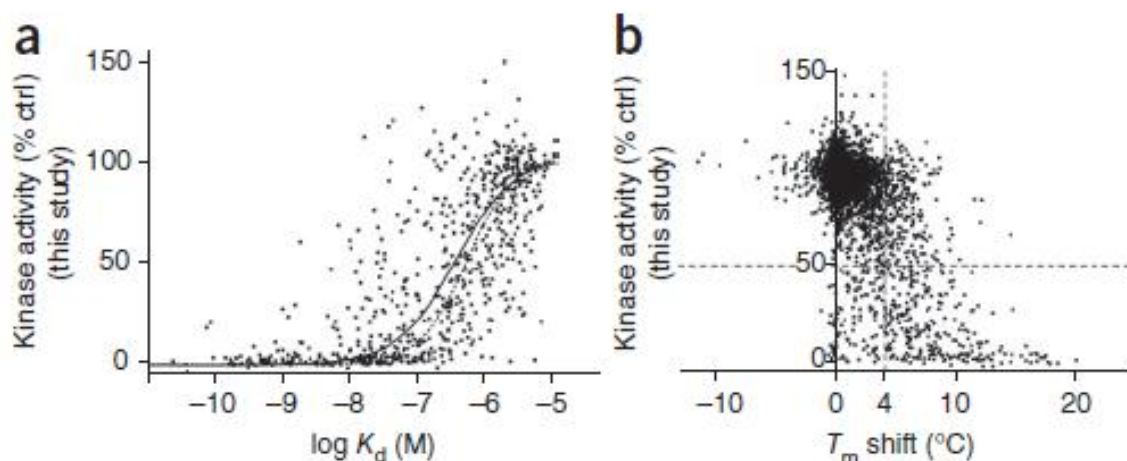
**CONCLUSION: From the results of Davis *et al.*, and from our unpublished data (toceranib), it appears clear that masitinib is as selective as imatinib and tofacitinib, and that all others competitors are less selective or totally unselective.**

However, there are two notable limitations to the study of Davis *et al.*:

First, the quantification of kinase compound interaction ( $K_d$  determination) is not strictly correlated to the inhibition of the catalytic activity as illustrated in figure 5A. Effectively, the comparison of kinase-compound pairs inhibition data from this study with the overlapping ones from large-scale binding studies show that 90% of high affinity kinase-compound interaction ( $K_d < 100$  nM) correspond to a functional inhibition (>50%). Moreover, when considering weak affinity kinase-compound interaction ( $K_d < 1000$  nM) only 13% showed >50% inhibition. The same finding is made when considering the variation of the melting temperature ( $T_m$ ) induced by the binding of an

inhibitor to its target kinase. In general, compounds that induce a  $T_m$  variation  $>4^\circ\text{C}$  are inhibitory compounds but the analysis of disposable data show a significant proportion of both false-positive and false negative (Figure 5B).

**Figure 5: Comparison of functional inhibition data from Anastassiadis et al. study with previous kinase-inhibitor interaction profiling studies; (a) binding studies ( $K_d$ ); (b) thermal shift studies ( $T_m$  Shift)**



Second, the selectivity score (defined as the number of kinase bound divided by the total number of kinase tested) depends upon an arbitrary hit threshold ( $x\mu\text{M}$ ), and it appears that selectivity scores generated by the same dataset but using different hit thresholds can produce different ranking of compounds, particularly for compounds of closest selectivity. This point is illustrated in table 2, where masitinib and its competitors are ranked either using the  $S(300\text{ nM})$  or the  $S(3\mu\text{M})$   $K_d$  thresholds.

**Table 2: Ranking of PKIs by their selectivity scores at two different  $K_d$  thresholds (300 nM and 3  $\mu\text{M}$ ).**

S(300nM) ranking		S(3uM) ranking	
Compound	S(300nM)	Compound	S(3uM)
CP-690550	0.0207	Imatinib	0.0570
Imatinib	0.0233	AB1010	0.0622
Erlotinib	0.0285	CP-690550	0.0622
AB1010	0.0337	Nilotinib	0.1244
Nilotinib	0.0440	Erlotinib	0.1813
INCB18424	0.0803	INCB18424	0.2565
Sunitinib	0.3109	Sunitinib	0.5959
R406	0.3420	R406	0.6088

AB1010 = masitinib; CP-690550 = tofacitinib; INCB18424 = ruxolitinib; R406 = fostamatinib.

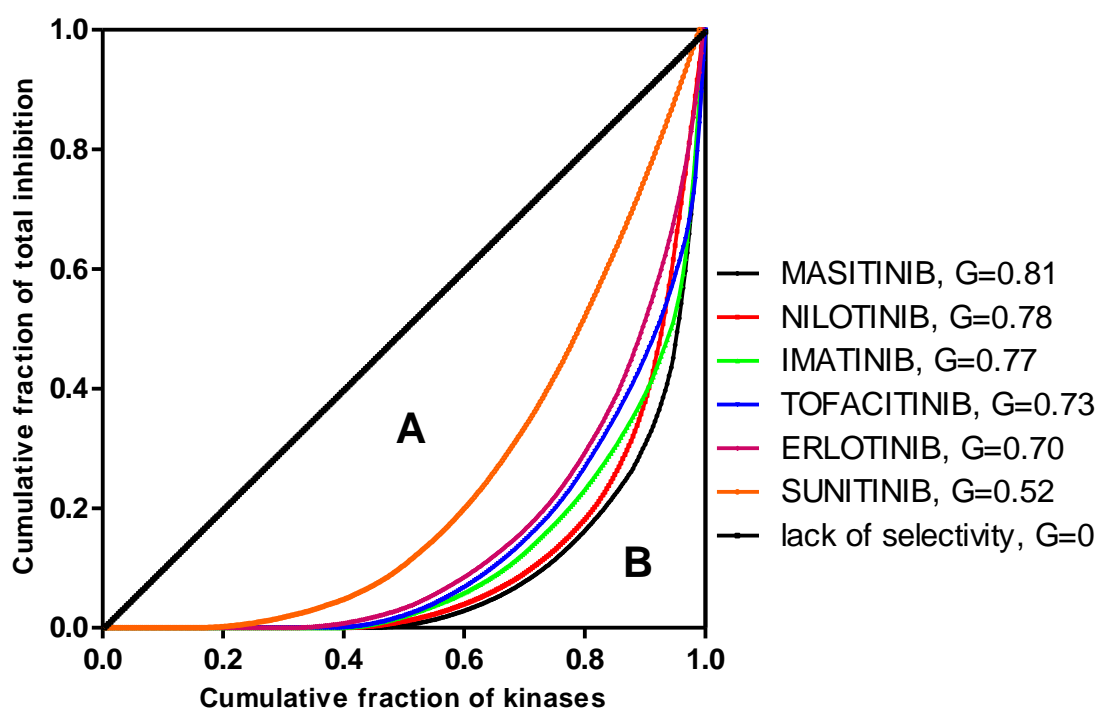
The experimental method and the results analysis used in the second article from Nature Biotechnology (Anastassiadis et al.) permit a response to these two limitations.

« Comprehensive assay of kinase catalytic activity reveals features of kinase inhibitor selectivity », Anastassiadis T, Deacon SW, Devarajan K, Ma H, Peterson JR. Nat Biotechnol. 2011 Oct 30;29(11):1039-45.

In this study only five of masitinib's seven competitors were evaluated; those missing being, ruxolitinib and fostamatinib. However, these are all unambiguously less selective than masitinib when considering results from the Davis *et al.* study, with their selectivity scores higher than that of masitinib at all K<sub>d</sub> thresholds considered, i.e. S(300 nM) or S(3μM). Moreover, the internal AB Science functional data (IC<sub>50</sub>, not shown) have confirmed the weak selectivity of these three compounds.

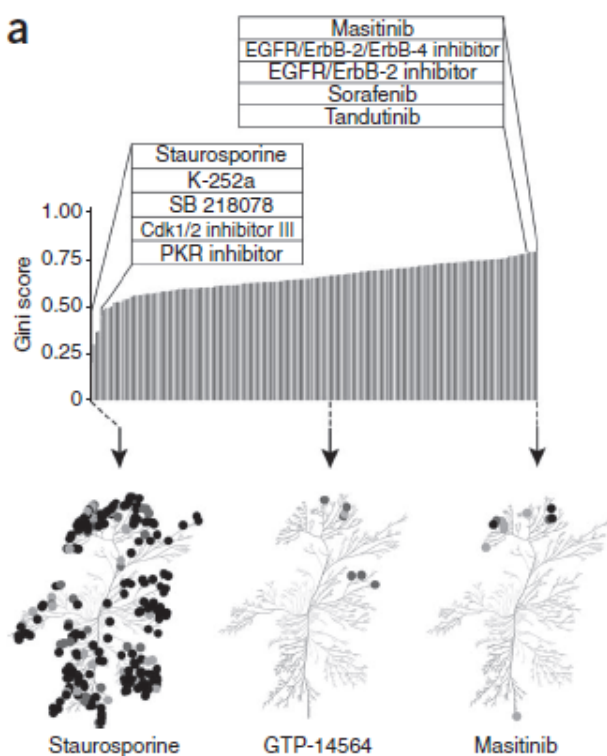
The results obtained from inhibition experiments of each kinase-compound pair were analyzed with a metric for kinase inhibitors based on the Gini coefficient. The application of this statistical method of analyze to PKIs was described in detail by P. Graczyk (Graczyk 2007). In summary, the total inhibition for a given compound is calculated as the sum of magnitudes of inhibition for all kinases tested. After sorting of the kinases in order of increasing inhibition, the cumulative fraction of total inhibition is plotted against the cumulative fraction of kinases. If all kinases are inhibited to an equal extent, the cumulative fraction of total inhibition increases linearly with the cumulative fraction of kinases. This situation of complete lack of selectivity corresponds to the black diagonal line in Figure 6. Conversely, if a compound only strongly inhibits a small number of kinases, the cumulative fraction of total inhibition will initially increase slowly following a Lorenz curve and steeply increase to 1 for the last small fraction of potentially inhibited kinases (Figure 6). Considering that the area between the diagonal line and Lorenz curve is A and the area under the Lorenz curve is B, the Gini coefficient (G), is defined as follow:  $G=A/(A+B)$ , taking account that  $A+B=0.5$ , the Gini coefficient equals  $G=1-2B$ . The Gini coefficient reflects, on a scale from 0 to 1, the manner in which the degree of aggregate inhibitory activity of a compound is directed against a single target ( $G=1$ ) or distributed equally against all kinase tested ( $G=0$ ).

Figure 6: Lorenz Curves Gini scores for masitinib and its competitors at 0.5 μM compound/10 μM ATP.



From these curves it appears clear that masitinib is the most selective compound of this panel since it had the smaller B area and by consequence the higher Gini coefficient. The full results of the study (178 inhibitors against 300 kinases, available on line <http://kir.fccc.edu>) are represented in the Figure 7, where the PKIs are ranked by Gini score.

**Figure 7: Ranked list of kinase inhibitors sorted by Gini scores as a measure of inhibitor selectivity**



Remarkably, when considering the full inhibitor panel (178 compounds), masitinib remains the most selective compound with the highest Gini score.

## CONCLUSION

**Two independent large scale studies of kinase inhibitor selectivity have been recently published in the journal Nature Biotechnology. From these data it appears clear that masitinib, developed by AB Science, is to date the most selective kinase inhibitor under clinical development or already approved.**

## BIBLIOGRAPHY

- Anastassiadis, T., S. W. Deacon, et al. "Comprehensive assay of kinase catalytic activity reveals features of kinase inhibitor selectivity." *Nat Biotechnol* **29**(11): 1039-45.
- Bantscheff, M., D. Eberhard, et al. (2007). "Quantitative chemical proteomics reveals mechanisms of action of clinical ABL kinase inhibitors." *Nat Biotechnol* **25**(9): 1035-44.
- Brehmer, D., Z. Greff, et al. (2005). "Cellular targets of gefitinib." *Cancer Res* **65**(2): 379-82.
- Davis, M. I., J. P. Hunt, et al. "Comprehensive analysis of kinase inhibitor selectivity." *Nat Biotechnol* **29**(11): 1046-51.
- Fabian, M. A., W. H. Biggs, 3rd, et al. (2005). "A small molecule-kinase interaction map for clinical kinase inhibitors." *Nat Biotechnol* **23**(3): 329-36.
- Graczyk, P. P. (2007). "Gini coefficient: a new way to express selectivity of kinase inhibitors against a family of kinases." *J Med Chem* **50**(23): 5773-9.
- Hantschel, O., U. Rix, et al. (2007). "The Btk tyrosine kinase is a major target of the Bcr-Abl inhibitor dasatinib." *Proc Natl Acad Sci U S A* **104**(33): 13283-8.
- Karaman, M. W., S. Herrgard, et al. (2008). "A quantitative analysis of kinase inhibitor selectivity." *Nat Biotechnol* **26**(1): 127-32.
- Kim, D. H. and T. Sim (2010). "Chemical kinomics: a powerful strategy for target deconvolution." *BMB Rep* **43**(11): 711-9.
- Manning, G., D. B. Whyte, et al. (2002). "The protein kinase complement of the human genome." *Science* **298**(5600): 1912-34.
- Rix, U., O. Hantschel, et al. (2007). "Chemical proteomic profiles of the BCR-ABL inhibitors imatinib, nilotinib, and dasatinib reveal novel kinase and nonkinase targets." *Blood* **110**(12): 4055-63.
- Rix, U. and G. Superti-Furga (2009). "Target profiling of small molecules by chemical proteomics." *Nat Chem Biol* **5**(9): 616-24.

# Comprehensive analysis of kinase inhibitor selectivity

Mindy I Davis<sup>1-3</sup>, Jeremy P Hunt<sup>1-3</sup>, Sanna Herrgard<sup>1,3</sup>, Pietro Ciceri<sup>1-3</sup>, Lisa M Wodicka<sup>1,2</sup>, Gabriel Pallares<sup>1,2</sup>, Michael Hocker<sup>1</sup>, Daniel K Treiber<sup>1,2</sup> & Patrick P Zarrinkar<sup>1,2</sup>

**We tested the interaction of 72 kinase inhibitors with 442 kinases covering >80% of the human catalytic protein kinome. Our data show that, as a class, type II inhibitors are more selective than type I inhibitors, but that there are important exceptions to this trend. The data further illustrate that selective inhibitors have been developed against the majority of kinases targeted by the compounds tested. Analysis of the interaction patterns reveals a class of ‘group-selective’ inhibitors broadly active against a single subfamily of kinases, but selective outside that subfamily. The data set suggests compounds to use as tools to study kinases for which no dedicated inhibitors exist. It also provides a foundation for further exploring kinase inhibitor biology and toxicity, as well as for studying the structural basis of the observed interaction patterns. Our findings will help to realize the direct enabling potential of genomics for drug development and basic research about cellular signaling.**

The vast majority of small-molecule kinase inhibitors interact with multiple members of the protein kinase family. The extent of cross-reactivity for this class of compounds only became apparent once large panels of kinase assays and other approaches to interrogate the kinome with small molecules became available<sup>1-6</sup>. Systematic kinase profiling of known inhibitors, including compounds that have been or are currently in clinical trials, has revealed diverse interaction patterns across the kinome and has provided a common resource to further study these compounds.

We previously described the interaction patterns of a set of 38 known kinase inhibitors against a panel of 317 kinase assays representing >50% of human protein kinase domains, and introduced the concept of a ‘selectivity score’ to facilitate an objective analysis of kinase profiling data and to quantify selectivity<sup>7</sup>. We now update and extend the data set to encompass a total of 72 known inhibitors, including 11 currently approved small-molecule kinase inhibitor drugs, tested against a panel of 442 kinase assays representing >80% of catalytically active, nonatypical human protein kinase domains.

The compounds tested here represent mature inhibitors that have been optimized against specific targets of interest. The data therefore provide insight into the interaction patterns and selectivity characteristics that can be achieved with optimized compounds, and complement information from screening large libraries comprising unoptimized compounds<sup>8-10</sup>. We show that most type II inhibitors, which contact a binding pocket adjacent to the ATP site and prefer a ‘DFG-out’ inactive kinase conformation<sup>11</sup>, are indeed relatively selective as expected. In contrast, type I inhibitors, which do not require a ‘DFG-out’ conformation of the activation loop and do not contact this pocket, vary widely in overall selectivity. Several type I inhibitors are among the most selective, whereas two type II inhibitors are among the least selective compounds tested. This shows that selectivity may be achieved with a type I binding mode and is not guaranteed with a type II binding mode. The compound set contains

selective inhibitors for the majority of the 28 kinases that represent the intended, primary targets of the compounds tested. This suggests that it is indeed possible to develop selective inhibitors for a diversity of kinases. Furthermore, a quantitative analysis of selectivity across the major kinase groups or subfamilies reveals a class of ‘group-selective’ compounds that interact broadly with one kinase group, but are selective outside of the targeted group. Selectivity within a kinase subfamily or group is therefore not always predictive of overall selectivity. Therefore, testing compounds against kinases closely related to the primary, intended target, as has frequently been done to estimate compound selectivity, does not reliably address global selectivity.

## RESULTS

### A comprehensive assay set for protein kinases

We used competition binding assays<sup>3</sup> to undertake a 10-year effort to develop a biochemical assay panel that would enable comprehensive and direct testing of compounds across the kinome. The primary emphasis was on building assays for catalytically active human protein kinase domains in the eight major ‘typical’ groups, as defined<sup>12</sup>. Due to their high therapeutic and biological relevance, we also included assays for PI3K-family lipid kinases, several atypical protein kinases such as mTOR, and kinases from human pathogens, as well as disease-linked mutant variants and noncatalytic kinase domains. The effort has yielded 442 assays representing >80% of catalytic, nonatypical human protein kinase domains (363 distinct kinase domains, not counting mutant variants). The panel also includes seven atypical kinases, 11 lipid kinases (not counting mutant variants), two kinases from *Plasmodium falciparum* and one from *Mycobacterium tuberculosis*, 7 activation-state variants, 49 disease-relevant mutant variants and two kinase domains believed to be noncatalytic (**Supplementary Table 1**).

We screened a diverse set of 72 known kinase inhibitors against the assay panel to generate a robust overview of what types of

<sup>1</sup>Ambit Biosciences, San Diego, California, USA. <sup>2</sup>Present addresses: National Institutes of Health, Bethesda, Maryland, USA (M.I.D.), KINOMEscan Division of DiscoverRx Corporation, San Diego, California, USA (J.P.H., P.C., L.M.W., G.P., D.K.T.) and Blueprint Medicines Corporation, San Diego, California, USA (P.P.Z.).

<sup>3</sup>These authors contributed equally to this work. Correspondence should be addressed to P.P.Z. (pzarrinkar@yahoo.com) or D.K.T. (dtreiber@discoverx.com).

Received 10 May; accepted 30 August; published online 30 October 2011; doi:10.1038/nbt.1990

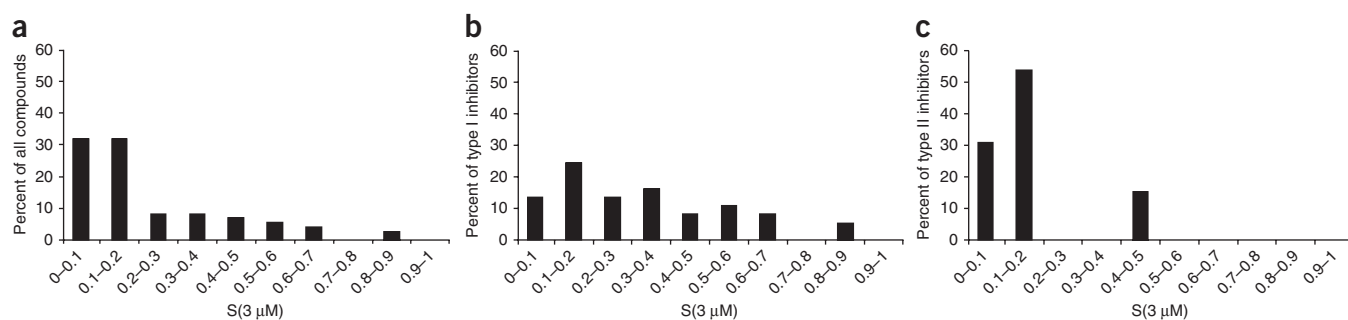


**Figure 1** Quantitative distribution of kinome-wide selectivity of compounds. A kinome selectivity score ( $S(3 \mu\text{M})$ ) was calculated for each compound as described in the text, and compounds were binned according to their scores. (a) Distribution of selectivity for the entire set of 72 compounds. (b) Distribution of selectivity for 37 compounds classified as type I inhibitors based on relative binding affinity for phosphorylated and nonphosphorylated variants of ABL1 (Supplementary Table 5). (c) Distribution of selectivity for 13 compounds classified as type II inhibitors based on relative binding affinity for phosphorylated and nonphosphorylated variants of ABL1 (Supplementary Table 5).

small molecule–kinome interaction patterns can be observed (Supplementary Table 2). At least 28 different kinases, representing six of the eight ‘typical’ kinase groups as well as the atypical and lipid kinase subfamilies, are among the primary, intended targets of these compounds (Supplementary Table 3). The compound set therefore represents a cross-section of inhibitors optimized for activity against a variety of kinases. We initially screened each compound against the panel at a single concentration (10  $\mu\text{M}$ ) to identify candidate kinase targets, and determined a quantitative dissociation constant ( $K_d$ ) for each interaction observed in this primary screen (Supplementary Table 4). Data for 40 of the compounds against smaller assay panels have been published previously<sup>7,13</sup> and are included once more here in the interest of presenting a single, systematic and unified data set that may readily be accessed and used as a resource for further studies and analyses. The updated and extended data set represents close to a 2.5-fold increase in the number of data points available compared to the previously published results, assessed by the number of compound/kinase combinations queried. As before<sup>7</sup>, the binding constants measured here generally agree well with published values determined using biochemical enzyme activity assays (Supplementary Table 3 and Supplementary Fig. 1).

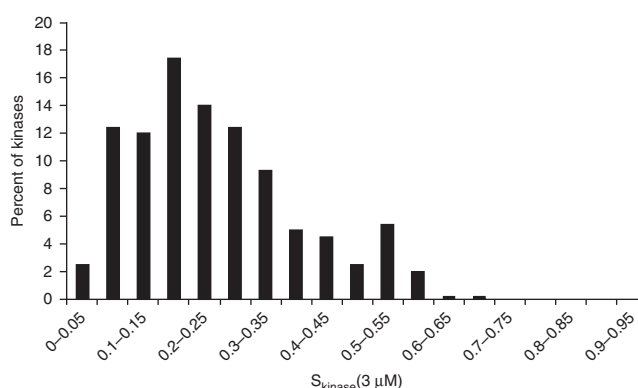
### Selectivity of type I and type II inhibitors

To provide an overview of global kinome selectivity, we prepared kinome interaction maps (Supplementary Fig. 2) and calculated selectivity scores for each compound by dividing the number of kinases bound with  $K_d < 3 \mu\text{M}$  by the total number of distinct kinase domains queried (386, after excluding mutant and activation state variants), as described previously<sup>7</sup> ( $S(3 \mu\text{M})$ ). For the majority of compounds (46 of 72, or 64%),  $S(3 \mu\text{M}) < 0.2$ , indicating that they bind <20% of the kinases tested (Fig. 1a and Supplementary Table 5). The scores for most of the remaining compounds are broadly distributed between 0.2 and 0.7, with the exception of two highly promiscuous outliers with scores >0.8. The outliers are the staurosporine analog CEP-701 and staurosporine itself, which is known to interact with a large fraction of kinases. The lowest selectivity scores, and therefore the greatest selectivity, were observed for the MEK inhibitors AZD-6244/ARRY-886 and CI-1040, the MET inhibitor SGX-523, the CSF1R inhibitor GW-2580 and the ERBB2/EGFR inhibitor lapatinib (Tykerb). Each of these highly selective compounds exploits a structural feature that may distinguish the target kinase from most other kinases. The MEK inhibitors bind an allosteric pocket adjacent to the ATP site, distinct from the pocket exploited by type II inhibitors, without contacting the ATP site itself<sup>14</sup>; SGX-523 requires a unique inactive conformation of

the kinase activation loop<sup>15</sup>; GW-2580 is a type II inhibitor, characterized by requiring an inactive ‘DFG-out’ conformation of the kinase<sup>11</sup>; and lapatinib, although not a typical type II inhibitor, requires an unusual displacement of the alpha-C helix<sup>16</sup>.

One of the potential advantages frequently noted for type II inhibitors is that there may be greater conformational heterogeneity among inactive kinase states than in the canonical active state, providing opportunities for optimizing selectivity for the inactive-like conformation specific to a target kinase<sup>11,17</sup>. A broad comparison of selectivity across a diverse set of type I and type II inhibitors has not been performed, however. We have recently shown that differential binding to phosphorylated and nonphosphorylated forms of ABL1 can functionally differentiate compounds that prefer an inactive, ‘DFG-out’ kinase conformation (type II inhibitors) from those that do not (type I inhibitors), even for compounds that are not primarily ABL1 inhibitors but exhibit at least modest affinity for ABL1 or a mutant variant of ABL1 (ref. 18). To functionally classify the inhibitors tested in the current study we therefore used binding affinities measured for the phosphorylated and nonphosphorylated forms of wild-type ABL1 and five ABL1 mutant variants included in our assay panel. Although this classification method is robust, we cannot completely rule out the possibility that some inhibitors have kinase-specific binding modes. Of the 72 compounds tested, 50 (69%) bind at least one of the paired ABL1 variants with  $K_d < 3 \mu\text{M}$  and could be classified based on these data. Of these 50 compounds, 37 exhibit little or no preference for the nonphosphorylated state and were classified as type I inhibitors. The remaining 13 have a marked preference for the nonphosphorylated state and therefore were classified as type II inhibitors (Supplementary Table 5). We then plotted the distribution of selectivity scores separately for type I and type II inhibitors (Fig. 1b,c). The scores for type I inhibitors are fairly evenly distributed across the range observed for the compound set as a whole. In contrast, all but two of the type II inhibitors had scores <0.2. A similar pattern was observed when the analysis was repeated using selectivity scores based on a 300 nM affinity cutoff ( $S(300 \text{ nM})$ ) (Supplementary Table 5 and Supplementary Fig. 3). The type II inhibitors therefore are largely responsible for the bias toward selective compounds observed for the compound set as a whole (Fig. 1a). Importantly, there are two type II inhibitors, EXEL-2880/GSK1363089 and AST-487, with  $S(3 \mu\text{M})$  of 0.44 and 0.49, respectively, which interact with a large number of kinases. These two compounds remain outliers when the analysis is repeated with a range of affinity cutoffs for calculating selectivity scores. Understanding why these compounds behave differently from other type II inhibitors will likely require structural studies, and

**Figure 2** Quantitative distribution of compound selectivity of kinases. A selectivity score ( $S_{\text{kinase}}(3 \mu\text{M})$ ) was calculated for each of the 442 kinases in the assay panel as described in the text, based on the number of compounds each kinase binds, and kinases binned according to their scores.



should provide important insights into the interplay between binding mode, kinase conformation and selectivity. Our analysis therefore confirms that, in general, type II inhibitors are more likely to be selective than type I inhibitors. However, the data highlight that a type II binding mode does not guarantee high selectivity, nor is it required to achieve selectivity. Several type I inhibitors, including CP-690550 (tofacitinib) and BIBW-2992, are as selective as any of the type II inhibitors, whereas the type II inhibitors EXEL-2880/GSK1363089 and AST-487 are among the least selective compounds tested here.

### Selectivity of kinases

It is apparent from the data set that just as some compounds are selective and others are broadly reactive, there are some kinases that interact with many of the compounds tested, whereas others interact with only one or two. To quantify these observations, we calculated selectivity scores for each kinase by dividing the number of compounds bound with  $K_d < 3 \mu\text{M}$  by the total number of compounds screened ( $S_{\text{kinase}}(3 \mu\text{M})$ ) (Fig. 2 and Supplementary Table 1). The overall distribution of kinase selectivities is fairly narrow, with >60% of kinases interacting with 10–40% of the compounds tested, and each kinase interacting with at least one compound. Three kinases, ERK1, ERK2 and TRPM6, bind only one compound each with  $K_d < 3 \mu\text{M}$ , and are the least frequently hit, whereas LCK and YSK4 each interact with >60% of the compounds tested, and are the most frequently hit. A similar pattern was observed when the analysis was repeated using a 300 nM affinity cutoff to calculate  $S_{\text{kinase}}(300 \text{ nM})$  (Supplementary Table 1). There is generally good agreement between our results and

the kinase selectivities observed previously in single-concentration primary screens of very different collections of unoptimized compounds against much smaller panels of kinases<sup>8,9</sup>. Differences in the frequencies with which individual kinases are hit in these studies likely reflect the different nature of the compounds tested and the scale of the experiments.

### Selective inhibitors for many kinases

One major question that has been difficult to address is whether it is possible to develop reasonably selective inhibitors for most kinases, or whether there is a significant subset of kinases for which it is difficult to identify selective inhibitors. The compounds used here are, with the exception of staurosporine, mature inhibitors that in most cases are the result of significant optimization against an intended, primary target. As such, they are well suited to begin to address this question. There are 28 distinct kinases that collectively may be considered to represent the primary targets of the compound set tested here (Primary Target 1 in Supplementary Table 3). Of these, 27 are

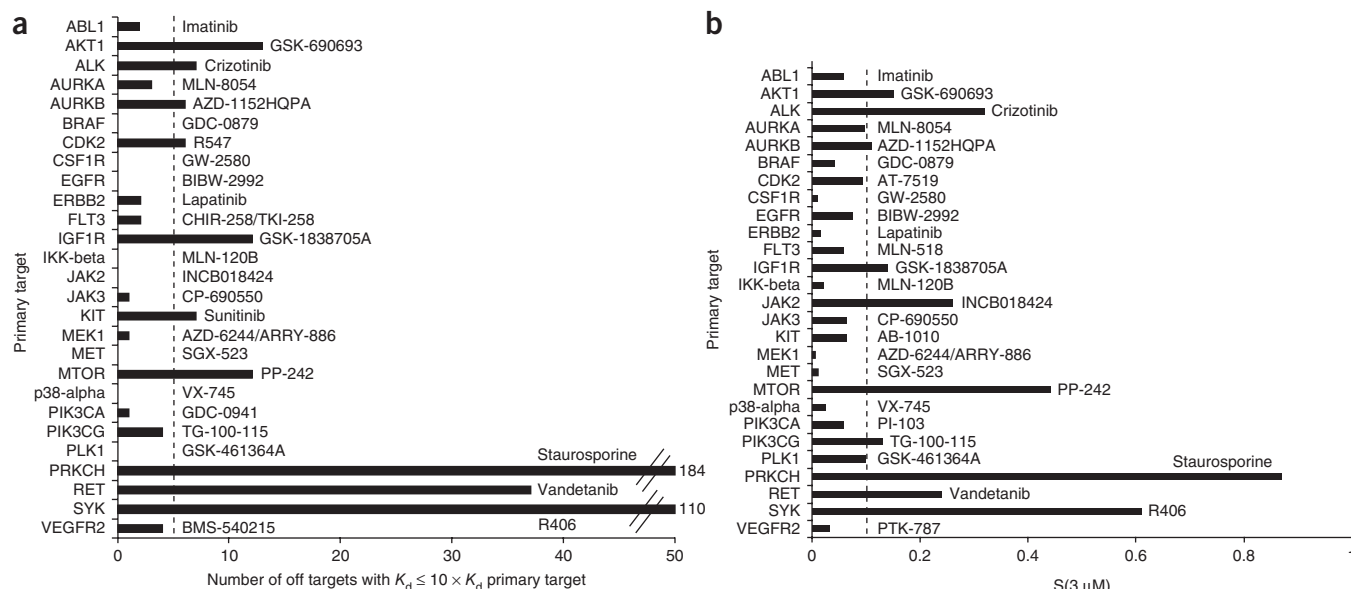


**Figure 3** Selective inhibitors for primary targets. Each kinase on the y axis is a primary, intended target of one or more compounds in the set tested here (Supplementary Table 3). The most selective compound for each target is shown. (a) Relative selectivity. For each of these primary targets, the compound with the greatest relative selectivity for that target was identified by counting the number of kinases bound with a  $K_d$  within tenfold or better of the  $K_d$  for the primary target for each compound targeting the kinase. The number of kinases bound with  $K_d$  within tenfold of that for the primary target is shown for the most selective compound targeting each of the kinases shown. (b) Absolute selectivity. For each of the primary targets the compound with the greatest absolute selectivity for that target was identified, using the  $S(3 \mu\text{M})$  as a measure of absolute selectivity (Supplementary Table 5). The  $S(3 \mu\text{M})$  is shown for the most selective compound targeting each of the kinases shown.



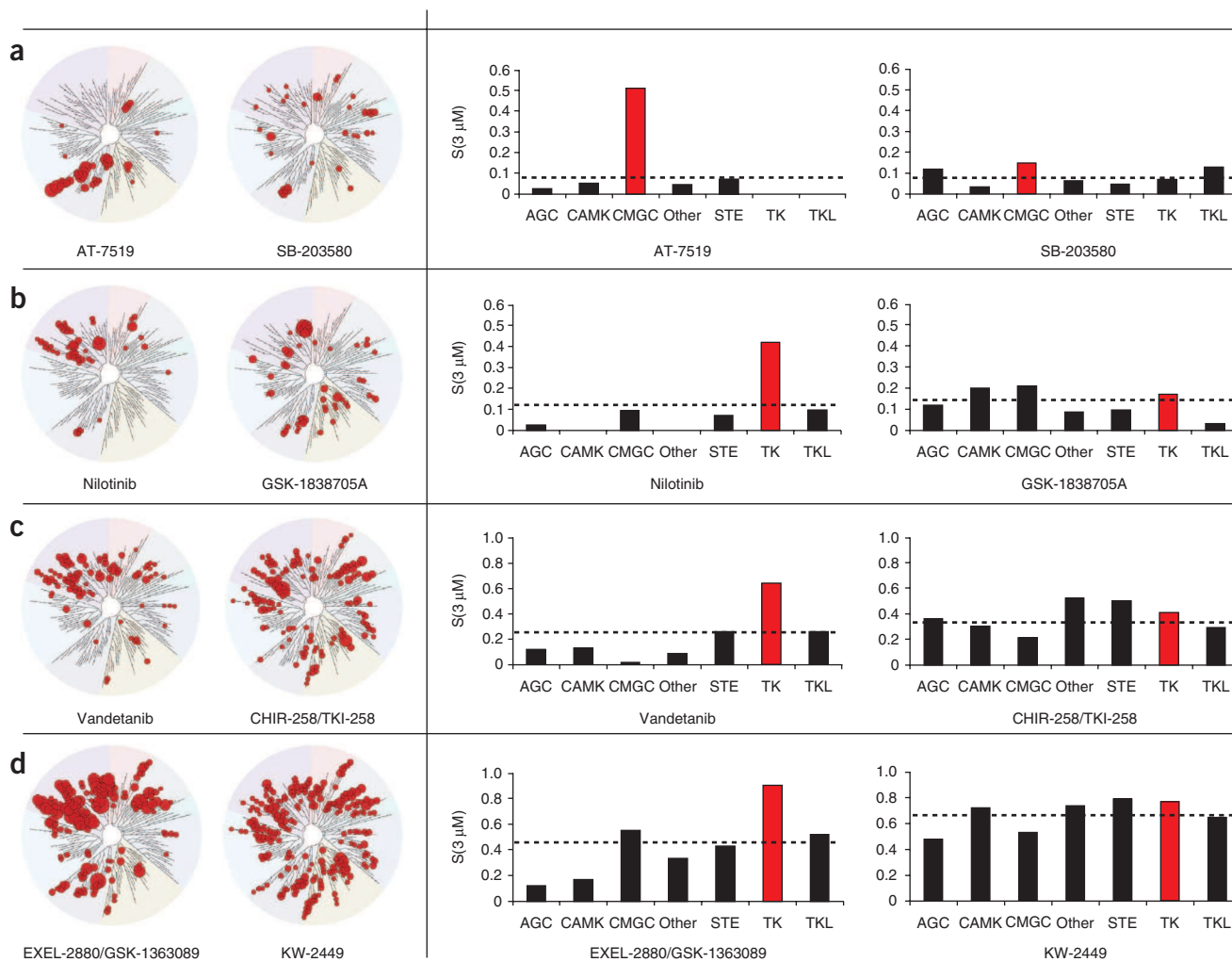


**Figure 4** Group-selective compounds. Compounds were divided into selectivity bins based on their overall selectivity ( $S(3 \mu\text{M})$ ) 0–0.1, 0.1–0.2, 0.2–0.4, >0.4, and selectivity scores ( $S(3 \mu\text{M})$ ) were calculated for each compound for the kinase groups for which more than fifteen kinases are represented in the assay panel (thereby excluding atypical, lipid and CK1 kinases). Shown here are the kinase interaction maps and kinase group fingerprints for one group-selective and one non-group-selective compound from each selectivity bin. (a) Compounds from the  $S(3 \mu\text{M}) = 0\text{--}0.1$  bin. (b) Compounds from the  $S(3 \mu\text{M}) = 0.1\text{--}0.2$  bin. (c) Compounds from the  $S(3 \mu\text{M}) = 0.2\text{--}0.4$  bin. (d) Compounds from the  $S(3 \mu\text{M}) > 0.4$  bin. The interaction maps were generated using TREEspot software (<http://www.kinomescan.com/>) and display a circular representation of the kinase family tree based on kinase domain sequence. The bars in each bar graph indicate  $S(3 \mu\text{M})$  for the individual kinase groups. Red bars indicate the kinase group containing the primary target for each compound. Dashed lines signify the overall  $S(3 \mu\text{M})$  for each compound.

represented in the assay panel. To determine which of these 27 kinases are targeted selectively by compounds in our set, we used two approaches. First, we counted for each compound the number of kinases bound with  $K_d$  within tenfold of the  $K_d$  for the compound's primary target, and thereby identified for each primary target the compound with the greatest relative selectivity for that target (Fig. 3a). For 17 of the 27 primary target kinases, there was at least one inhibitor in our set that bound fewer than five other kinases with affinities comparable to that for the intended, primary target. Second, we determined for each primary target the compound with the lowest overall selectivity score ( $S(3 \mu\text{M})$ ), and thereby identified for each primary target the compound with the greatest absolute selectivity (Fig. 3b). For 16 of the 27 primary target kinases, there was at least one inhibitor in our set with  $S(3 \mu\text{M}) < 0.1$ . For 15 of the 27 primary target kinases, there was at least one compound that featured both fewer than five off-targets (kinases other than the primary target) with affinity comparable to that for the primary target, and an  $S(3 \mu\text{M}) < 0.1$ .

Although the set of 27 primary targets examined here certainly is not an unbiased selection of kinases, these results nevertheless suggest that it is possible to develop reasonably selective inhibitors for a diversity of kinase targets.

**A quantitative fingerprint of interaction patterns**

We have previously noted that the pattern of interactions across the various kinase groups or subfamilies can vary widely, even among compounds that share a primary target<sup>7</sup>. To describe the interaction patterns of compounds quantitatively, we calculated individual selectivity scores, again using a  $3 \mu\text{M}$  affinity cutoff, for each of the major kinase groups<sup>12</sup>. The relative pattern, or fingerprint, of these group-specific selectivity scores reveals whether a compound preferentially targets one or more kinase subfamilies, or whether the interaction pattern is distributed across the kinome. This quantitative approach provides an objective description of compounds' kinase group preferences that is difficult to obtain

from a more qualitative visual assessment of interaction patterns, or from screening a limited number of kinases.

For many compounds, the selectivity scores for the individual kinase groups are relatively similar, and close to the overall kinome-wide score. For a subset of compounds, however, the score for one kinase group (generally the group that includes the compounds' primary target) is substantially higher both than that for the remaining groups, and than the overall score (Fig. 4). These compounds can thus be considered 'kinase group selective', but are not necessarily selective for their specific target. Group-selective inhibitors may have broad reactivity against members of the primary targeted kinase group, and testing kinases closely related to the primary target is therefore unlikely to yield an accurate assessment of their overall selectivity. Group-selective inhibitors included compounds with a wide range of overall selectivity (Fig. 4), both type I and type II inhibitors, and compounds with diverse chemical structures. These observations suggest that group selectivity is not governed by gross binding mode, chemical scaffold or global propensity to interact with a range of kinases. Three of the four cyclin-dependent kinase (CDK) inhibitors tested (AT-7519, R547, BMS-387032/SNS-032) were strongly group selective (Supplementary Fig. 2). This may reflect similar strategies taken to optimize selectivity for CDKs over non-CMGC kinases, or may signal a more fundamental structural feature that distinguishes CMGC kinases from kinases in other groups that each of these compounds exploits.

## DISCUSSION

Our data set represents the most detailed comprehensive assessment of the reactivity of known and clinical kinase inhibitors across the kinome published to date. The assay panel approaches near-complete coverage of the human protein kinome and, together with the diversity of chemical scaffolds and of primary targets represented by the compound collection tested, yields a broad overview of how optimized small-molecule inhibitors interact with the kinome.

An assessment of overall selectivity of the compounds tested here by compound class shows that, as a class, type II inhibitors are more likely to be selective than type I inhibitors, and that type I inhibitors can have a wide range of selectivities. This observation is consistent with the general assumption that the inactive conformation preferred by type II inhibitors is more kinase-specific than an active conformation that can accommodate typical type I inhibitors. However, the data also demonstrate that several type II inhibitors exhibit poor selectivity, whereas a number of type I inhibitors are quite selective. Therefore, inhibitor type does not dictate selectivity. A common theme for the most selective compounds, regardless of inhibitor type, is that they exploit structural features or kinase conformations that can help distinguish the target kinase from other kinases. The data also show that for at least 15 of the 27 kinases that are the primary, intended targets for the compounds tested and that are represented in the assay panel, selective inhibitors, as assessed by both absolute selectivity across the kinome and selectivity relative to the primary target, are among the 72 tested here. Although the number of primary targets and compounds assessed is still limited, these results nevertheless provide an initial encouraging suggestion that it may be possible to develop selective inhibitors for a majority of kinases.

Small-molecule inhibitors are valuable tools to study the biology and therapeutic potential of specific kinases. Nonetheless, dedicated inhibitors are available for only a very small fraction of protein kinases. Our data set reveals a large number of previously undescribed activities of known and available inhibitors, along with the overall selectivity

and interaction pattern for each compound. The information may enable the use of compounds in the set studied here as tools for kinases for which no specifically targeted inhibitors are currently available. In some cases, it may suggest possible novel applications to explore for known drugs or starting points for the development of optimized inhibitors targeting novel kinases. Interesting novel activities include the high affinity of sunitinib (Sutent) for RET harboring gatekeeper mutations (RET(V804L/M)), which are not bound with high affinity by the approved RET inhibitor vandetanib (Zactima)<sup>19</sup>; the interaction of PKC-412, a compound in late-stage clinical development, with EGFR(T790M), which is a major resistance mutation for EGFR inhibitors in lung cancer and against which no drugs are currently available; and the interaction of PFCDPK1 from the malaria parasite with PLX-4720, a compound closely related to the recently approved drug vemurafenib (Zelboraf).

One of the most compelling applications of comprehensive kinase assay panels is the screening of large compound collections to efficiently identify novel inhibitors and starting points for drug discovery<sup>8–10,20–22</sup>. Identifying compounds of interest from the large data sets generated by this application requires computational handles for classifying compounds and revealing the most promising and interesting hits. The approach we describe here of calculating selectivity scores for each of the major kinase groups or subfamilies provides such a handle by generating a quantitative and numeric description of not only the overall kinome selectivity of compounds, but their detailed interaction pattern across kinase groups. This kinase group fingerprint makes it possible to systematically search large data sets to identify compounds with specific interaction patterns without the need to manually examine large numbers of qualitative interaction map images.

A major rationale for sequencing the human genome was the promise that the genome sequence would facilitate and enable drug discovery. The most commonly assumed path from genome to drugs is through the identification of novel gene-disease associations and of potential new drug targets. An alternative path by which the genome can affect drug discovery is through enabling the development of technologies that directly facilitate drug discovery, rather than target discovery. This path is exemplified by the application of high-throughput kinase profiling to drug discovery. The genome sequence was essential to enumerate the human protein kinome<sup>12</sup>, which in turn has been essential to systematically build panels of kinase assays to interrogate the kinome with small molecules, and for understanding how complete and representative the assay panels were<sup>2–4,6</sup>. Profiling of known inhibitors, including approved drugs, across the assay panels has revealed many previously unrecognized activities, and has yielded a more complete understanding of how these compounds may affect biology<sup>2–4,6,7,23–27</sup>. The assay panels further have enabled a novel approach to kinase inhibitor discovery, based on screening entire libraries of compounds against panels of kinases, which has resulted in the discovery of several promising new inhibitors<sup>8,9,13,20–22,28,29</sup>. At least one of these inhibitors is currently in clinical trials and has exhibited efficacy in patients<sup>30</sup>. This direct path from genome sequence to kinome, from kinome to kinase profiling-based drug discovery, and from kinase profiling to novel drugs and a greater understanding of existing drugs illustrates one way in which the genome sequence is living up to the promise of improving human health.

## METHODS

Methods and any associated references are available in the online version of the paper at <http://www.nature.com/naturebiotechnology/>.

Note: Supplementary information is available on the Nature Biotechnology website.

ACKNOWLEDGMENTS

We thank W. Wierenga for critical reading of the manuscript, A. Torres, G. Riggs and M. Costa for compound management, M. Floyd and L. Ramos for expert molecular biology technical assistance, C. Shewmaker and J. Lowe for expert compound screening technical assistance, R. Faraoni for advice on compound synthesis and D. Jones for assistance preparing Figure 4.

AUTHOR CONTRIBUTIONS

M.I.D. coordinated development of the assay panel, J.P.H. developed technology to enhance the efficiency of compound screening, S.H. analyzed data, M.I.D., J.P.H., P.C. and L.M.W. developed binding assay technology and performed assay development, G.P. coordinated and executed the measurement of  $K_d$  values, M.H. synthesized compounds, D.K.T. conceived the technology, designed assay development strategies, and supervised technology and assay development, S.H. and D.K.T. contributed to preparation of the manuscript, P.P.Z. designed the study, supervised the project, analyzed data and wrote the manuscript.

COMPETING FINANCIAL INTERESTS

The authors declare competing financial interests: details accompany the full-text HTML version of the paper at <http://www.nature.com/nbt/index.html>.

Published online at <http://www.nature.com/nbt/index.html>.

Reprints and permissions information is available online at <http://www.nature.com/reprints/index.html>.

1. Bain, J., McLauchlan, H., Elliott, M. & Cohen, P. The specificities of protein kinase inhibitors: an update. *Biochem. J.* **371**, 199–204 (2003).
2. Bantscheff, M. *et al.* Quantitative chemical proteomics reveals mechanisms of action of clinical ABL kinase inhibitors. *Nat. Biotechnol.* **25**, 1035–1044 (2007).
3. Fabian, M.A. *et al.* A small molecule-kinase interaction map for clinical kinase inhibitors. *Nat. Biotechnol.* **23**, 329–336 (2005).
4. Melnick, J.S. *et al.* An efficient rapid system for profiling the cellular activities of molecular libraries. *Proc. Natl. Acad. Sci. USA* **103**, 3153–3158 (2006).
5. Patricelli, M.P. *et al.* Functional interrogation of the kinome using nucleotide acyl phosphates. *Biochemistry* **46**, 350–358 (2007).
6. Fedorov, O. *et al.* A systematic interaction map of validated kinase inhibitors with Ser/Thr kinases. *Proc. Natl. Acad. Sci. USA* **104**, 20523–20528 (2007).
7. Karaman, M.W. *et al.* A quantitative analysis of kinase inhibitor selectivity. *Nat. Biotechnol.* **26**, 127–132 (2008).
8. Bamborough, P., Drewry, D., Harper, G., Smith, G.K. & Schneider, K. Assessment of chemical coverage of kinome space and its implications for kinase drug discovery. *J. Med. Chem.* **51**, 7898–7914 (2008).
9. Posy, S.L. *et al.* Trends in kinase selectivity: insights for target class-focused library screening. *J. Med. Chem.* **54**, 54–66 (2011).
10. Metz, J.T. *et al.* Navigating the kinome. *Nat. Chem. Biol.* **7**, 200–202 (2011).

11. Liu, Y. & Gray, N.S. Rational design of inhibitors that bind to inactive kinase conformations. *Nat. Chem. Biol.* **2**, 358–364 (2006).
12. Manning, G., Whyte, D.B., Martinez, R., Hunter, T. & Sudarsanam, S. The protein kinase complement of the human genome. *Science* **298**, 1912–1934 (2002).
13. Zarrinkar, P.P. *et al.* AC220 is a uniquely potent and selective inhibitor of FLT3 for the treatment of acute myeloid leukemia (AML). *Blood* **114**, 2984–2992 (2009).
14. Ohren, J.F. *et al.* Structures of human MAP kinase kinase 1 (MEK1) and MEK2 describe novel noncompetitive kinase inhibition. *Nat. Struct. Mol. Biol.* **11**, 1192–1197 (2004).
15. Buchanan, S.G. *et al.* SGX523 is an exquisitely selective, ATP-competitive inhibitor of the MET receptor tyrosine kinase with antitumor activity in vivo. *Mol. Cancer Ther.* **8**, 3181–3190 (2009).
16. Wood, E.R. *et al.* A unique structure for epidermal growth factor receptor bound to GW572016 (Lapatinib): relationships among protein conformation, inhibitor off-rate, and receptor activity in tumor cells. *Cancer Res.* **64**, 6652–6659 (2004).
17. Simard, J.R. *et al.* Fluorophore labeling of the glycine-rich loop as a method of identifying inhibitors that bind to active and inactive kinase conformations. *J. Am. Chem. Soc.* **132**, 4152–4160 (2010).
18. Wodicka, L.M. *et al.* Activation state-dependent binding of small molecule kinase inhibitors: structural insights from biochemistry. *Chem. Biol.* **17**, 1241–1249 (2010).
19. Carlomagno, F. *et al.* Disease associated mutations at valine 804 in the RET receptor tyrosine kinase confer resistance to selective kinase inhibitors. *Oncogene* **23**, 6056–6063 (2004).
20. Goldstein, D.M., Gray, N.S. & Zarrinkar, P.P. High-throughput kinase profiling as a platform for drug discovery. *Nat. Rev. Drug Discov.* **7**, 391–397 (2008).
21. Kwiatkowski, N. *et al.* Small-molecule kinase inhibitors provide insight into Mps1 cell cycle function. *Nat. Chem. Biol.* **6**, 359–368 (2010).
22. Deng, X. *et al.* Characterization of a selective inhibitor of the Parkinson's disease kinase LRRK2. *Nat. Chem. Biol.* **7**, 203–205 (2011).
23. Hasinoff, B.B. & Patel, D. The lack of target specificity of small molecule anticancer kinase inhibitors is correlated with their ability to damage myocytes in vitro. *Toxicol. Appl. Pharmacol.* **249**, 132–139 (2010).
24. Huang, D., Zhou, T., Lafleur, K., Nevado, C. & Caflish, A. Kinase selectivity potential for inhibitors targeting the ATP binding site: a network analysis. *Bioinformatics* **26**, 198–204 (2010).
25. Olaharski, A.J. *et al.* Identification of a kinase profile that predicts chromosome damage induced by small molecule kinase inhibitors. *PLOS Comput. Biol.* **5**, e1000446 (2009).
26. Yang, X. *et al.* Kinase inhibition-related adverse events predicted from in vitro kinome and clinical trial data. *J. Biomed. Inform.* **43**, 376–384 (2010).
27. Remsing Rix, L.L. *et al.* Global target profile of the kinase inhibitor bosutinib in primary chronic myeloid leukemia cells. *Leukemia* **23**, 477–485 (2009).
28. Knight, Z.A., Lin, H. & Shokat, K.M. Targeting the cancer kinome through polypharmacology. *Nat. Rev. Cancer* **10**, 130–137 (2010).
29. Miduturu, C.V. *et al.* High-throughput kinase profiling: a more efficient approach toward the discovery of new kinase inhibitors. *Chem. Biol.* **18**, 868–879 (2011).
30. Cortes, J. *et al.* AC220, a potent, selective, second generation FLT3 receptor tyrosine kinase (RTK) inhibitor, in a first-in-human (FIH) phase I clinical trial. *Blood (ASH Annual Meeting Abstracts)* **114**, Abstract 636 (2009).



## ONLINE METHODS

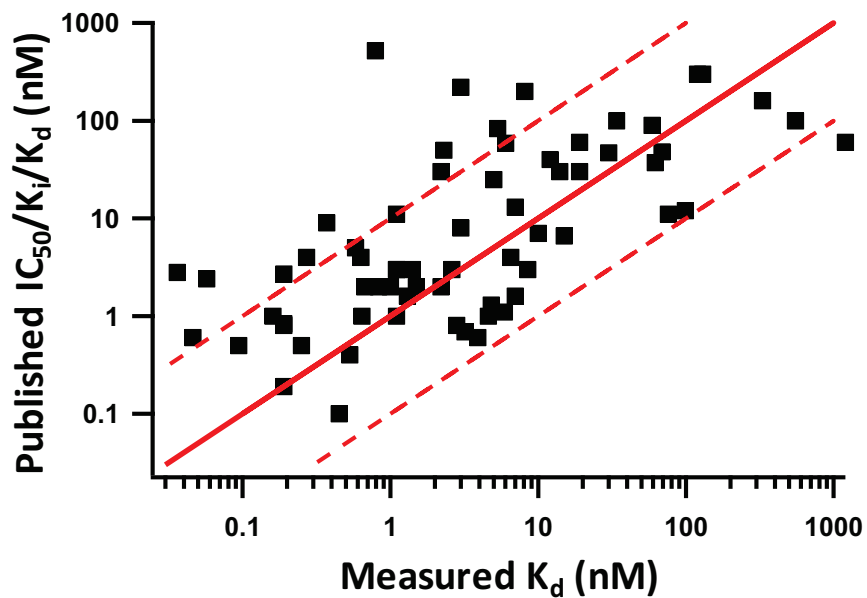
**Compounds.** Inhibitors were either purchased from A.G. Scientific, Calbiochem/EMD Chemicals, Tocris Bioscience, Archerchem, Axon Medchem or SYNthesismedchem, custom synthesized by Qventas, SAI Advantium, CiVentiChem, Shangai SynCores Technologies, WuXi AppTec, BioDuro, SynChem or synthesized at Ambit Biosciences.

**Competition binding assays.** Competition binding assays were developed, validated and performed as described previously<sup>3,18</sup>. Kinases were produced either as fusions to T7 phage<sup>3</sup>, or were expressed as fusions to NF- $\kappa$ B in HEK-293 cells and subsequently tagged with DNA for PCR detection<sup>18</sup>. In general, full-length constructs were used for small, single-domain kinases, and catalytic domain constructs including appropriate flanking sequences were used for multidomain kinases. Briefly, for the binding assays, streptavidin-coated magnetic beads were treated with biotinylated affinity ligands to

generate affinity resins. The liganded beads were blocked to reduce nonspecific binding and washed to remove unbound ligand. Binding reactions were assembled by combining kinase, liganded affinity beads and test compounds prepared as 100 $\times$  stocks in DMSO. DMSO was added to control assays lacking a test compound. Primary screen interactions were performed in 384-well plates, whereas  $K_d$  determinations were performed in 96-well plates. Assay plates were incubated at 25 °C with shaking for 1 h, and the affinity beads were washed extensively to remove unbound protein. Bound kinase was eluted in the presence of nonbiotinylated affinity ligands for 30 min at 25 °C with shaking. The kinase concentration in the eluates was measured by quantitative PCR.  $K_d$ s were determined using 11 serial threefold dilutions of test compound and a DMSO control. Kinase interaction maps shown in **Figure 4** were generated using TREEspot software (<http://www.kinomescan.com/>).

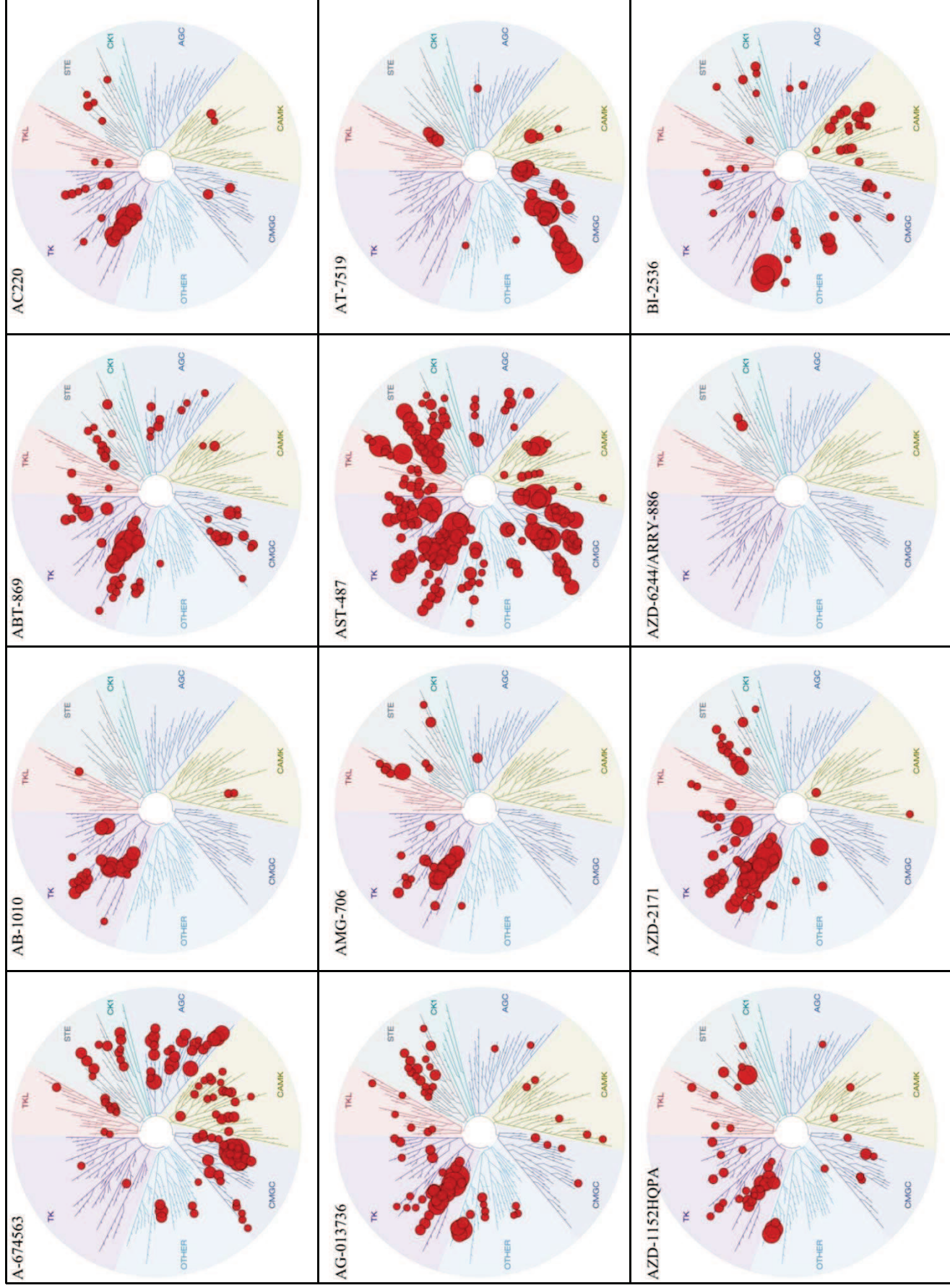
False-positive and false-negative rates for single-concentration primary screens have been previously determined<sup>7</sup>.

Supplementary Figure 1.

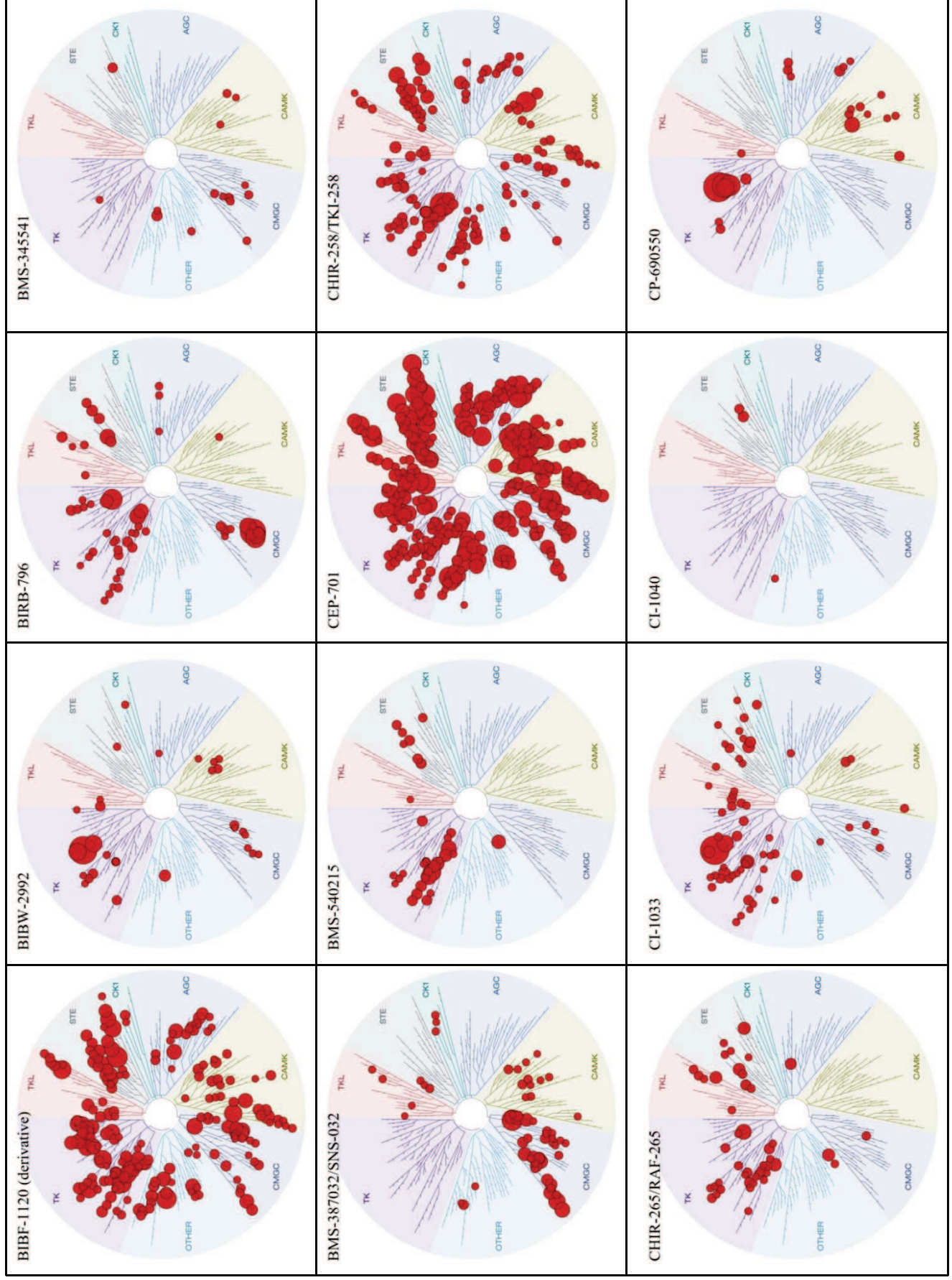


**Supplementary Figure 1. Comparison of  $K_d$  values reported here and published biochemical  $IC_{50}/K_i/K_d$  values for interactions between inhibitors and their primary, intended targets.** Values used to create this plot are reported in Supplementary Table 3. Comparative data were available for 66 of the 72 compounds addressed in this study. The line of equivalence is indicated in solid red, and dashed red lines indicate 10-fold offsets.

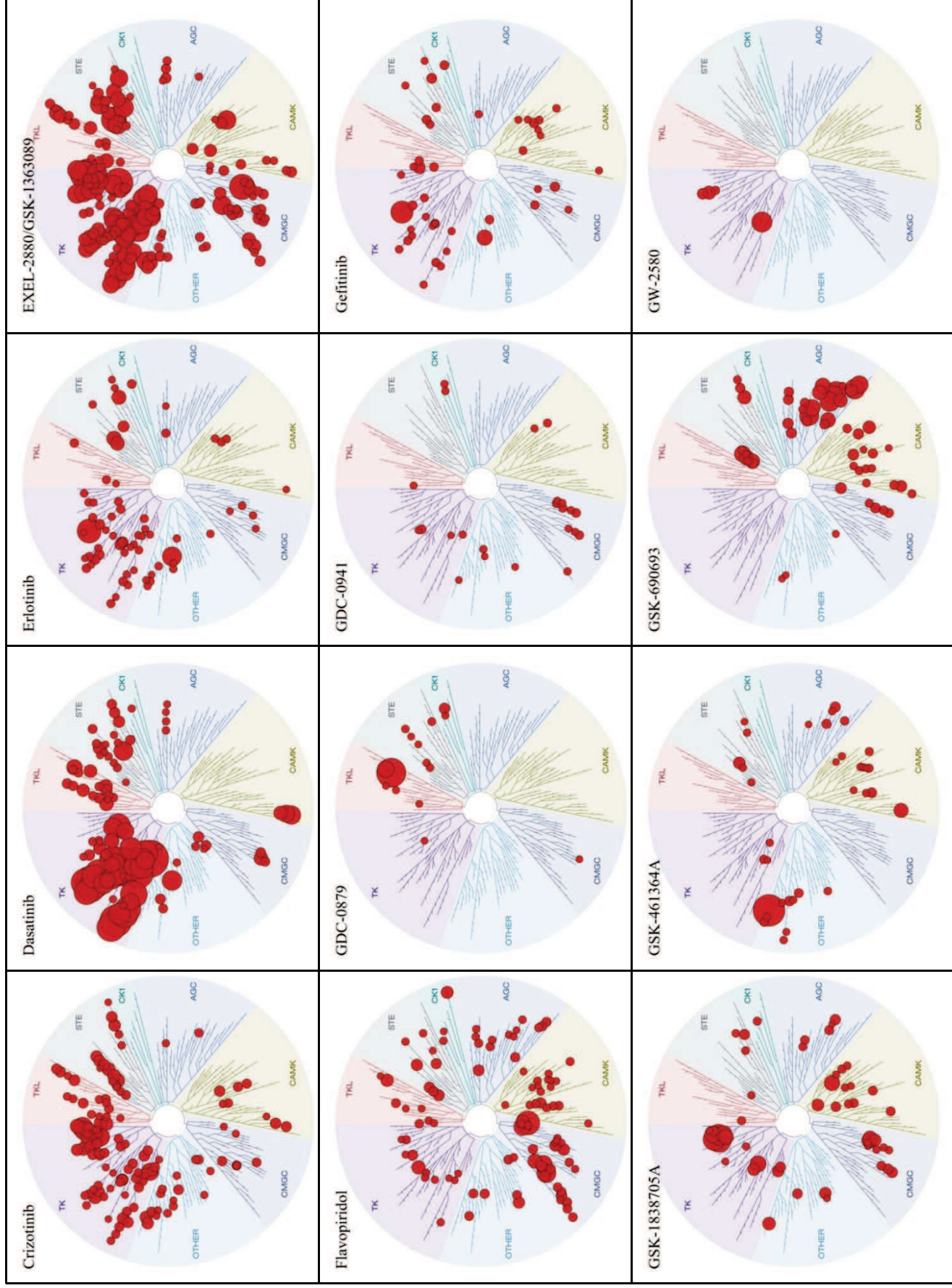
Supplementary Figure 2.



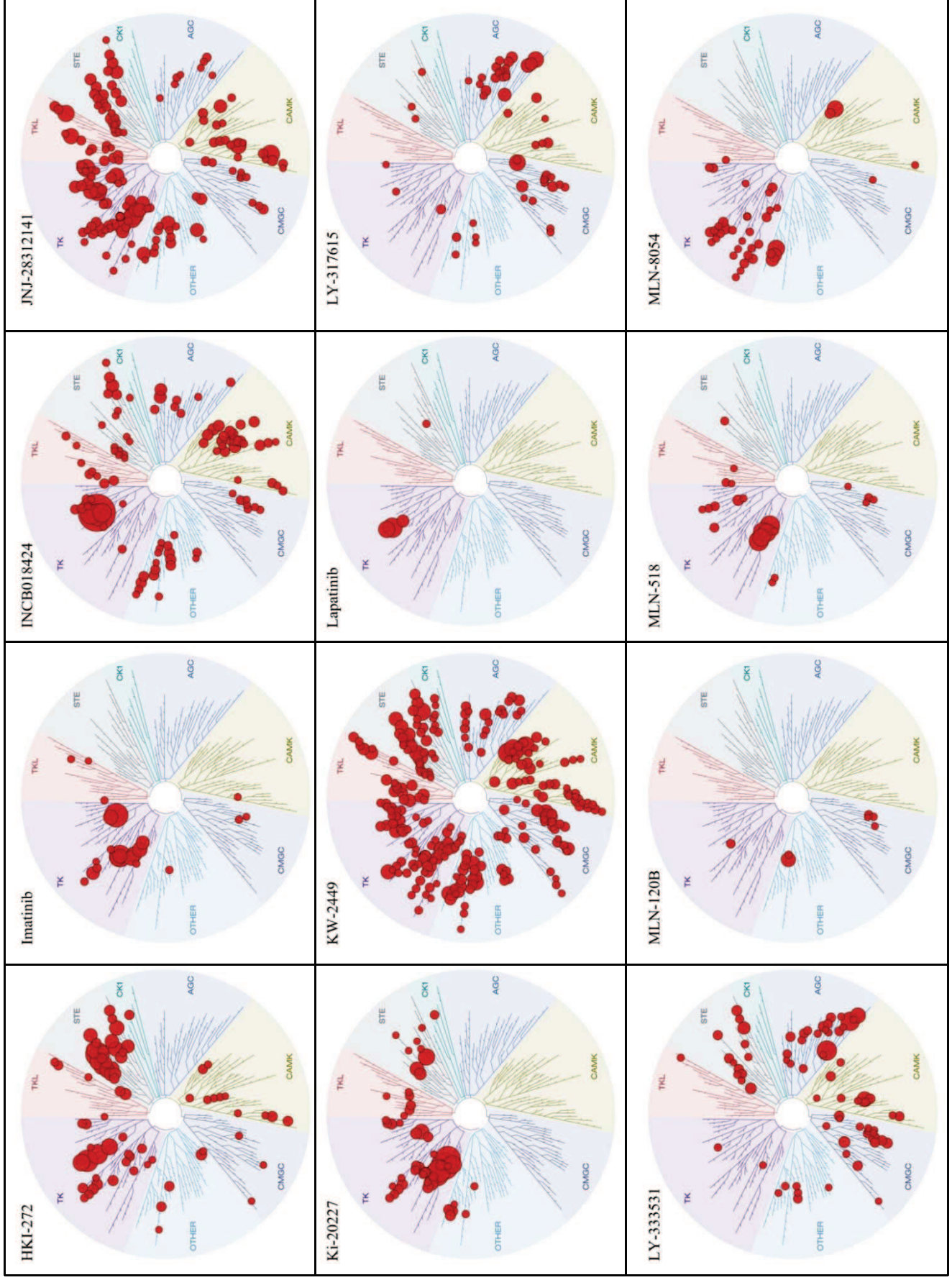
Supplementary Figure 2.



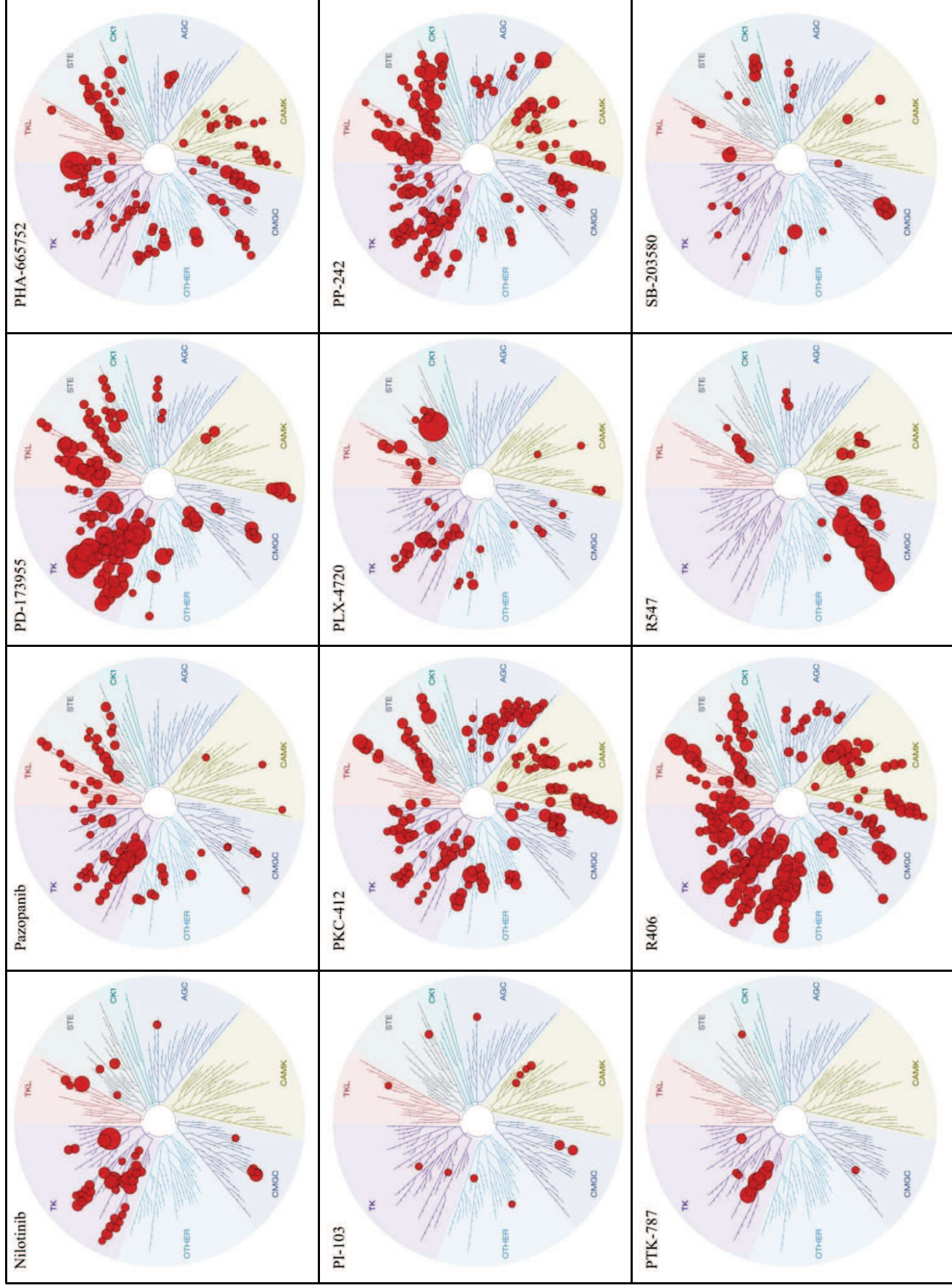
Supplementary Figure 2.



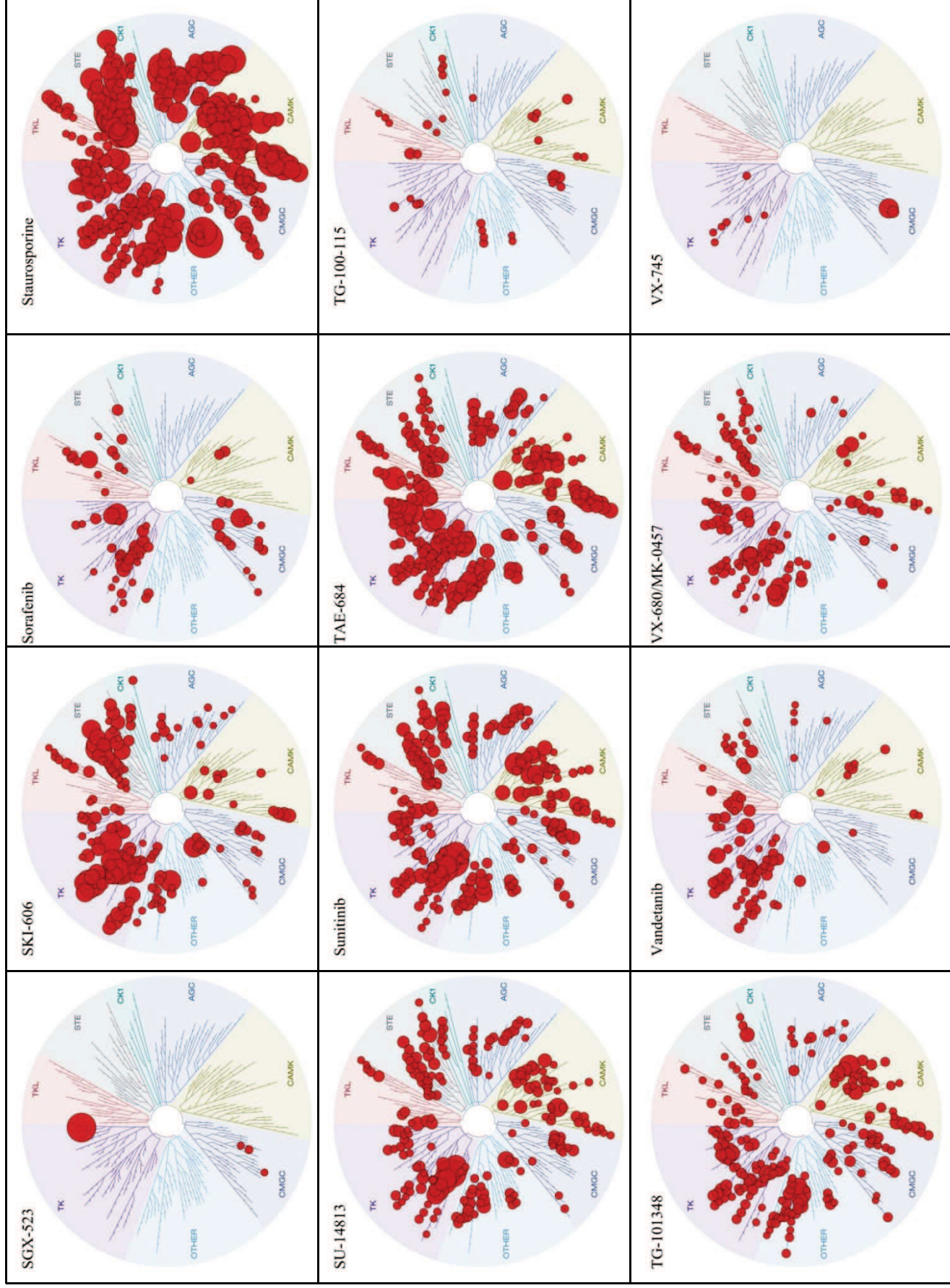
Supplementary Figure 2.



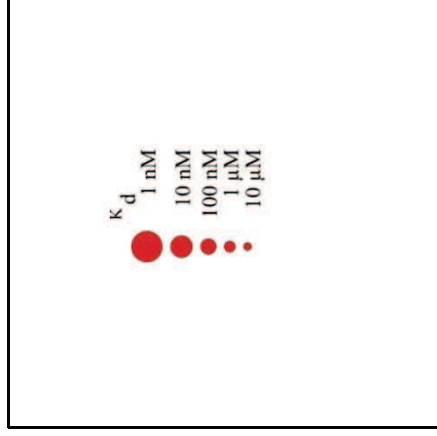
Supplementary Figure 2.



Supplementary Figure 2.

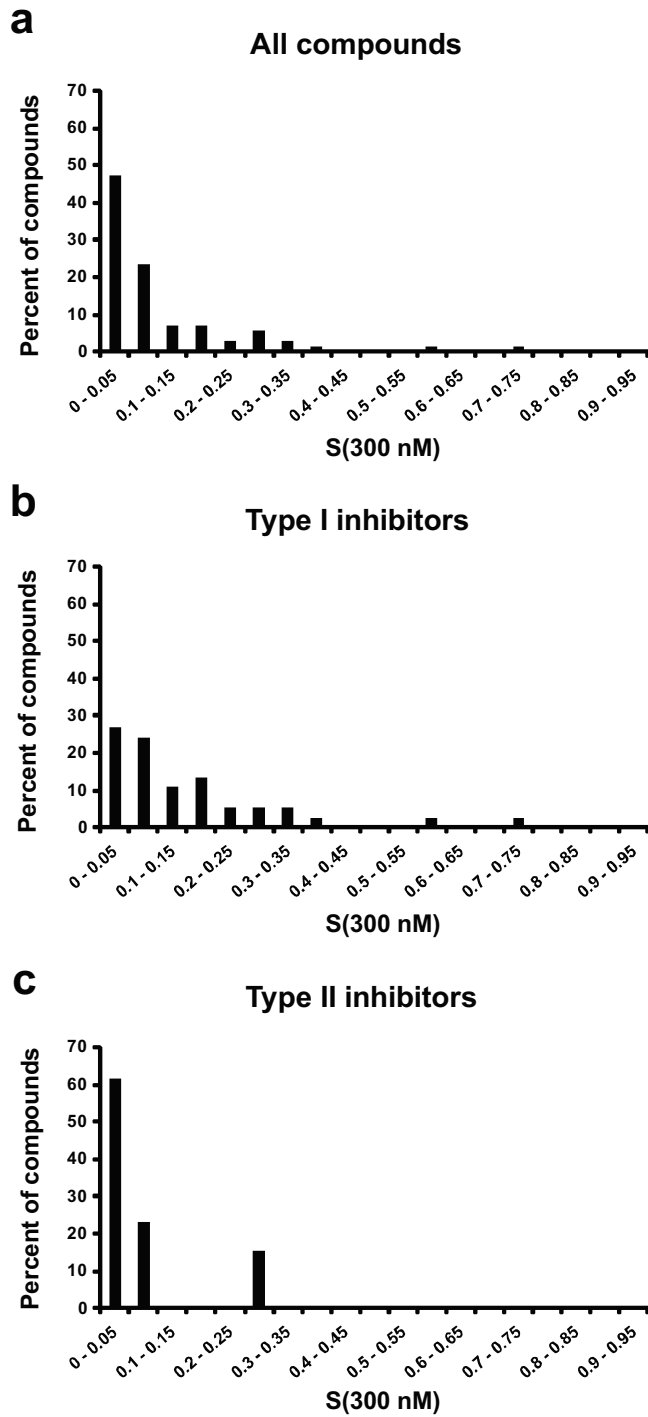


**Supplementary Figure 2.**



**Supplementary Figure 2. Kinome interaction maps for the 72 compounds tested.** Each red circle indicates a kinase found to bind to a compound. Larger circles indicate higher affinity interactions. Interactions with  $K_d < 3 \mu$ M are shown.

Supplementary Figure 3.



**Supplementary Figure 3. Quantitative distribution of kinome-wide selectivity of compounds.** An alternative analysis of the data shown in Figure 1 using a cutoff of S(300 nM) instead of S(3  $\mu$ M) and reduced bin sizes (0.05 units instead of 0.1). (a), (b), and (c) are otherwise as described in Figure 1.



Supplementary Table 2. Compound structures and highest affinity target kinases (excluding mutants)

Compound	Structure	Kinase	Kd, nM
AT-7519		PCK2	0.95
		PCK1	1.1
		CDK5	2.6
		CDK7	2.8
		CDC2L5	3.2
		CDC2L2	5.2
		CDK9	5.8
		ICK	8.3
		CDC2L1	8.4
		GSK3B	11
		AZD-1152HQA	
AURKC	4.4		
AURKB	4.6		
FLT3	8.2		
KIT	17		
PDGFRA	38		
PDGFRB	41		
EPHB6	50		
RET	80		
HIPK4	97		
PDGFRB	0.32		
AZD-2171		KIT	0.38
		PDGFRA	0.41
		FLT1	0.74
		VEGFR2	1.1
		DDR1	1.7
		FLT4	4.3
		STK35	5.4
		RET	6.1
		CSF1R	13
		MEK1	99
		AZD-6244/ARRY-886	
EGFR	7000		
BI-2536		PLK1	0.19
		PLK2	0.81
		PLK3	4
		RPS6KA4(Kin.Dom.2-C-terminal)	12
		CAMKK1	22
		CAMKK2	23
		MYLK	97
		PIP5K2C	110
		DAPK3	130
		FAK	150
		BIBF-1120 (derivative)	
BIKE	2.2		
VEGFR2	2.9		
PKNB(M.tuberculosis)	3.6		
FLT3	3.8		
TAK1	4.1		
TRKA	4.5		
JAK1(JH2domain-pseudokinase)	4.8		
MELK	4.9		
YSK4	5.2		
BIBW-2992			
		ERBB2	5
		ERBB4	6.3
		GAK	79
		BLK	220
		IRAK1	240
		EPHA6	340
		HIPK4	360
		PHKG2	470
		ABL1-phosphorylated	570

Supplementary Table 2. Compound structures and highest affinity target kinases (excluding mutants)

Compound	Structure	Kinase	Kd, nM		
BIRB-796		p38-alpha	0.45		
		DDR1	1.9		
		p38-gamma	2.9		
		p38-beta	7.2		
		JNK2	7.3		
		TIE1	8.3		
		LOK	12		
		TIE2	20		
		DDR2	33		
		p38-delta	78		
		BMS-345541		IKK-beta	130
				YSK4	260
CDC2L2	390				
CDC2L1	420				
ERK5	620				
CDK7	680				
MYLK4	700				
CDC2L5	800				
PCTK1	890				
ERN1	1000				
BMS-387032/SNS-032				CDKL5	1.7
				PCTK1	7.1
		PCTK2	13		
		CDC2L5	23		
		GSK3A	28		
		CDK7	31		
		GSK3B	37		
		CDKL2	41		
		PCTK3	44		
		CDC2L2	48		
		BMS-540215		VEGFR2	5
				FLT1	10
PDGFRA	11				
STK35	26				
KIT	36				
PDGFRB	50				
FLT4	56				
FGFR1	99				
FGFR2	110				
DDR1	160				
CEP-701				PHKG1	0.39
				YSK4	0.52
		LATS2	1		
		SNARK	1		
		MKNK2	1.4		
		PLK4	1.5		
		IRAK4	1.7		
		PHKG2	1.7		
		PKN2	1.8		
		JAK3(JH1domain-catalytic)	2.3		
		CHIR-258/TKI-258		FLT3	0.64
				MLCK	2
PDGFRB	3.8				
KIT	7.5				
MINK	9.1				
YSK4	12				
TNIK	24				
MEK5	32				
MAST1	40				
HPK1	44				
CHIR-265/RAF-265				DDR1	13
				EPHB6	43
		YSK4	54		
		GCN2(Kin.Dom.2,S808G)	55		
		LOK	60		
		ZAK	63		
		CIT	87		
		TAOK2	140		
		RET	150		
		TIE1	150		

Supplementary Table 2. Compound structures and highest affinity target kinases (excluding mutants)

Compound	Structure	Kinase	Kd, nM
CI-1033		EGFR	0.19
		ERBB4	6.5
		ABL1-phosphorylated	30
		BLK	45
		ERBB2	56
		MEK5	60
		GAK	100
		MKK7	110
		ABL1-nonphosphorylated	210
		ERBB3	210
		CI-1040	
MEK2	370		
AURKC	1800		
PDGFRB	3100		
CAMK2A	3400		
CP-690550		JAK3(JH1domain-catalytic)	0.16
		JAK2(JH1domain-catalytic)	0.58
		JAK1(JH1domain-catalytic)	1.6
		TYK2(JH1domain-catalytic)	4.8
		DCAMKL3	12
		TNK1	120
		PKN1	170
		SNARK	240
		ROCK2	420
		LCK	460
		MET	2.1
Crizotinib		ALK	3.3
		MERTK	3.6
		ROS1	4.1
		EPHB6	6
		AXL	7.8
		LTK	12
		SLK	18
		MST1R	25
		LCK	30
Dasatinib		ABL1-nonphosphorylated	0.029
		EPHB6	0.039
		ABL1-phosphorylated	0.046
		EPHA3	0.093
		ABL2	0.17
		LCK	0.2
		BLK	0.21
		SRC	0.21
		EPHA5	0.24
		EPHA8	0.24
Erlotinib		EGFR	0.67
		GAK	3.1
		LOK	19
		YSK4	25
		SLK	26
		ABL1-phosphorylated	76
		MEK5	96
		BLK	190
		ABL2	200
		ERBB4	230
EXEL-2880/GSK-1363089		AXL	0.093
		DDR1	0.2
		MERTK	0.27
		HIPK4	0.51
		LOK	0.53
		RET	0.74
		TIE1	0.79
		FLT3	0.9
		PDGFRB	0.96
		EPHA3	1

Supplementary Table 2. Compound structures and highest affinity target kinases (excluding mutants)

Compound	Structure	Kinase	Kd, nM		
Flavopiridol		ICK	0.69		
		CDK4-cyclinD3	3.3		
		CDK9	6.4		
		CDKL5	7.1		
		CDK4-cyclinD1	9		
		CDK7	23		
		MAK	28		
		TYK2(JH2domain-pseudokinase)	35		
		TNNI3K	55		
		CDK11	57		
		GDC-0879		BRAF	0.19
RAF1	6.6				
CSNK1E	130				
YSK4	910				
MINK	1000				
RIOK2	1200				
LOK	1300				
SLK	1300				
CSNK1D	1400				
BMPR1B	1800				
GDC-0941				PIK3CA	1.1
				PIK3CD	5
				PIK3CB	16
				PIK3CG	48
		PIK3C2B	130		
		MTOR	200		
		PIK3C2G	300		
		JAK1(JH2domain-pseudokinase)	430		
		HIPK2	520		
		JNK3	560		
Gefitinib		EGFR	1		
		GAK	13		
		IRAK1	69		
		YSK4	240		
		MKMK1	290		
		HIPK4	310		
		ERBB4	410		
		CSNK1E	430		
		LOK	470		
		ABL1-phosphorylated	480		
		ALK	0.55		
GSK-1838705A		LTK	1.1		
		INSR	1.7		
		IGF1R	7		
		INSRR	8.6		
		FER	9.3		
		MYLK	11		
		ROS1	15		
		CLK2	16		
		CLK1	21		
		PLK1	0.094		
		SNARK	23		
		LOK	69		
		RSK2(Kin.Dom.1-N-terminal)	190		
GSK-461364A		PIM1	250		
		NEK2	260		
		RSK4(Kin.Dom.1-N-terminal)	350		
		BIKE	470		
		PLK2	500		
		CAMK2D	620		
		GSK-690693		AKT2	2.1
				AKT1	2.2
				PRKCH	2.4
				AKT3	3
PRKG2	3.1				
PKNB(M.tuberculosis)	3.2				
PRKCE	5.3				
PRKX	7.2				
PAK7	8.9				
PKAC-beta	13				

Supplementary Table 2. Compound structures and highest affinity target kinases (excluding mutants)

Compound	Structure	Kinase	Kd, nM
GW-2580		CSF1R	2.2
		TRKB	36
		TRKC	120
		TRKA	630
HKI-272		MAP4K5	0.65
		EGFR	1.1
		ERBB4	2.4
		ERBB2	6
		MST3	6.5
		MST4	7.4
		ERBB3	7.7
		MAP4K3	7.7
		YSK1	12
		LOK	13
		DDR1	0.7
		ABL1-nonphosphorylated	1.1
		ABL2	10
Imatinib		CSF1R	11
		KIT	13
		PDGFRB	14
		DDR2	15
		ABL1-phosphorylated	21
		PDGFRA	31
		LCK	40
		JAK2(JH1domain-catalytic)	0.036
		TYK2(JH1domain-catalytic)	0.9
		JAK3(JH1domain-catalytic)	2
		JAK1(JH1domain-catalytic)	3.4
		MAP3K2	41
		CAMK2A	46
ROCK2	52		
ROCK1	60		
DCAMK1	68		
DAPK1	72		
JNJ-28312141		CSF1R	3.2
		KIT	3.6
		AMPK-alpha2	4.1
		AXL	5.3
		TYK2(JH1domain-catalytic)	5.8
		TAK1	7.2
		RET	9.2
		DDR1	9.4
		CHEK1	9.9
		JAK2(JH1domain-catalytic)	9.9
		PDGFRB	0.29
		PDGFRA	0.49
		KIT	0.69
CSF1R	0.83		
EPHB6	5		
MEK5	7.4		
DDR1	12		
VEGFR2	18		
LOK	22		
SLK	60		
KW-2449		DRAK1	2.9
		MLCK	4.3
		DRAK2	4.8
		YSK4	5.2
		BIKE	9.6
		MAP4K2	11
		LOK	13
		SLK	13
		FLT3	15
		SRPK2	15



Supplementary Table 2. Compound structures and highest affinity target kinases (excluding mutants)

Compound	Structure	Kinase	Kd, nM
Pazopanib		PDGFRB	2
		KIT	2.8
		PDGFRA	4.9
		CSF1R	7.9
		FLT1	14
		VEGFR2	14
		FLT4	27
		TAOK3	45
		DDR1	57
		EPHB6	81
		PD-173955	
CSF1R	0.67		
ABL2	0.69		
SRC	0.71		
LCK	1.1		
PDGFRB	1.4		
ABL1-nonphosphorylated	1.5		
BLK	1.5		
KIT	1.8		
EPHB6	2		
PHA-665752			
		SRPK1	41
		TAOK3	43
		BIKE	47
		GRK7	61
		HIPK3	63
		CAMKK1	64
		DDR1	70
		CAMKK2	73
		YSK4	78
		PI-103	
PIK3CB	1.7		
PIK3C2B	10		
MTOR	12		
PIK3CG	16		
PIK3CD	17		
PIK3C2G	41		
HIPK2	290		
HIPK3	310		
PIP5K2C	620		
PKC-412			
		TBK1	9.3
		FLT3	11
		JAK3(JH1domain-catalytic)	12
		MLK1	15
		PKN2	15
		YSK4	15
		MLK3	17
		CAMK2A	20
		MARK3	21
		PLX-4720	
PFCDPK1(P.falciparum)	1.7		
SRMS	21		
ZAK	41		
BRK	48		
FGR	62		
RAF1	170		
KIT	180		
MEK4	190		
NEK11	190		
PP-242			
		ACVRL1	2.9
		MTOR	3
		ACVR1	4
		RET	4.8
		YSK4	5.1
		MEK5	7.3
		ACVR2B	7.6
		PRKCE	9
		JAK2(JH1domain-catalytic)	11

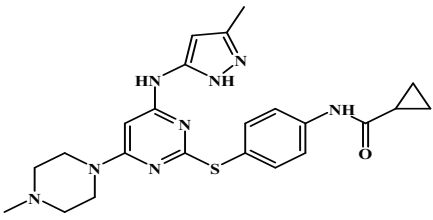
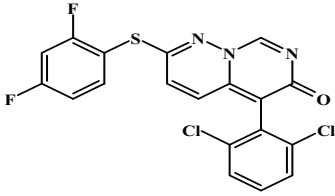
Supplementary Table 2. Compound structures and highest affinity target kinases (excluding mutants)

Compound	Structure	Kinase	Kd, nM
PTK-787		KIT	5.1
		FLT1	9.6
		PDGFRB	25
		CSF1R	45
		VEGFR2	62
		PDGFRA	96
		DDR1	270
		FLT4	330
		CDK11	1500
		FRK	1800
		R406	
STK16	1.7		
GCN2(Kin.Dom.2,S808G)	3.3		
PDGFRB	3.3		
JAK2(JH1domain-catalytic)	3.5		
MLK2	3.8		
RET	4.1		
PLK4	4.2		
MLK1	4.3		
PLK3	5.1		
CDK2	0.53		
R547		PCTK1	0.54
		CDK7	0.58
		CDK4-cyclinD1	0.61
		CDK4-cyclinD3	0.81
		PCTK2	0.86
		ICK	2.2
		CDK3	3.2
		PPTAIRE2	7.2
		CDK5	7.4
		p38-alpha	12
		GAK	19
SB-203580		RIPK2	24
		NLK	25
		JNK3	35
		CSNK1D	37
		p38-beta	70
		CSNK1A1	75
		CSNK1E	100
		JNK2	130
		MET	0.19
		DYRK1A	780
		DYRK1B	1800
SGX-523		JNK3	1900
		PIP5K2C	3300
		JNK1	4200
		YSK4	6400
		ABL1-phosphorylated	0.057
		ABL1-nonphosphorylated	0.12
SKI-606		MAP4K5	0.5
		LCK	0.59
		ERBB3	0.77
		SRC	1
		GAK	1.3
		FRK	1.4
		ABL2	1.5
		STK35	2
		DDR1	1.5
		HIPK4	3.3
Sorafenib		ZAK	6.3
		DDR2	6.6
		FLT3	13
		RET	13
		CSF1R	28
		KIT	28
		FLT1	31
		PDGFRB	37

Supplementary Table 2. Compound structures and highest affinity target kinases (excluding mutants)

Compound	Structure	Kinase	Kd, nM		
Staurosporine		SLK	0.024		
		LOK	0.037		
		CAMKK1	0.039		
		SNARK	0.086		
		PHKG2	0.14		
		CAMK2A	0.16		
		CAMKK2	0.16		
		MST2	0.18		
		MST1	0.19		
		TAOK3	0.22		
		PDGFRB	0.29		
		FLT3	0.54		
SU-14813		KIT	0.68		
		PDGFRA	1.1		
		VEGFR2	2.3		
		CSF1R	3.6		
		HUNK	3.7		
		FLT1	4.7		
		STK35	8.2		
		YSK4	12		
		PDGFRB	0.075		
		KIT	0.37		
		FLT3	0.41		
		PDGFRA	0.79		
Sunitinib		DRAK1	1		
		VEGFR2	1.5		
		FLT1	1.8		
		CSF1R	2.5		
		BIKE	5.5		
		PHKG1	5.5		
		ROS1	0.49		
		ULK1	0.83		
		BMPR1B	0.85		
		PLK4	0.93		
		LTK	0.95		
		ALK	1.1		
TAE-684		FAK	1.1		
		PYK2	1.1		
		SNARK	1.2		
		FER	1.4		
		PIK3C2G	3.2		
		PIK3CG	5.3		
		PIK3C2B	7.3		
		TRPM6	7.9		
		CLK2	43		
		PIK3CA	59		
		PIK3CB	80		
		ADCK3	94		
RIPK4	97				
CLK4	130				
TG-100-115		GAK	1.1		
		JAK2(JH1domain-catalytic)	1.1		
		DAPK3	1.2		
		STK16	6.6		
		DCAMKL3	13		
		FLT3	13		
		DAPK1	16		
		JAK1(JH1domain-catalytic)	18		
		YSK4	19		
		TYK2(JH1domain-catalytic)	21		
		RIPK2	4.6		
		EGFR	9.5		
TG-101348		DDR1	11		
		ABL1-phosphorylated	16		
		LCK	17		
		RET	34		
		ABL1-nonphosphorylated	48		
		MEK5	49		
		EPHA6	50		
		STK35	56		
		Vandetanib			

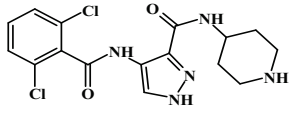
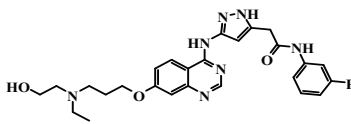
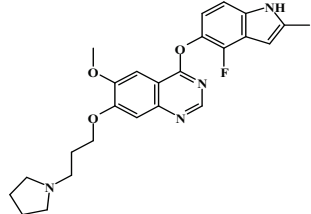
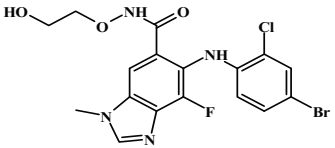
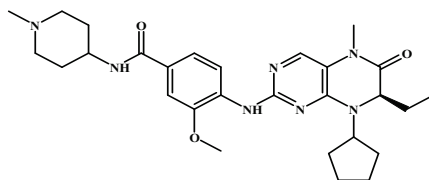
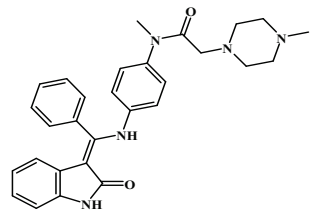
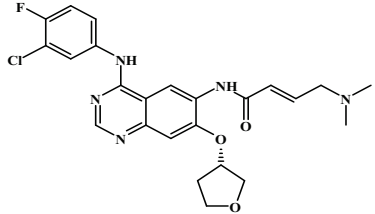
Supplementary Table 2. Compound structures and highest affinity target kinases (excluding mutants)

Compound	Structure	Kinase	Kd, nM
VX-680/MK-0457		AURKA	3.9
		ABL2	4
		AURKC	6.3
		FLT3	6.5
		AURKB	7.4
		ABL1-phosphorylated	7.5
		PLK4	9.2
		ABL1-nonphosphorylated	13
		MLCK	15
		RIPK1	20
		p38-alpha	2.8
		p38-beta	74
		DDR1	1100
		FGR	1300
YES	1600		
LYN	1700		
ABL2	1900		
FYN	2100		
CSF1R	2600		
BLK	3100		
VX-745		p38-alpha	2.8
		p38-beta	74
		DDR1	1100
		FGR	1300
		YES	1600
		LYN	1700
		ABL2	1900
		FYN	2100
		CSF1R	2600
		BLK	3100

Supplementary Table 2. Compound structures and highest affinity target kinases (excluding mutants)

Compound	Structure	Kinase	Kd, nM		
A-674563		CLK2	0.51		
		CLK4	0.53		
		CLK1	1.4		
		DYRK1A	2.1		
		DYRK1B	3.9		
		PRKCH	9.5		
		PRKCE	11		
		PRKCCQ	12		
		CIT	13		
		PRKG2	19		
		ABL1-nonphosphorylated	2.1		
		CSF1R	7.6		
		AB-1010		KIT	8.1
PDGFRB	8.4				
DDR1	8.7				
PDGFRA	25				
DDR2	26				
LCK	31				
ABL1-phosphorylated	55				
LYN	61				
FLT3	0.63				
PDGFRB	1.9				
KIT	2				
CSF1R	3.4				
PDGFRA	4.2				
ABT-869		FLT1	7.5		
		VEGFR2	8.1		
		MUSK	10		
		FLT4	16		
		EPHB6	33		
		FLT3	1.3		
		KIT	4.8		
		PDGFRB	7.7		
		RET	8		
		CSF1R	10		
		PDGFRA	11		
		FLT1	41		
		FLT4	41		
AC220		DDR1	81		
		VEGFR2	87		
		PDGFRA	0.51		
		PDGFRB	0.57		
		AURKC	1.3		
		KIT	3.2		
		FLT1	5.8		
		VEGFR2	5.9		
		AURKB	11		
		PLK4	16		
		CSF1R	21		
		ABL1-phosphorylated	36		
		KIT	3.7		
AG-013736		CSF1R	5.6		
		ZAK	8		
		PDGFRB	9.1		
		FLT4	9.7		
		PDGFRA	10		
		FLT1	12		
		RET	14		
		VEGFR2	26		
		FLT3	71		
		TIE1	0.29		
		CDKL2	0.52		
		ABL1-nonphosphorylated	0.68		
		DDR1	0.69		
AMG-706		FLT3	0.79		
		LOK	0.92		
		CDC2L5	0.94		
		CDK8	1.4		
		CDK11	1.5		
		TAK1	1.5		
		AST-487		CDK11	1.5

Supplementary Table 2. Compound structures and highest affinity target kinases (excluding mutants)

Compound	Structure	Kinase	Kd, nM
AT-7519		PCK2	0.95
		PCK1	1.1
		CDK5	2.6
		CDK7	2.8
		CDC2L5	3.2
		CDC2L2	5.2
		CDK9	5.8
		ICK	8.3
		CDC2L1	8.4
		GSK3B	11
		AZD-1152HQA	
AURKC	4.4		
AURKB	4.6		
FLT3	8.2		
KIT	17		
PDGFRA	38		
PDGFRB	41		
EPHB6	50		
RET	80		
HIPK4	97		
PDGFRB	0.32		
AZD-2171		KIT	0.38
		PDGFRA	0.41
		FLT1	0.74
		VEGFR2	1.1
		DDR1	1.7
		FLT4	4.3
		STK35	5.4
		RET	6.1
		CSF1R	13
		MEK1	99
		AZD-6244/ARRY-886	
EGFR	7000		
BI-2536		PLK1	0.19
		PLK2	0.81
		PLK3	4
		RPS6KA4(Kin.Dom.2-C-terminal)	12
		CAMKK1	22
		CAMKK2	23
		MYLK	97
		PIP5K2C	110
		DAPK3	130
		FAK	150
		BIBF-1120 (derivative)	
BIKE	2.2		
VEGFR2	2.9		
PKNB(M.tuberculosis)	3.6		
FLT3	3.8		
TAK1	4.1		
TRKA	4.5		
JAK1(JH2domain-pseudokinase)	4.8		
MELK	4.9		
YSK4	5.2		
BIBW-2992			
		ERBB2	5
		ERBB4	6.3
		GAK	79
		BLK	220
		IRAK1	240
		EPHA6	340
		HIPK4	360
		PHKG2	470
		ABL1-phosphorylated	570

Supplementary Table 2. Compound structures and highest affinity target kinases (excluding mutants)

Compound	Structure	Kinase	Kd, nM
BIRB-796		p38-alpha	0.45
		DDR1	1.9
		p38-gamma	2.9
		p38-beta	7.2
		JNK2	7.3
		TIE1	8.3
		LOK	12
		TIE2	20
		DDR2	33
		p38-delta	78
BMS-345541		IKK-beta	130
		YSK4	260
		CDC2L2	390
		CDC2L1	420
		ERK5	620
		CDK7	680
		MYLK4	700
		CDC2L5	800
		PCTK1	890
		ERN1	1000
BMS-387032/SNS-032		CDKL5	1.7
		PCTK1	7.1
		PCTK2	13
		CDC2L5	23
		GSK3A	28
		CDK7	31
		GSK3B	37
		CDKL2	41
		PCTK3	44
		CDC2L2	48
BMS-540215		VEGFR2	5
		FLT1	10
		PDGFRA	11
		STK35	26
		KIT	36
		PDGFRB	50
		FLT4	56
		FGFR1	99
		FGFR2	110
		DDR1	160
CEP-701		PHKG1	0.39
		YSK4	0.52
		LATS2	1
		SNARK	1
		MKNK2	1.4
		PLK4	1.5
		IRAK4	1.7
		PHKG2	1.7
		PKN2	1.8
		JAK3(JH1domain-catalytic)	2.3
CHIR-258/TKI-258		FLT3	0.64
		MLCK	2
		PDGFRB	3.8
		KIT	7.5
		MINK	9.1
		YSK4	12
		TNIK	24
		MEK5	32
		MAST1	40
		HPK1	44
CHIR-265/RAF-265		DDR1	13
		EPHB6	43
		YSK4	54
		GCN2(Kin.Dom.2,S808G)	55
		LOK	60
		ZAK	63
		CIT	87
		TAOK2	140
		RET	150
		TIE1	150

Supplementary Table 2. Compound structures and highest affinity target kinases (excluding mutants)

Compound	Structure	Kinase	Kd, nM
CI-1033		EGFR	0.19
		ERBB4	6.5
		ABL1-phosphorylated	30
		BLK	45
		ERBB2	56
		MEK5	60
		GAK	100
		MKK7	110
		ABL1-nonphosphorylated	210
		ERBB3	210
		CI-1040	
MEK2	370		
AURKC	1800		
PDGFRB	3100		
CAMK2A	3400		
CP-690550		JAK3(JH1domain-catalytic)	0.16
		JAK2(JH1domain-catalytic)	0.58
		JAK1(JH1domain-catalytic)	1.6
		TYK2(JH1domain-catalytic)	4.8
		DCAMKL3	12
		TNK1	120
		PKN1	170
		SNARK	240
		ROCK2	420
		LCK	460
		MET	2.1
Crizotinib		ALK	3.3
		MERTK	3.6
		ROS1	4.1
		EPHB6	6
		AXL	7.8
		LTK	12
		SLK	18
		MST1R	25
		LCK	30
Dasatinib		ABL1-nonphosphorylated	0.029
		EPHB6	0.039
		ABL1-phosphorylated	0.046
		EPHA3	0.093
		ABL2	0.17
		LCK	0.2
		BLK	0.21
		SRC	0.21
		EPHA5	0.24
		EPHA8	0.24
Erlotinib		EGFR	0.67
		GAK	3.1
		LOK	19
		YSK4	25
		SLK	26
		ABL1-phosphorylated	76
		MEK5	96
		BLK	190
		ABL2	200
		ERBB4	230
EXEL-2880/GSK-1363089		AXL	0.093
		DDR1	0.2
		MERTK	0.27
		HIPK4	0.51
		LOK	0.53
		RET	0.74
		TIE1	0.79
		FLT3	0.9
		PDGFRB	0.96
		EPHA3	1

Supplementary Table 2. Compound structures and highest affinity target kinases (excluding mutants)

Compound	Structure	Kinase	Kd, nM		
Flavopiridol		ICK	0.69		
		CDK4-cyclinD3	3.3		
		CDK9	6.4		
		CDKL5	7.1		
		CDK4-cyclinD1	9		
		CDK7	23		
		MAK	28		
		TYK2(JH2domain-pseudokinase)	35		
		TNNI3K	55		
		CDK11	57		
		GDC-0879		BRAF	0.19
RAF1	6.6				
CSNK1E	130				
YSK4	910				
MINK	1000				
RIOK2	1200				
LOK	1300				
SLK	1300				
CSNK1D	1400				
BMPR1B	1800				
GDC-0941				PIK3CA	1.1
				PIK3CD	5
				PIK3CB	16
				PIK3CG	48
		PIK3C2B	130		
		MTOR	200		
		PIK3C2G	300		
		JAK1(JH2domain-pseudokinase)	430		
		HIPK2	520		
		JNK3	560		
		Gefitinib		EGFR	1
GAK	13				
IRAK1	69				
YSK4	240				
MKMK1	290				
HIPK4	310				
ERBB4	410				
CSNK1E	430				
LOK	470				
ABL1-phosphorylated	480				
GSK-1838705A				ALK	0.55
		LTK	1.1		
		INSR	1.7		
		IGF1R	7		
		INSRR	8.6		
		FER	9.3		
		MYLK	11		
		ROS1	15		
		CLK2	16		
		CLK1	21		
		PLK1	0.094		
		SNARK	23		
		LOK	69		
		RSK2(Kin.Dom.1-N-terminal)	190		
GSK-461364A		PIM1	250		
		NEK2	260		
		RSK4(Kin.Dom.1-N-terminal)	350		
		BIKE	470		
		PLK2	500		
		CAMK2D	620		
		GSK-690693		AKT2	2.1
				AKT1	2.2
				PRKCH	2.4
				AKT3	3
				PRKG2	3.1
PKNB(M.tuberculosis)	3.2				
PRKCE	5.3				
PRKX	7.2				
PAK7	8.9				
PKAC-beta	13				

Supplementary Table 2. Compound structures and highest affinity target kinases (excluding mutants)

Compound	Structure	Kinase	Kd, nM
GW-2580		CSF1R	2.2
		TRKB	36
		TRKC	120
		TRKA	630
HKI-272		MAP4K5	0.65
		EGFR	1.1
		ERBB4	2.4
		ERBB2	6
		MST3	6.5
		MST4	7.4
		ERBB3	7.7
		MAP4K3	7.7
		YSK1	12
		LOK	13
		DDR1	0.7
		ABL1-nonphosphorylated	1.1
		ABL2	10
Imatinib		CSF1R	11
		KIT	13
		PDGFRB	14
		DDR2	15
		ABL1-phosphorylated	21
		PDGFRA	31
		LCK	40
		JAK2(JH1domain-catalytic)	0.036
		TYK2(JH1domain-catalytic)	0.9
		JAK3(JH1domain-catalytic)	2
		JAK1(JH1domain-catalytic)	3.4
		MAP3K2	41
		CAMK2A	46
ROCK2	52		
ROCK1	60		
DCAMKL1	68		
DAPK1	72		
JNJ-28312141		CSF1R	3.2
		KIT	3.6
		AMPK-alpha2	4.1
		AXL	5.3
		TYK2(JH1domain-catalytic)	5.8
		TAK1	7.2
		RET	9.2
		DDR1	9.4
		CHEK1	9.9
		JAK2(JH1domain-catalytic)	9.9
		PDGFRB	0.29
		PDGFRA	0.49
		KIT	0.69
CSF1R	0.83		
EPHB6	5		
MEK5	7.4		
DDR1	12		
VEGFR2	18		
LOK	22		
SLK	60		
KW-2449		DRAK1	2.9
		MLCK	4.3
		DRAK2	4.8
		YSK4	5.2
		BIKE	9.6
		MAP4K2	11
		LOK	13
		SLK	13
		FLT3	15
		SRPK2	15



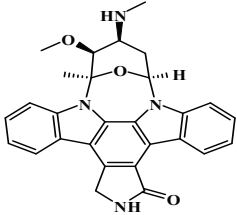
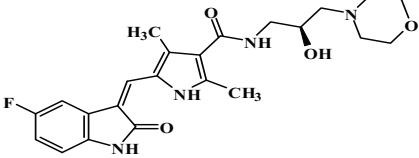
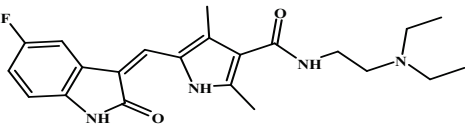
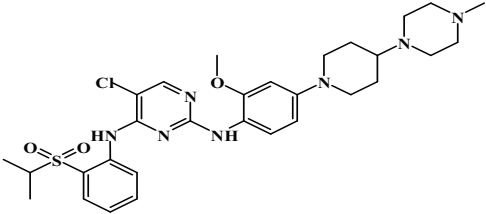
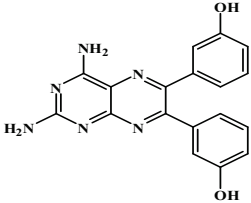
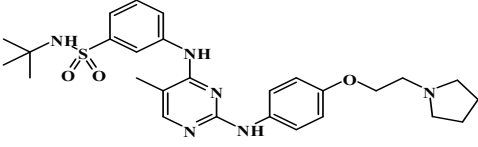
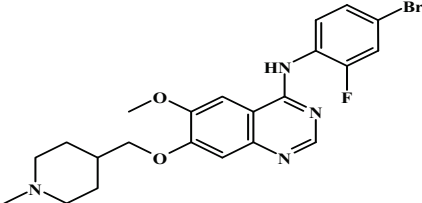
Supplementary Table 2. Compound structures and highest affinity target kinases (excluding mutants)

Compound	Structure	Kinase	Kd, nM
Pazopanib		PDGFRB	2
		KIT	2.8
		PDGFRA	4.9
		CSF1R	7.9
		FLT1	14
		VEGFR2	14
		FLT4	27
		TAOK3	45
		DDR1	57
		EPHB6	81
		PD-173955	
CSF1R	0.67		
ABL2	0.69		
SRC	0.71		
LCK	1.1		
PDGFRB	1.4		
ABL1-nonphosphorylated	1.5		
BLK	1.5		
KIT	1.8		
EPHB6	2		
MET	0.27		
PHA-665752		SRPK1	41
		TAOK3	43
		BIKE	47
		GRK7	61
		HIPK3	63
		CAMKK1	64
		DDR1	70
		CAMKK2	73
		YSK4	78
		PIK3CA	1.5
		PIK3CB	1.7
PI-103		PIK3C2B	10
		MTOR	12
		PIK3CG	16
		PIK3CD	17
		PIK3C2G	41
		HIPK2	290
		HIPK3	310
		PIP5K2C	620
		PKN1	9.3
		TBK1	9.3
		FLT3	11
PKC-412		JAK3(JH1domain-catalytic)	12
		MLK1	15
		PKN2	15
		YSK4	15
		MLK3	17
		CAMK2A	20
		MARK3	21
		MEK5	0.16
		PFCDPK1(P.falciparum)	1.7
		SRMS	21
		ZAK	41
PLX-4720		BRK	48
		FGR	62
		RAF1	170
		KIT	180
		MEK4	190
		NEK11	190
		BMPR1B	2.1
		ACVRL1	2.9
		MTOR	3
		ACVR1	4
		RET	4.8
PP-242		YSK4	5.1
		MEK5	7.3
		ACVR2B	7.6
		PRKCE	9
		JAK2(JH1domain-catalytic)	11

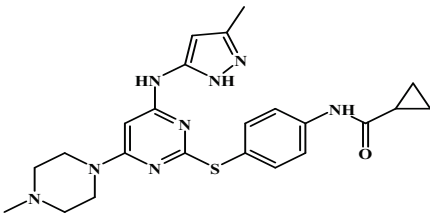
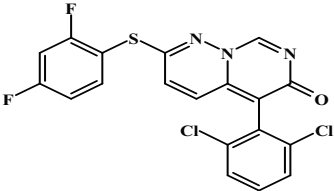
Supplementary Table 2. Compound structures and highest affinity target kinases (excluding mutants)

Compound	Structure	Kinase	Kd, nM
PTK-787		KIT	5.1
		FLT1	9.6
		PDGFRB	25
		CSF1R	45
		VEGFR2	62
		PDGFRA	96
		DDR1	270
		FLT4	330
		CDK11	1500
		FRK	1800
		R406	
STK16	1.7		
GCN2(Kin.Dom.2,S808G)	3.3		
PDGFRB	3.3		
JAK2(JH1domain-catalytic)	3.5		
MLK2	3.8		
RET	4.1		
PLK4	4.2		
MLK1	4.3		
PLK3	5.1		
CDK2	0.53		
R547		PCTK1	0.54
		CDK7	0.58
		CDK4-cyclinD1	0.61
		CDK4-cyclinD3	0.81
		PCK2	0.86
		ICK	2.2
		CDK3	3.2
		PFTAIR2	7.2
		CDK5	7.4
		p38-alpha	12
		GAK	19
SB-203580		RIPK2	24
		NLK	25
		JNK3	35
		CSNK1D	37
		p38-beta	70
		CSNK1A1	75
		CSNK1E	100
		JNK2	130
		MET	0.19
		DYRK1A	780
		SGX-523	
JNK3	1900		
PIP5K2C	3300		
JNK1	4200		
YSK4	6400		
ABL1-phosphorylated	0.057		
ABL1-nonphosphorylated	0.12		
MAP4K5	0.5		
LCK	0.59		
ERBB3	0.77		
SRC	1		
SKI-606		GAK	1.3
		FRK	1.4
		ABL2	1.5
		STK35	2
		DDR1	1.5
		HIPK4	3.3
		ZAK	6.3
		DDR2	6.6
		FLT3	13
		RET	13
		CSF1R	28
Sorafenib		KIT	28
		FLT1	31
		PDGFRB	37

Supplementary Table 2. Compound structures and highest affinity target kinases (excluding mutants)

Compound	Structure	Kinase	Kd, nM
Staurosporine		SLK	0.024
		LOK	0.037
		CAMKK1	0.039
		SNARK	0.086
		PHKG2	0.14
		CAMK2A	0.16
		CAMKK2	0.16
		MST2	0.18
		MST1	0.19
		TAOK3	0.22
		PDGFRB	0.29
		SU-14813	
KIT	0.68		
PDGFRA	1.1		
VEGFR2	2.3		
CSF1R	3.6		
HUNK	3.7		
FLT1	4.7		
STK35	8.2		
YSK4	12		
PDGFRB	0.075		
KIT	0.37		
Sunitinib			
		PDGFRA	0.79
		DRAK1	1
		VEGFR2	1.5
		FLT1	1.8
		CSF1R	2.5
		BIKE	5.5
		PHKG1	5.5
		ROS1	0.49
		ULK1	0.83
		BMPR1B	0.85
		TAE-684	
LTK	0.95		
ALK	1.1		
FAK	1.1		
PYK2	1.1		
SNARK	1.2		
FER	1.4		
PIK3C2G	3.2		
PIK3CG	5.3		
PIK3C2B	7.3		
TRPM6	7.9		
CLK2	43		
TG-100-115		PIK3CA	59
		PIK3CB	80
		ADCK3	94
		RIPK4	97
		CLK4	130
		GAK	1.1
		JAK2(JH1domain-catalytic)	1.1
		DAPK3	1.2
		STK16	6.6
		DCAMKL3	13
		FLT3	13
		DAPK1	16
TG-101348		JAK1(JH1domain-catalytic)	18
		YSK4	19
		TYK2(JH1domain-catalytic)	21
		RIPK2	4.6
		EGFR	9.5
		DDR1	11
		ABL1-phosphorylated	16
		LCK	17
		RET	34
		ABL1-nonphosphorylated	48
		MEK5	49
		Vandetanib	
STK35	56		

Supplementary Table 2. Compound structures and highest affinity target kinases (excluding mutants)

Compound	Structure	Kinase	Kd, nM
VX-680/MK-0457		AURKA	3.9
		ABL2	4
		AURKC	6.3
		FLT3	6.5
		AURKB	7.4
		ABL1-phosphorylated	7.5
		PLK4	9.2
		ABL1-nonphosphorylated	13
		MLCK	15
		RIPK1	20
		p38-alpha	2.8
		p38-beta	74
		DDR1	1100
		FGR	1300
YES	1600		
LYN	1700		
ABL2	1900		
FYN	2100		
CSF1R	2600		
BLK	3100		
VX-745		p38-alpha	2.8
		p38-beta	74
		DDR1	1100
		FGR	1300
		YES	1600
		LYN	1700
		ABL2	1900
		FYN	2100
		CSF1R	2600
		BLK	3100

# Comprehensive assay of kinase catalytic activity reveals features of kinase inhibitor selectivity

Theonie Anastassiadis<sup>1</sup>, Sean W Deacon<sup>2</sup>, Karthik Devarajan<sup>1</sup>, Haiching Ma<sup>2</sup> & Jeffrey R Peterson<sup>1</sup>

Small-molecule protein kinase inhibitors are widely used to elucidate cellular signaling pathways and are promising therapeutic agents. Owing to evolutionary conservation of the ATP-binding site, most kinase inhibitors that target this site promiscuously inhibit multiple kinases. Interpretation of experiments that use these compounds is confounded by a lack of data on the comprehensive kinase selectivity of most inhibitors. Here we used functional assays to profile the activity of 178 commercially available kinase inhibitors against a panel of 300 recombinant protein kinases. Quantitative analysis revealed complex and often unexpected interactions between protein kinases and kinase inhibitors, with a wide spectrum of promiscuity. Many off-target interactions occur with seemingly unrelated kinases, revealing how large-scale profiling can identify multitargeted inhibitors of specific, diverse kinases. The results have implications for drug development and provide a resource for selecting compounds to elucidate kinase function and for interpreting the results of experiments involving kinase inhibitors.

Protein kinases are among the most important classes of therapeutic targets because of their central roles in cellular signaling and the presence of a highly conserved ATP-binding pocket that can be exploited by synthetic chemical compounds. However, achieving highly selective kinase inhibition is a major challenge<sup>1–6</sup>. Knowing the selectivity of kinase inhibitors for their targets is critical for predicting and interpreting the effects of inhibitors in both research and clinical settings. However, the selectivity of kinase inhibitors is seldom assessed across a substantial part of the kinome. Recent technological advances have led to the development of methods to profile kinase target selectivity against sizable fractions of the 518 human protein kinases<sup>7,8</sup>. In many cases, however, these methods measure the binding of small molecules to kinases, rather than functional inhibition of catalytic activity. The ability of these assays to predict functional inhibition thus remains an important unknown.

Traditionally, kinase inhibitors have been discovered in a target-centric manner involving high-throughput screening of large numbers of small molecules and a kinase of interest. The resulting compounds are then tested for selectivity against a panel of representative kinases. An alternative approach, involves screening libraries of compounds in a target-blind manner against a comprehensive panel of recombinant protein kinases to reveal the selectivity of each compound<sup>9,10</sup>. Compounds showing desired selectivity patterns are identified and then chemically optimized. This parallel approach is predicted to identify unexpected new inhibitors for kinases of interest and reveal multitargeted inhibitors, whose inhibitory activity is focused toward a small number of specific kinase targets rather than toward a single primary target<sup>11,12</sup>. Indeed, multitargeted inhibitors are challenging to identify by conventional target-centric screens<sup>13</sup>.

We used a high-throughput enzymatic assay to conduct a large-scale parallel screen of 178 known kinase inhibitors against a panel of 300 protein kinases in duplicate. Our goals were to identify novel

inhibitor chemotypes for specific kinase targets and to reveal the target specificities of a large panel of kinase inhibitors. The compounds tested represent widely used research compounds and clinical agents targeting all of the major kinase families. The resulting data set, to our knowledge the largest of its type available in the public domain, comprises results generated from >100,000 independent functional assays measuring pairwise inhibition of a single enzyme by a single compound. Systematic, quantitative analysis of the results revealed kinases that are commonly inhibited by many compounds, kinases that are resistant to small-molecule inhibition, and unexpected off-target activities of many commonly used kinase inhibitors. In addition, we report potential leads, for orphan kinases for which few inhibitors currently exist and starting points for the development of multitargeted kinase inhibitors.

## RESULTS

### A kinase-inhibitor interaction map

To directly test the kinase selectivity of a large number of kinase inhibitors, we conducted low-volume kinase assays using a panel of 300 recombinant human protein kinases. We used HotSpot, a radiometric assay based on conventional filter-binding assays, which directly measures kinase catalytic activity toward a specific substrate. This well-validated method is the standard against which more indirect assays for kinase inhibition are compared<sup>7</sup>. Our collection of kinase inhibitors included US Food and Drug Administration–approved drugs, compounds in clinical testing, and compounds primarily used as research tools. The library comprised 178 compounds known to inhibit kinases from all major protein kinase subfamilies (**Fig. 1a** and **Supplementary Table 1**).

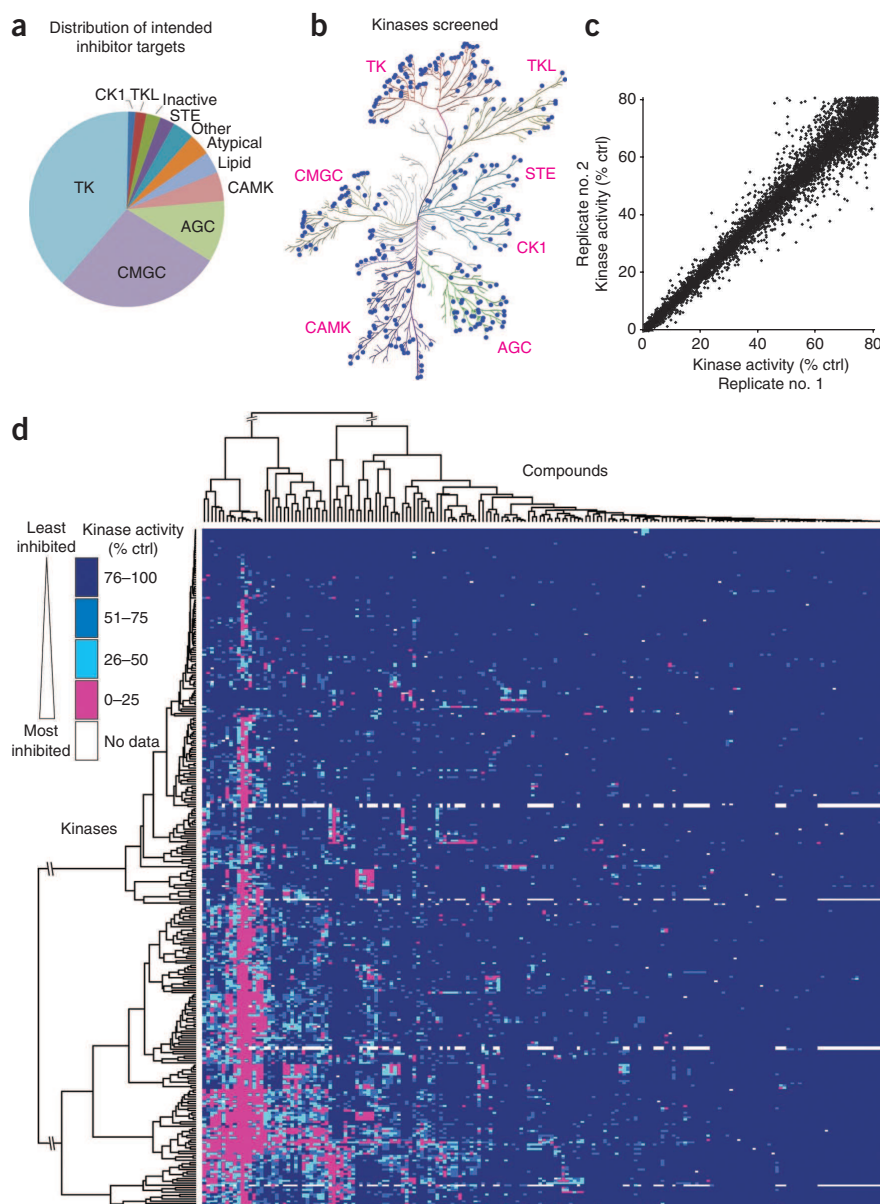
The kinase panel tested includes members of all major human protein kinase families (**Fig. 1b**) and includes the intended targets of 87.6% of the compounds tested. A complete listing of the kinase constructs and substrates used is provided in **Supplementary Table 2**.

<sup>1</sup>Cancer Biology Program, Fox Chase Cancer Center, Philadelphia, Pennsylvania, USA. <sup>2</sup>Reaction Biology Corporation, Malvern, Pennsylvania, USA. Correspondence should be addressed to J.R.P. (jeffrey.peterson@fccc.edu).

Received 1 September; accepted 23 September; published online 30 October 2011; doi:10.1038/nbt.2017

## RESOURCE

**Figure 1** Large-scale kinase-inhibitor interaction analysis. **(a)** Distribution of the intended targets of the inhibitor library, by kinase family. **(b)** The distribution of kinases in the screening panel is represented by blue dots on a dendrogram representing the human kinome (kinome illustration was adapted and is reproduced courtesy of Cell Signaling Technology based on ref. 33). **(c)** Scatter plot of the kinase activity in replicate 1 versus replicate 2 for each kinase-inhibitor pair for which >20% inhibition of kinase activity was observed. **(d)** Two-way hierarchical clustering analysis of the entire kinase-inhibitor interaction map presented as a heat map of kinase activity. A fully labeled, high-resolution version of this heat map is presented in **Supplementary Figure 2**, as a data table in **Supplementary Table 3** and via the Kinase Inhibitor Resource (KIR) online tool (<http://kir.fccc.edu/>). Ctrl, control.



For simplicity, all compounds were tested at a concentration of 0.5  $\mu\text{M}$  in the presence of 10  $\mu\text{M}$  ATP. Despite an average reported half-maximum inhibitory concentration ( $\text{IC}_{50}$ ) for these compounds toward their primary targets of 66 nM, we chose to use 0.5  $\mu\text{M}$  to capture weaker off-target inhibitory activity.

We tested each protein kinase and kinase inhibitor combination (kinase-inhibitor pair) in duplicate and expressed the average substrate phosphorylation results as a percentage of solvent control reactions (henceforth referred to as remaining kinase activity). We identified and eliminated disparate replicates (0.18% of the data set) from the analysis (Online Methods and **Supplementary Fig. 1**). **Figure 1c** illustrates the reproducibility of the resulting data set as a scatter plot in which each point represents one kinase-inhibitor pair plotted as the remaining kinase activity in one replicate versus the second replicate, for all kinase-inhibitor pairs in which at least 20% kinase inhibition was observed.

The mean remaining kinase activity for each kinase-inhibitor pair is presented as a heat map in **Figure 1d**, in high-resolution form in **Supplementary Figure 2** and as a spreadsheet in **Supplementary Table 3**. In addition, we created the Kinase Inhibitor Resource (KIR) database, an internet website that allows compound or kinase specific queries of the data set to be downloaded or analyzed within a browser window (<http://kir.fccc.edu/>). Two-way hierarchical clustering was performed to cluster both kinases and inhibitors based on the similarity of their activity patterns. As expected, structurally related compounds were generally grouped together. Similarly, kinases closely related by sequence identity were often clustered and were inhibited by similar patterns of compounds. Exceptions included members of the clinically relevant Aurora, PDGFR and FGFR family kinases (**Supplementary Fig. 2**), suggesting the possibility that members of these families can be differentially targeted by small molecules. Consistent with this finding, isoform-specific inhibitors of Aurora kinases have been reported and structural studies have revealed the structural basis for isoform-specific inhibition<sup>14</sup>.

### Comparison of data across multiple assay platforms

A variety of high-throughput screening approaches have been devised to detect kinase-compound interactions without directly measuring inhibition of kinase catalytic activity. Although convenient for screening, the extent to which these binding assays predict inhibition of catalytic activity remains uncertain. To assess this, we compared our kinase inhibition data with previous large-scale studies of the binding of small molecules to kinases. Two recent studies used a competitive binding assay to derive affinities for a large number of kinase-inhibitor interactions<sup>1,2</sup>. Six hundred fifty-four kinase-inhibitor pairs overlapped with our study and their affinities showed generally good agreement with the expected kinase activity measured in our single-dose study (**Fig. 2a**). Indeed, 90.2% of kinase-inhibitor interactions with high affinity (stronger than 100 nM  $K_d$ ) showed functional inhibition (>50%). Conversely, only 13.1% of the kinase-inhibitor pairs with low affinity (weaker than 1  $\mu\text{M}$   $K_d$ ) showed >50% inhibition, as expected.

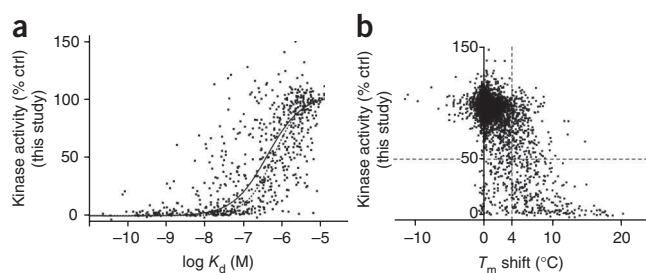
An alternative approach to monitoring kinase-compound binding involves protecting kinases from thermal denaturation by compound binding<sup>3</sup>. To assess this approach to predict kinase inhibition,

**Figure 2** Comparison of functional inhibition data generated in this study with previous kinase-inhibitor interaction profiling studies.

(a,b) Scatter plots compare our results with studies that examined interactions of overlapping kinase-inhibitor pairs by a quantitative kinase-inhibitor binding assay<sup>1,2</sup> (a), or an assay measuring resistance to thermal denaturation by kinases in the presence of individual inhibitors<sup>3</sup> (b).

In a, remaining kinase activity is plotted as a function of kinase-compound binding affinity ( $K_d$ ) for 654 kinase-inhibitor pairs. The resulting data were fit to a sigmoidal dose-response curve (solid line) and can be compared with a theoretical curve (dotted line) for expected remaining kinase activity for an inhibitor of the given affinity.

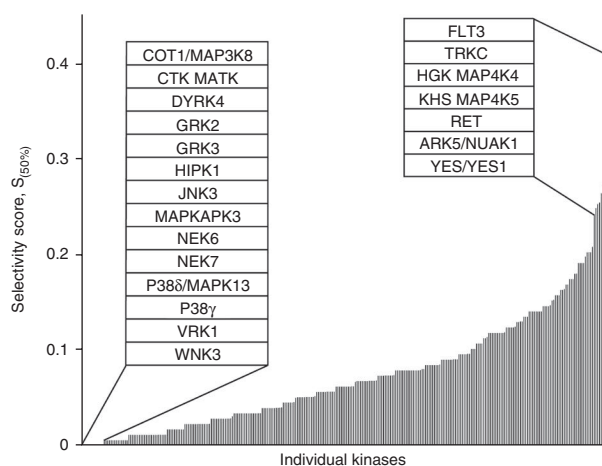
In b remaining kinase activity is plotted against the change in  $T_m$ , relative to solvent control, caused by compound binding for 3,926 kinase-inhibitor pairs. The dashed vertical line denotes the  $T_m$  shift threshold used in ref. 3. The dashed horizontal line highlights the 50% threshold for inhibition of catalytic activity. The resulting upper right quadrant includes compounds that showed significant thermal stabilization without inhibiting kinase activity whereas the lower left quadrant contains compounds which only marginally affect thermal stability yet show >50% inhibition of catalytic activity. Ctrl, control.



we plotted the remaining kinase activity in our functional assay as a function of the change in reported melting temperature ( $T_m$ ) of each kinase-inhibitor pair (Fig. 2b). Generally, compounds that increased the kinase melting temperature also showed inhibition of catalytic activity, as predicted. However, a significant number of compounds showed  $T_m$  changes >4 °C, the hit threshold used previously<sup>3</sup>, without inhibiting kinase activity by >50% (Fig. 2b, upper right dashed quadrant). Likewise, 117 out of 3,926 inhibitor pairs showed >50% inhibition of kinase activity without exhibiting  $T_m$  changes >4 °C (Fig. 2b, lower left dashed quadrant). The findings from these comparisons, taken together, suggest that kinase-inhibitor binding assays exhibit appreciable false-positive and false-negative rates with respect to their ability to predict compounds that functionally inhibit catalytic activity, although binding and inhibition are significantly correlated.

### Analysis of kinase druggability

We next asked whether each kinase in the panel was equally likely to be inhibited by a given compound or whether kinases differed in their sensitivity to small-molecule inhibition. To do this, we ranked the kinases with respect to a selectivity score ( $S_{(50\%)}$ ), the fraction of all compounds tested that inhibited the catalytic activity of each kinase by >50% (Fig. 3 and Supplementary Table 4). Only 14 kinases in the panel were not inhibited by any of the compounds tested (Fig. 3, left inset), demonstrating good coverage of the kinome by this inhibitor set. The untargeted kinases, including COT1, NEK6/7 and p38 $\delta$ , suggest a target list for which screens using traditional ATP-mimetic scaffolds may be less successful. By contrast, a subset of kinases including FLT3, TRKC and HGK/MAP4K4 were broadly inhibited



by large numbers of compounds (right inset), potentially representing kinases highly susceptible to chemical inhibition. This broad range of kinase sensitivity to small molecules has important implications for the assessment of kinase inhibitor selectivity with small kinase panels and suggests that screening panels should include these sensitive kinases. We cannot completely exclude the possibility, however, that the results could reflect hidden biases in our compound library.

### Kinase inhibitor selectivity

Kinase inhibitors are commonly used as research tools to reveal the biological consequence of acute inactivation of their kinase targets. Interpretation of the results of such experiments depends critically on knowing the inhibitor target(s). The selectivity of novel kinase inhibitors is frequently assessed by testing against a limited panel of closely related kinases based on the assumption that off-target interactions are more likely to be found with kinases most closely related by amino acid sequence. To test this quantitatively, we assessed the fraction of kinase targets that are within the same kinase subfamily versus outside the family of the primary target. As highly promiscuous compounds would increase the apparent frequency of out-of-family targets, we removed the top ten most promiscuous compounds before the analysis. On average, 42% of the kinases inhibited by a given compound were from a different kinase subfamily than the subfamily of the intended kinase target (Supplementary Fig. 3). For inhibitors developed against tyrosine kinases, 24% of off-target hits were serine/threonine kinases. The within-family selectivity of tyrosine kinase-targeting compounds may be explained, in part, by the fact that these compounds include almost all of the clinical agents in our compound set and are, therefore, likely more optimized with regard to specificity than research tool compounds. These results highlight the importance of assessing the selectivity of kinase inhibitors against as broad a panel of kinases as possible.

Inhibitors that exhibit selectivity for a very limited number of kinase targets are most valuable as research tools for probing kinase function. Various methods have been proposed to quantitatively assess kinase inhibitor selectivity. A selectivity score  $S(x)$  has been defined, where  $S$  is the number of kinases bound by an inhibitor

**Figure 3** Kinase selectivity. A ranked bar chart of selectivity scores ( $S_{(50\%)}$ ) for all tested kinases. This score corresponds to the fraction of all tested inhibitors that inhibit catalytic activity by >50%. Each bar represents the selectivity score of an individual kinase. Insets identify the 14 kinases that were not inhibited by any compound (left) and the seven most frequently inhibited kinases (right). The complete table is presented in Supplementary Table 4.

(with an affinity greater than  $x \mu\text{M}$ ) divided by the number of kinases tested<sup>2</sup>. A critical limitation of the selectivity score is its dependence on an arbitrary hit threshold ( $x \mu\text{M}$ ). For example, when we analyzed our data using an arbitrary percent inhibition as the hit criterion, several compounds scored favorably because they met the hit threshold with a limited number of kinases, despite a great deal of inhibition of other kinases just below this threshold (not shown). Indeed, selectivity scores generated from the same data set but using different hit thresholds can produce different rank orders of compounds<sup>2</sup>. In addition, compounds that did not meet the hit threshold for any kinase could not be scored. We therefore calculated a previously described metric for kinase inhibitor selectivity based on the Gini coefficient<sup>15</sup>. Importantly, this method does not depend on defining an arbitrary hit threshold, although it is strongly influenced by the compound screening concentration. The Gini score reflects, on a scale of 0 to 1, the degree to which the aggregate inhibitory activity of a compound (calculated as the sum of inhibition for all kinases) is directed toward only a single target (a Gini score of 1) or is distributed equally across all tested kinases (a Gini score of 0). We used the results of this analysis to rank the compounds from the most promiscuous to the most selective (Fig. 4a; complete list in Supplementary Table 5). Not surprisingly, staurosporine and several of its structural analogs exhibited the lowest Gini scores (Fig. 4a, left inset), consistent with their known broad target spectrum. Among the most selective compounds (Fig. 4a, right inset) were several structurally distinct inhibitors of ErbB family kinases. The target spectra of the three compounds with the lowest, median and highest Gini scores are shown in the bottom panels. Although a comparable number of kinases were targeted by the compounds with the median and highest Gini scores (middle and right dendrograms), masitinib achieves a higher Gini score by producing lower residual kinase activity in its targets (darker spots).

To understand the molecular features that contribute to inhibitor promiscuity, previous kinase-inhibitor profiling studies have identified correlations between compound physicochemical properties and promiscuity<sup>13,16</sup>. We analyzed a variety of compound physicochemical properties with respect to either the Gini score or the selectivity score but did not observe a consistent linear correlation with any single

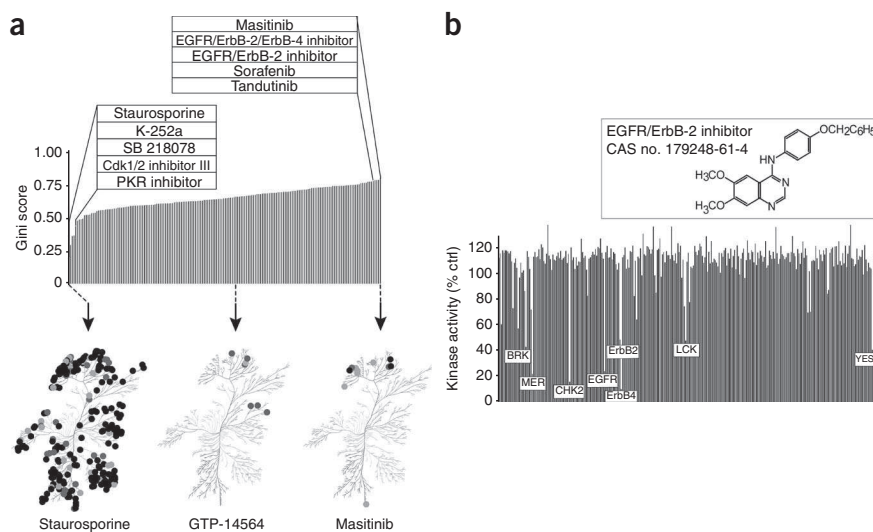
compound property (Supplementary Fig. 4). This finding and the discrepant findings of the previous studies suggest that compound promiscuity is unlikely to be strongly related to any one physical parameter in a simple, linear manner.

The clinical success of some kinase inhibitors that show poor kinase selectivity *in vitro* (e.g., dasatinib (Sprycel), sunitinib (Sutent)) has led to increasing interest in so-called multitargeted kinase inhibitors<sup>12,17</sup>. Ideally, such compounds differ from promiscuous inhibitors in that they should show significant selectivity toward a limited number of clinically relevant targets with the goal of achieving greater therapeutic effect than targeting a single kinase<sup>18</sup>. Despite the promise of polypharmacology, it remains a difficult technical challenge to rationally develop single compounds with a desired target spectrum<sup>18,19</sup>. Parallel kinase profiling of large inhibitor libraries has been suggested as an approach to identify compound scaffolds that show promising activity against specific kinases of interest<sup>9,19</sup>. We interrogated our data for examples of inhibitors with off-target activities against a limited number of cancer-relevant kinases. The ErbB family kinase inhibitor 4-(4-benzoyloxyanilino)-6,7-dimethoxyquinazoline<sup>20</sup> showed potent inhibition of a few tyrosine kinases beyond ErbB family members and, most surprisingly, potent inhibition of the serine/threonine kinase CHK2, a critical component of the DNA damage checkpoint (Fig. 4b). CHK2 inhibition has been proposed as a strategy to increase the therapeutic impact of DNA-damaging cancer therapies and inhibitors of CHK2 are in clinical trials<sup>21</sup>. This illustrates how kinase profiling can reveal unanticipated novel scaffolds that show activity against highly divergent kinases of therapeutic interest. Data mining of this and similar data sets can facilitate the identification of inhibitor scaffolds with activity toward multiple targets of interest.

### Novel targets of uni-specific kinase inhibitors

Even among the most selective inhibitors identified by the screen, most still targeted multiple kinases with similar potency (Fig. 4a, rightmost dendrogram), therefore confounding their use as research tools to elucidate the function of a single kinase. We therefore asked whether any compounds inhibited a single kinase more potently than any other in our panel, a characteristic we termed 'uni-specificity'. Importantly, this stringent criterion excludes compounds that target

**Figure 4** Kinase inhibitor selectivity. (a) A ranked list of kinase inhibitors sorted by Gini score<sup>15</sup> as a measure of inhibitor selectivity. A Gini score of 0 indicates equal inhibition of all kinases (promiscuous inhibition) whereas a score of 1 indicates inhibition of only one kinase (selective inhibition). Left inset highlights the five compounds with the lowest Gini scores and the right inset, the five highest scoring compounds. The complete table is presented in Supplementary Table 5. Below, the selectivity of three representative compounds are presented on a dendrogram of all human kinases based on amino acid sequence similarity<sup>33</sup>. Spot color represents inhibitory potency: darkest, 0–10% remaining activity; lighter, 10–25% activity; lightest, 25–50% activity. The kinome dendrogram was adapted and is reproduced courtesy of Cell Signaling Technology. (b) Target spectrum of 4-(4-benzoyloxyanilino)-6,7-dimethoxyquinazoline, a multitargeted inhibitor, highly selective for ErbB family members, a limited number of other tyrosine kinase targets and the serine/threonine kinase CHK2. Each bar corresponds to the percent remaining activity for an individual kinase.



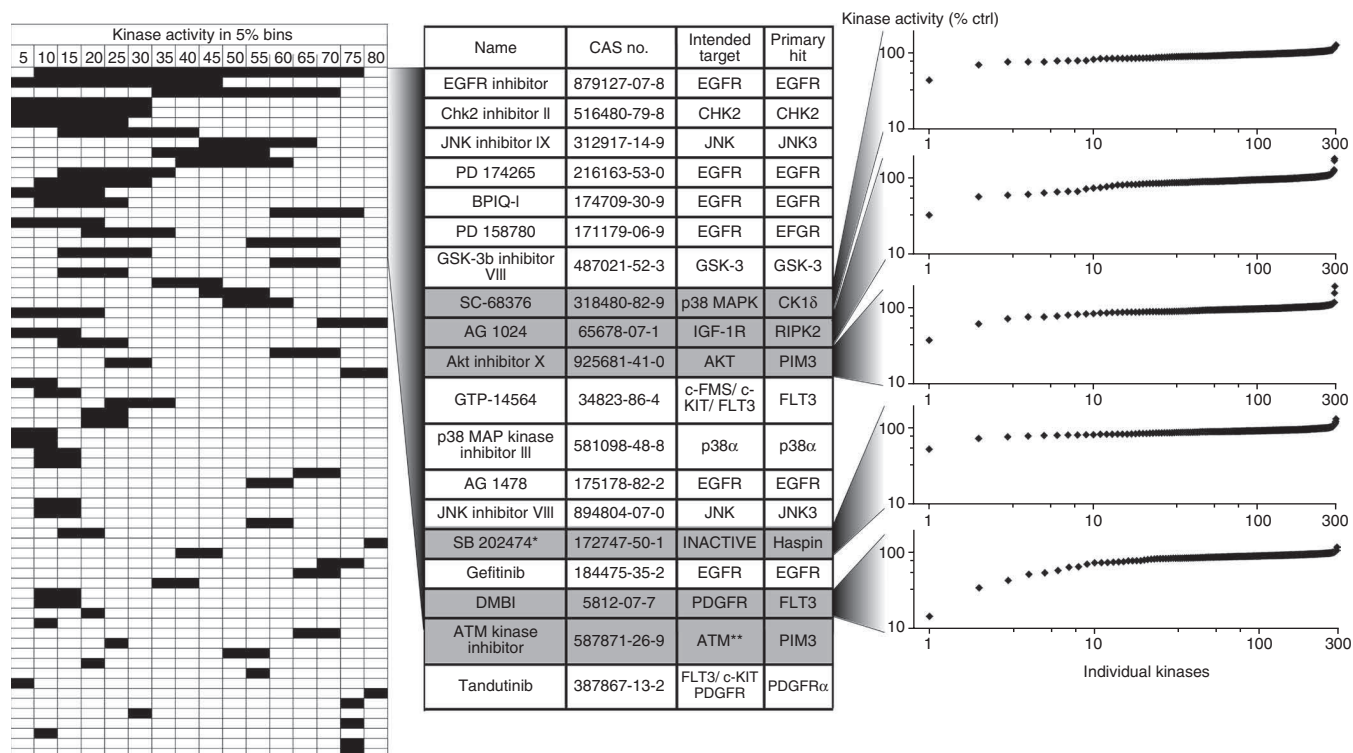


**Figure 5** Uni-specific kinase inhibitors. The left panel presents a graphical table of compounds ranked based on the compound's ability to inhibit a single kinase more potently than any other kinase tested. The left boundary of each horizontal bar depicts the potency with which the compound inhibits its most sensitive target and the right boundary reflects the potency with which the next most sensitive kinase is inhibited (% remaining kinase activity is shown in bins of 5%). Thus, the horizontal length of each bar reflects the differential activity of the corresponding inhibitor against its two most potently inhibited targets. Only compounds with a differential potency of at least 5% are shown. The central table identifies the compounds that showed at least 20% differential potency, their intended targets, and their most sensitive targets. Six compounds for which the most sensitive target is not the intended target are shown in gray. In the right panel, the effect of the individual compounds on each kinase in the panel is shown in a ranked plot. \*, SB 202474 is a negative control compound for the p38 MAP kinase inhibitor SB 202190. \*\*, ATM kinase was not included in our test panel. Ctrl, control.

more than one kinase with similar potency, even if those kinases are closely related isoforms from the same subfamily. In addition, it has a bias for kinase targets without close homologs in the screening panel. A uni-specificity score was calculated for each compound by subtracting the remaining kinase activity of the most potently inhibited kinase from the activity of the next most potently inhibited kinase. Compounds were then ranked from most uni-specific (highest numerical score) to least. We plotted the results as a horizontal bar graph in which the leftmost edge of the bar denotes the remaining kinase activity for the most potently inhibited kinase and the rightmost edge indicates the remaining kinase activity of the second most potently inhibited target (Fig. 5, leftmost panel). The length of each bar, therefore, denotes the differential potency of inhibition of these two most sensitive kinase targets, and the left-right positioning of this bar indicates the absolute potency against these targets.

Few compounds in the panel showed any degree of uni-specificity and most of these showed only slight potency differences between their primary and secondary targets (short bars in Fig. 5, leftmost panel). This finding highlights the challenge of achieving differential inhibition of closely related kinases. Nineteen compounds inhibited their primary target at least 20% more potently than any other kinase in the panel (Fig. 5, middle). Among these 19 most uni-specific kinases are several inhibitors intended to target the epidermal growth factor receptor (EGFR). In fact, the most uni-specific inhibitor, a 4,6-dianilino-pyrimidine EGFR inhibitor (CAS no. 879127-07-8) with a reported  $IC_{50}$  of 21 nM for EGFR<sup>22</sup>, inhibited EGFR catalytic

activity by >94% but inhibited its next most potently inhibited target, MRCKα, by only 22%. In contrast to other EGFR inhibitors tested, this compound also highlights the ability to achieve isoform-selective inhibition among the closely related ErbB family kinases<sup>22</sup>. The dramatic selectivity of this and other uni-specific EGFR inhibitors identified here could reflect unique features of EGFR or, more likely, the unequal attention devoted to the development of inhibitors of this important therapeutic target.

Strikingly, 6 of the top 17 uni-specific compounds inhibited other kinases more potently than the kinases they were intended to target (Fig. 5, center, gray rows). The rightmost panel of Figure 5 shows the activity of 5 of these 6 compounds against all kinases in the panel as a sorted plot. The ATM kinase inhibitor was not included because ATM was not a part of the screening panel. In all cases these more potent off-target hits represent hitherto unknown kinase targets of these compounds. Remarkably, in all but one case, that of the compound DMBI, the most potent off-target hit falls outside of the kinase subfamily of the intended target. For example, we identified the serine/threonine kinase RIPK2 as a much more sensitive target of the IGF1R tyrosine kinase inhibitor AG1024, one of the most uni-specific compounds identified.

To validate the use of our single-dose screening data to rank the sensitivity of different kinases to the same compound, we determined the dose-response relationship for five uni-specific compounds against both their intended and novel targets. In all cases the greater potency against the novel targets were confirmed (Supplementary Fig. 5).

These findings confirm the accuracy of our single-dose data and reveal potentially inhibited new targets for these compounds. For example, the results revealed the weak platelet-derived growth factor receptor inhibitor, DMBI to be a highly potent inhibitor of FLT3 and TrkC. Additionally, SB202474, an inactive analog of the p38 MAP kinase inhibitor SB202190 (ref. 23), showed significant inhibition of only one kinase, the haploid germ cell-specific nuclear protein kinase Haspin (Fig. 5). This atypical family kinase phosphorylates histone H3 and contributes to chromosomal organization and has been suggested as an anti-cancer target, though few inhibitors have been reported<sup>24–26</sup>. Thus, the uni-specific compounds described here provide new and selective inhibitors for their novel targets and in some cases, starting points for multitargeted kinase inhibition.

## DISCUSSION

Previous kinase inhibitor profiling studies have revealed an unexpected number of interactions with off-target kinases, even for highly characterized kinase inhibitors<sup>1,2</sup>. These findings have emphasized the importance of broad kinase profiling of these compounds and are supported by our data. Quantitative assessment of inhibitor selectivity is increasingly important as ever-larger kinase profiling data sets are reported. Although strong kinase selectivity may not be essential for efficacy of therapeutic agents<sup>27</sup>, it is critical for tool compounds used to elucidate kinase biology. We therefore applied the Gini coefficient as a measure of kinase inhibitor selectivity<sup>15</sup>, thus avoiding the necessity for arbitrary hit thresholds used by previous methods<sup>2</sup>. Comparison of Gini scores across multiple inhibitors targeting a specific kinase of interest should provide a powerful basis for choosing the most selective inhibitor for investigating kinase function. For example, the compound collection contains four well-established inhibitors of the AGC subfamily kinase ROCK (Rho-associated kinase): Rockout, glycy-H-1152 (Rho Kinase Inhibitor IV), Y-27632 and the clinical agent fasudil (HA-1077)<sup>28,29</sup>. Gini score analysis revealed greatest selectivity for glycy-H-1152 (0.738) and, indeed, this compound inhibited both ROCK I and II significantly more potently than any other kinase (data not shown). By contrast, fasudil showed more potent inhibition of PRKX and KHS than ROCK. Strikingly, hierarchical clustering based on target spectrum clustered Rockout, Rho Kinase Inhibitor IV and Y-27632 together (Supplementary Fig. 2), despite no clear structural similarity in the compounds. In fact, the secondary targets shared by these compounds are almost all other members of the AGC kinase subfamily, demonstrating that a variety of distinct chemotypes can be employed to selectively inhibit AGC kinases, perhaps due to greater sequence divergence of this subfamily from other subfamilies. These findings illustrate the utility of the present data set in guiding both tool compound selection and the development of new inhibitors selective for particular kinase subfamilies.

We also introduce the concept of uni-specificity as a way of quantitatively assessing the differential activity of an inhibitor toward its most sensitive and its next most sensitive kinase targets. Compounds exhibiting the greatest degree of uni-specificity are expected to provide the widest dosing window within which only a single kinase target is inhibited. We used this metric to prioritize the characterization of new inhibitor targets. Six uni-specific compounds were found that inhibit other kinases more potently than their intended targets. In all cases, these compounds represent previously unknown targets for these compounds.

Although the high-throughput assay used here to systematically measure kinase activity is economical, rapid and robust, caution is warranted if attempting to extrapolate these *in vitro* results to the prediction of cellular efficacy. First, our screen was carried out in the

presence of 10  $\mu\text{M}$  ATP regardless of the affinity of individual kinases for ATP. Potency of ATP-competitive kinase inhibitors in the cellular context is dictated not only by the intrinsic affinity of the inhibitor for the kinase, but also by the Michaelis-Menten constant for ATP binding and the cellular concentration of ATP<sup>30</sup>. Thus, the relative rank order of inhibited kinases determined here may differ in the cellular context. Second, many kinases in the panel are represented by truncated constructs whose interactions with a compound could differ in the context of the full-length kinase or in the cellular milieu. In addition, many kinases can adopt multiple conformational states and only one such state was assayed for each kinase. Third, though the kinase panel tested here is among the largest available for biochemical measurements of kinase catalytic activity, a minority of kinases are not included in the panel. Thus, additional off-target activities against untested kinases can be reasonably expected. Nevertheless, the data presented here provide a rich resource of information concerning kinase-inhibitor interactions, and biochemical analysis of kinase-inhibitor interactions generally correlates with cellular efficacy<sup>30</sup>.

Protein kinase research has been predominantly focused on a small subset of the kinome<sup>31</sup>. The identification of selective inhibitors targeting poorly understood kinases would greatly facilitate elucidation of their function. Our identification of a uni-specific inhibitor of Haspin provides one example of how large-scale kinase profiling can identify new tool compounds to stimulate new research. Crystallographic studies may also benefit from the present study. Protein kinases exhibit considerable conformational plasticity, which can make it difficult to obtain diffracting crystals of unliganded kinases<sup>32</sup>. ATP-competitive kinase inhibitors can be used to stabilize kinases for crystallographic structure determination<sup>3</sup>. The data set presented here provides a library of candidates, on average nine per kinase, to support such studies. In addition, we illustrate how the present data set can be mined to reveal new opportunities for multitargeted kinase inhibition (Fig. 4b). Indeed, new statistical methods have been recently developed<sup>13</sup> to facilitate analysis of potential drug polypharmacology using robust kinase-inhibitor interaction maps such as this. Finally, we expect that the inhibitor collection characterized here, with activity against the majority of human protein kinases, will be a powerful tool to elucidate kinase functions in cell models.

## METHODS

Methods and any associated references are available in the online version of the paper at <http://www.nature.com/naturebiotechnology/>.

*Note: Supplementary information is available on the Nature Biotechnology website.*

## ACKNOWLEDGMENTS

We gratefully acknowledge B. Turk, A. Andrews and members of the Peterson laboratory for comments on the manuscript and R. Hartman of Reaction Biology Corp. for developing the Kinase Inhibitor Resource (KIR) web application tool. This work was supported by a W.W. Smith Foundation Award, funding from the Keystone Program in Head and Neck Cancer of Fox Chase Cancer Center and by US National Institutes of Health awards RO1 GM083025 to J.R.P. and P30 CA006927 to Fox Chase Cancer Center. HotSpot technology development was partially supported by the US National Institutes of Health (RO1 HG003818 and R44 CA114995 to H.M.).

## AUTHOR CONTRIBUTIONS

The study was conceived by J.R.P., S.W.D. and H.M., experimental data was collected by S.W.D., statistical analysis was performed by K.D., data were analyzed by T.A. and J.R.P. with input from S.W.D. and H.M., and the manuscript was written by J.R.P. with input from the other authors.

## COMPETING FINANCIAL INTERESTS

The authors declare competing financial interests: details accompany the full-text HTML version of the paper at <http://www.nature.com/nbt/index.html>.

Published online at <http://www.nature.com/nbt/index.html>.

Reprints and permissions information is available online at <http://www.nature.com/reprints/index.html>.

- Fabian, M.A. *et al.* A small molecule-kinase interaction map for clinical kinase inhibitors. *Nat. Biotechnol.* **23**, 329–336 (2005).
- Karaman, M.W. *et al.* A quantitative analysis of kinase inhibitor selectivity. *Nat. Biotechnol.* **26**, 127–132 (2008).
- Fedorov, O. *et al.* A systematic interaction map of validated kinase inhibitors with Ser/Thr kinases. *Proc. Natl. Acad. Sci. USA* **104**, 20523–20528 (2007).
- Bain, J. *et al.* The selectivity of protein kinase inhibitors: a further update. *Biochem. J.* **408**, 297–315 (2007).
- Davies, S.P., Reddy, H., Caivano, M. & Cohen, P. Specificity and mechanism of action of some commonly used protein kinase inhibitors. *Biochem. J.* **351**, 95–105 (2000).
- Bain, J., McLauchlan, H., Elliott, M. & Cohen, P. The specificities of protein kinase inhibitors: an update. *Biochem. J.* **371**, 199–204 (2003).
- Ma, H., Deacon, S. & Horiuchi, K. The challenge of selecting protein kinase assays for lead discovery optimization. *Expert Opin. Drug Discov.* **3**, 607–621 (2008).
- Smyth, L.A. & Collins, I. Measuring and interpreting the selectivity of protein kinase inhibitors. *J. Chem. Biol.* **2**, 131–151 (2009).
- Goldstein, D.M., Gray, N.S. & Zarrinkar, P.P. High-throughput kinase profiling as a platform for drug discovery. *Nat. Rev. Drug Discov.* **7**, 391–397 (2008).
- Miduturu, C.V. *et al.* High-throughput kinase profiling: a more efficient approach toward the discovery of new kinase inhibitors. *Chem. Biol.* **18**, 868–879 (2011).
- Daub, H., Specht, K. & Ullrich, A. Strategies to overcome resistance to targeted protein kinase inhibitors. *Nat. Rev. Drug Discov.* **3**, 1001–1010 (2004).
- Morphy, R., Kay, C. & Rankovic, Z. From magic bullets to designed multiple ligands. *Drug Discov. Today* **9**, 641–651 (2004).
- Metz, J.T. *et al.* Navigating the kinome. *Nat. Chem. Biol.* **7**, 200–202 (2011).
- Dodson, C.A. *et al.* Crystal structure of an Aurora-A mutant that mimics Aurora-B bound to MLN8054: insights into selectivity and drug design. *Biochem. J.* **427**, 19–28 (2010).
- Graczyk, P.P. Gini coefficient: a new way to express selectivity of kinase inhibitors against a family of kinases. *J. Med. Chem.* **50**, 5773–5779 (2007).
- Bamborough, P., Drewry, D., Harper, G., Smith, G.K. & Schneider, K. Assessment of chemical coverage of kinome space and its implications for kinase drug discovery. *J. Med. Chem.* **51**, 7898–7914 (2008).
- Favre, S., Djelloul, S. & Raymond, E. New paradigms in anticancer therapy: targeting multiple signaling pathways with kinase inhibitors. *Semin. Oncol.* **33**, 407–420 (2006).
- Morphy, R. Selectively nonselective kinase inhibition: striking the right balance. *J. Med. Chem.* **53**, 1413–1437 (2010).
- Knight, Z.A., Lin, H. & Shokat, K.M. Targeting the cancer kinome through polypharmacology. *Nat. Rev. Cancer* **10**, 130–137 (2010).
- Cockerill, S. *et al.* Indazolylamino quinazolines and pyridopyrimidines as inhibitors of the EGFR and c-erbB-2. *Bioorg. Med. Chem. Lett.* **11**, 1401–1405 (2001).
- Lapenna, S. & Giordano, A. Cell cycle kinases as therapeutic targets for cancer. *Nat. Rev. Drug Discov.* **8**, 547–566 (2009).
- Zhang, Q. *et al.* Discovery of EGFR selective 4,6-disubstituted pyrimidines from a combinatorial kinase-directed heterocycle library. *J. Am. Chem. Soc.* **128**, 2182–2183 (2006).
- Lee, J.C. *et al.* A protein kinase involved in the regulation of inflammatory cytokine biosynthesis. *Nature* **372**, 739–746 (1994).
- Cuny, G.D. *et al.* Structure-activity relationship study of acridine analogs as haspin and DYRK2 kinase inhibitors. *Bioorg. Med. Chem. Lett.* **20**, 3491–3494 (2010).
- Huertas, D. *et al.* Antitumor activity of a small-molecule inhibitor of the histone kinase Haspin. *Oncogene* published online, doi:10.1038/onc.2011.335 (1 August 2011).
- Patnaik, D. *et al.* Identification of small molecule inhibitors of the mitotic kinase haspin by high-throughput screening using a homogeneous time-resolved fluorescence resonance energy transfer assay. *J. Biomol. Screen.* **13**, 1025–1034 (2008).
- Mencher, S.K. & Wang, L.G. Promiscuous drugs compared to selective drugs (promiscuity can be a virtue). *BMC Clin. Pharmacol.* **5**, 3 (2005).
- Liao, J.K., Seto, M. & Noma, K. Rho kinase (ROCK) inhibitors. *J. Cardiovasc. Pharmacol.* **50**, 17–24 (2007).
- Yarrow, J.C., Totsukawa, G., Charras, G.T. & Mitchison, T.J. Screening for cell migration inhibitors via automated microscopy reveals a Rho-kinase inhibitor. *Chem. Biol.* **12**, 385–395 (2005).
- Knight, Z.A. & Shokat, K.M. Features of selective kinase inhibitors. *Chem. Biol.* **12**, 621–637 (2005).
- Fedorov, O., Muller, S. & Knapp, S. The (un)targeted cancer kinome. *Nat. Chem. Biol.* **6**, 166–169 (2010).
- Huse, M. & Kuriyan, J. The conformational plasticity of protein kinases. *Cell* **109**, 275–282 (2002).
- Manning, G., Whyte, D.B., Martinez, R., Hunter, T. & Sudarsanam, S. The protein kinase complement of the human genome. *Science* **298**, 1912–1934 (2002).

## ONLINE METHODS

**Materials.** Kinase inhibitors (**Supplementary Table 1**) were obtained either from EMD Biosciences or LC Laboratories with an average purity of >98%. A complete description of recombinant kinases used is provided in **Supplementary Table 2**.

**Kinase assays.** *In vitro* profiling of the 300 member kinase panel was performed at Reaction Biology Corporation using the “HotSpot” assay platform. Briefly, specific kinase/substrate pairs along with required cofactors were prepared in reaction buffer; 20 mM Hepes pH 7.5, 10 mM MgCl<sub>2</sub>, 1 mM EGTA, 0.02% Brij35, 0.02 mg/ml BSA, 0.1 mM Na<sub>3</sub>VO<sub>4</sub>, 2 mM DTT, 1% DMSO (for specific details of individual kinase reaction components see **Supplementary Table 2**). Compounds were delivered into the reaction, followed ~20 min later by addition of a mixture of ATP (Sigma) and <sup>33</sup>P ATP (PerkinElmer) to a final concentration of 10 μM. Reactions were carried out at 25 °C for 120 min, followed by spotting of the reactions onto P81 ion exchange filter paper (Whatman). Unbound phosphate was removed by extensive washing of filters in 0.75% phosphoric acid. After subtraction of background derived from control reactions containing inactive enzyme, kinase activity data were expressed as the percent remaining kinase activity in test samples compared to vehicle (dimethyl sulfoxide) reactions. IC<sub>50</sub> values and curve fits were obtained using Prism (GraphPad Software). Kinome tree representations were prepared using Kinome Mapper (<http://www.reactionbiology.com/apps/kinome/mapper/LaunchKinome.htm>).

**Statistical methods. Outlier detection.** Raw data were measured as percentage of compound activity for each kinase-inhibitor pair in duplicate. All negative values were truncated to zero and kinase-inhibitor pairs with either missing observations or identical values across duplicates were removed from further analysis and the coefficient of variation (CV) and the difference (D) from duplicate observations were computed for each kinase-inhibitor pair. Using kernel density estimation and quantile-quantile plots, the difference D was determined to be double exponentially distributed (**Supplementary Fig. 1a,b**). Its location and scale parameters (and hence the mean and s.d.) were estimated using maximum likelihood methods<sup>34</sup>. A scatter plot of CV versus D is displayed in **Supplementary Figure 1e** for all pairs of data points. To account for the inherent noise in the assay measurements, we retained observations within 1 s.d. of the mean of the distribution of differences D (as determined by the gray vertical lines in the double exponential density plot for D, **Supplementary Fig. 1a**) for further analyses of compound activity. The region enclosed by these vertical lines contains 75.6% of the observations based on the estimated mean and s.d. of this distribution. The red vertical lines in

**Supplementary Figure 1e** also represent these limits whereas the green and black circles within this region represent these observations. These observations were excluded from the current set of data and the CV recomputed for the remaining kinase-inhibitor pairs.

The distribution-based outlier detection method outlined by van der Loo<sup>35</sup> was then applied to the CV based on this reduced set of data points. First, the distribution of CV was determined and its parameters estimated using methods described earlier for D<sup>34</sup>. The log-normal distribution provided the best fit for these data (**Supplementary Fig. 1c,d**). For outlier detection, the data (excluding the top and bottom 1%) were fit to the quantile-quantile plot positions for the log-normal distribution and its parameters were robustly estimated. A test was then performed to determine whether extreme observations are outliers by computing the threshold beyond which a certain prespecified number of observations are expected. The pink horizontal line in **Supplementary Figure 1e** represents this threshold and corresponds to a CV cut-off of ~0.5. Based on this twofold approach, the remainder of the observations that were located above the CV cut-off of 0.5 and outside this band, represented by blue circles, were identified as outlying observations and excluded from further analysis. The outliers (black data points) are shown within the context of the complete data set in **Supplementary Figure 1f**.

**Hierarchical clustering.** Negative values for remaining kinase activity were truncated to zero and values >100 were truncated at that value. A reordered heat map of compound activity was obtained using two-way hierarchical clustering based on 1 – Spearman rank correlation as the distance metric and average linkage. No scaling was applied to the data.

Computations were carried out in the R statistical language and environment using libraries VGAM and extremevalues.

**Kinase activity analysis.** The theoretical kinase activity curve in **Figure 2a** was calculated according to the equation: activity = (100 – (100/(1 + (IC<sub>50</sub>/0.5 μM))) and the Cheng-Prusoff equation<sup>36</sup> relating K<sub>i</sub> and IC<sub>50</sub>. This calculation assumes a Hill coefficient of 1 for the binding and a K<sub>m,ATP</sub> of 10 μM for all kinases.

34. Yee, T.W. & Hastie, T.J. Reduced-rank vector generalized linear models. *Stat. Modelling* **3**, 15–41 (2003).

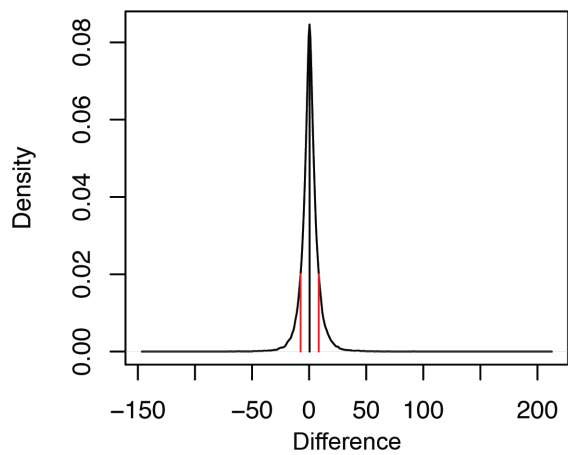
35. van der Loo, M.P.J. Distribution-based outlier detection for univariate data. Discussion paper 10003 (Statistics Netherlands, The Hague, 2010).

36. Cheng, Y. & Prusoff, W.H. Relationship between the inhibition constant (K<sub>i</sub>) and the concentration of inhibitor which causes 50 per cent inhibition (I<sub>50</sub>) of an enzymatic reaction. *Biochem. Pharmacol.* **22**, 3099–3108 (1973).

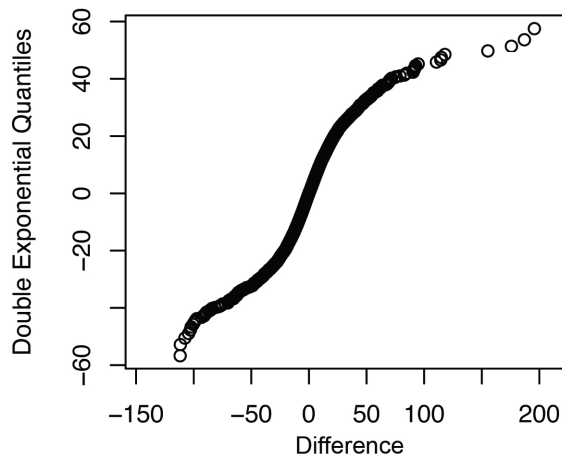
## **SUPPLEMENTARY DATA**

**Supplementary Figure 1.** Identification and elimination of statistical outliers. **(a)** Kernel density plot of difference (D) from duplicate observations for each kinase-inhibitor pair. The estimated double exponential density (y-axis) is plotted against D (x-axis). The grey vertical lines represent one standard deviation on either side of the mean of the distribution of D. **(b)** Quantile-quantile plot of D from duplicate observations for each kinase-inhibitor pair. Quantiles of the estimated double exponential distribution (y-axis) are plotted against D (x-axis). **(c)** Kernel density plot of the coefficient of variation (CV) from duplicate observations for each kinase-inhibitor pair. The estimated log-normal density (y-axis) is plotted against CV (x-axis). **(d)** Quantile-quantile plot of CV from duplicate observations for each kinase-inhibitor pair. Quantiles of the estimated log-normal distribution (y-axis) are plotted against CV (x-axis). **(e)** A scatter plot of CV versus D for all kinase-inhibitor pairs. The green and black circles that lie inside the band formed by the red vertical lines represent observations within one standard deviation of the mean of the estimated double exponential distribution of D. These observations were considered to be within acceptable noise levels in assay measurements and were retained for further analyses of compound activity. The pink horizontal line represents the CV threshold for outlier detection. The blue circles represent observations whose CV exceeded this threshold and were identified as outliers. **(f)** A scatter plot of the kinase activity in replicate 1 versus replicate 2 for all kinase-inhibitor pairs. Data points in black represent the identified outliers that were removed from the final data.

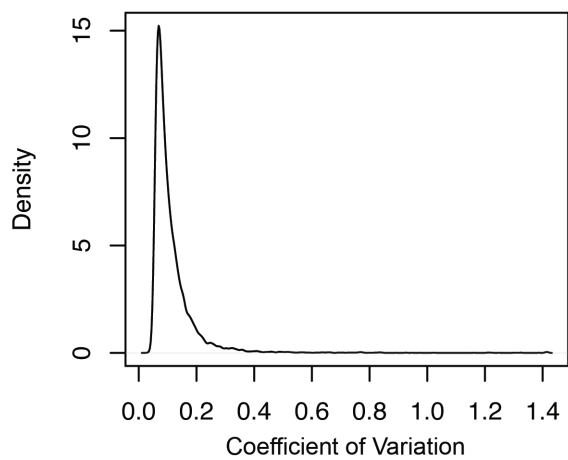
**a**



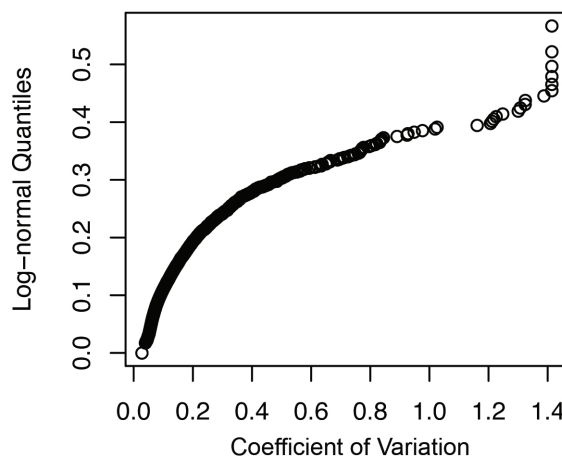
**b**



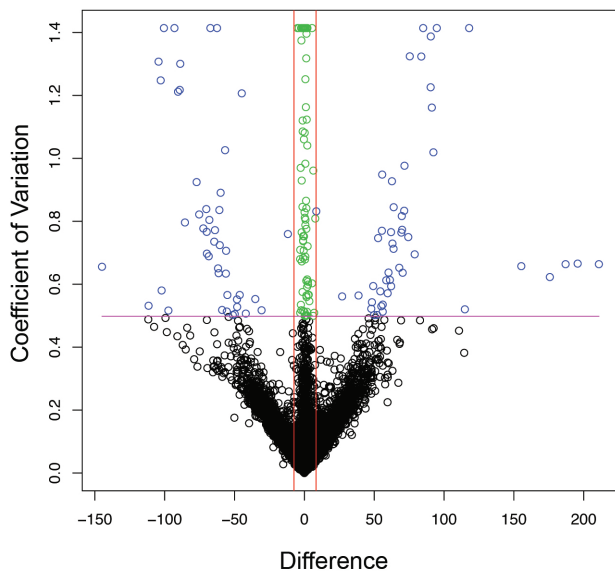
**c**



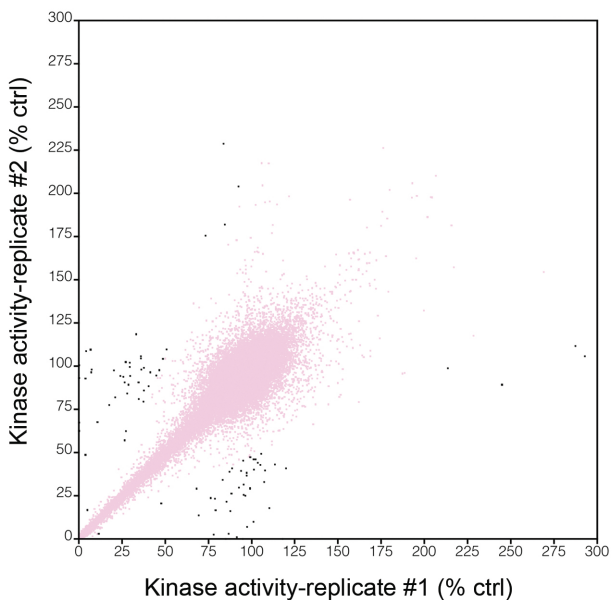
**d**



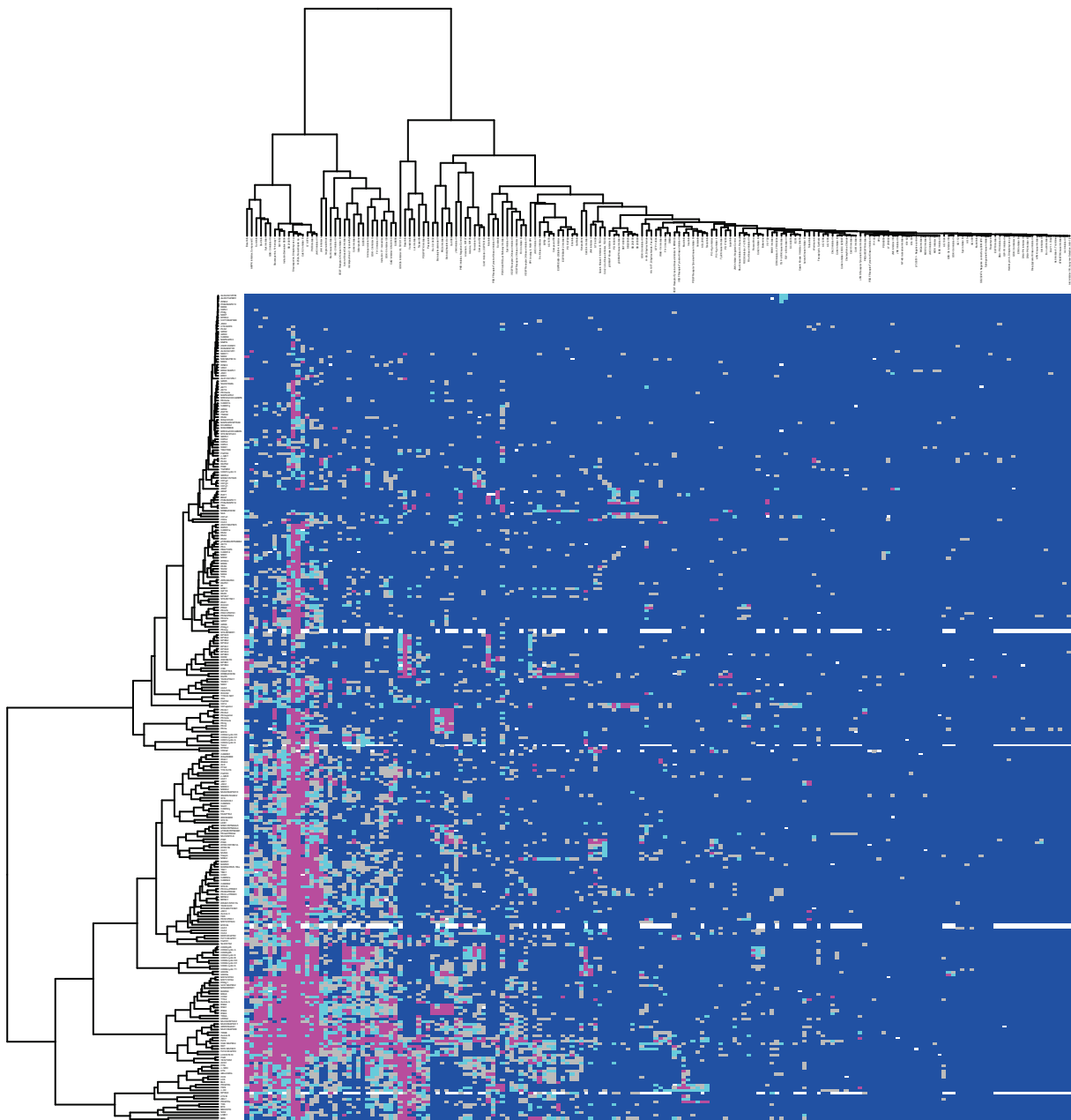
**e**



**f**



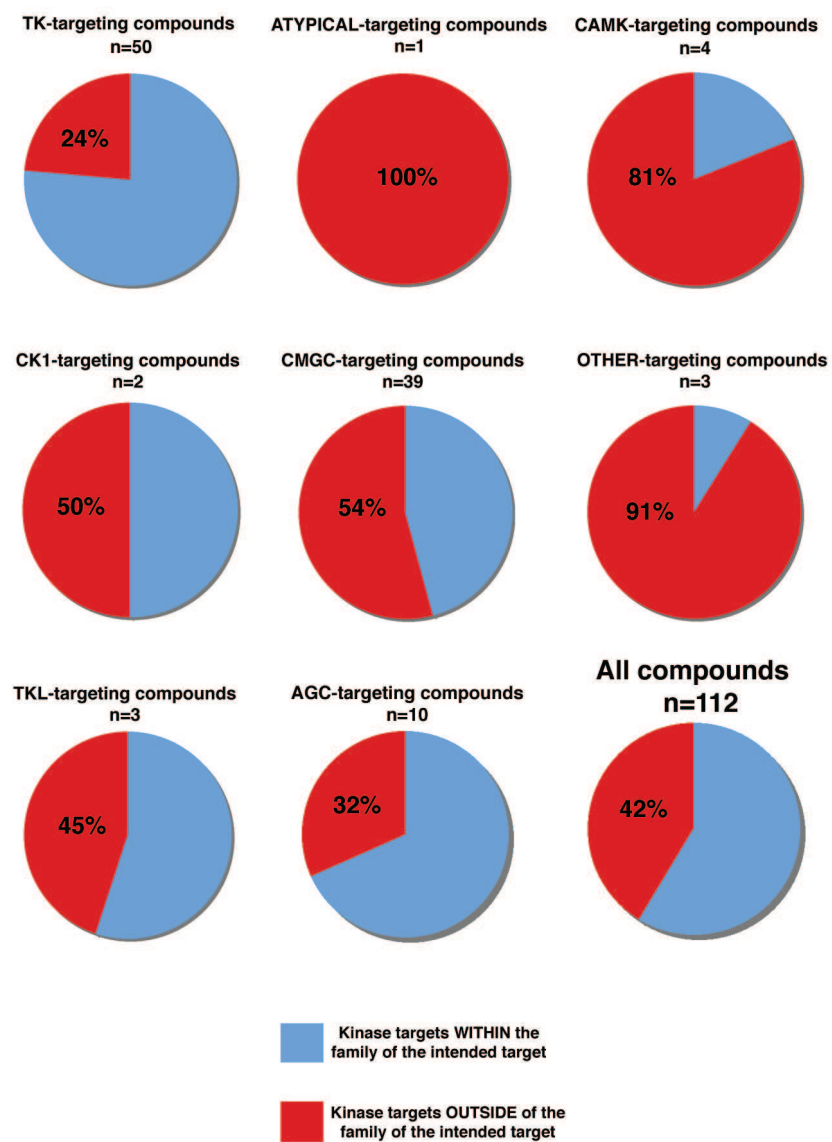
**Supplementary Figure 2.** A high-resolution version of **Figure 1d** showing two-way hierarchical clustering analysis of the entire kinase-inhibitor interaction network presented as a heatmap of inhibitory activity.



Nature Biotechnology: doi:10.1038/nbt.2017

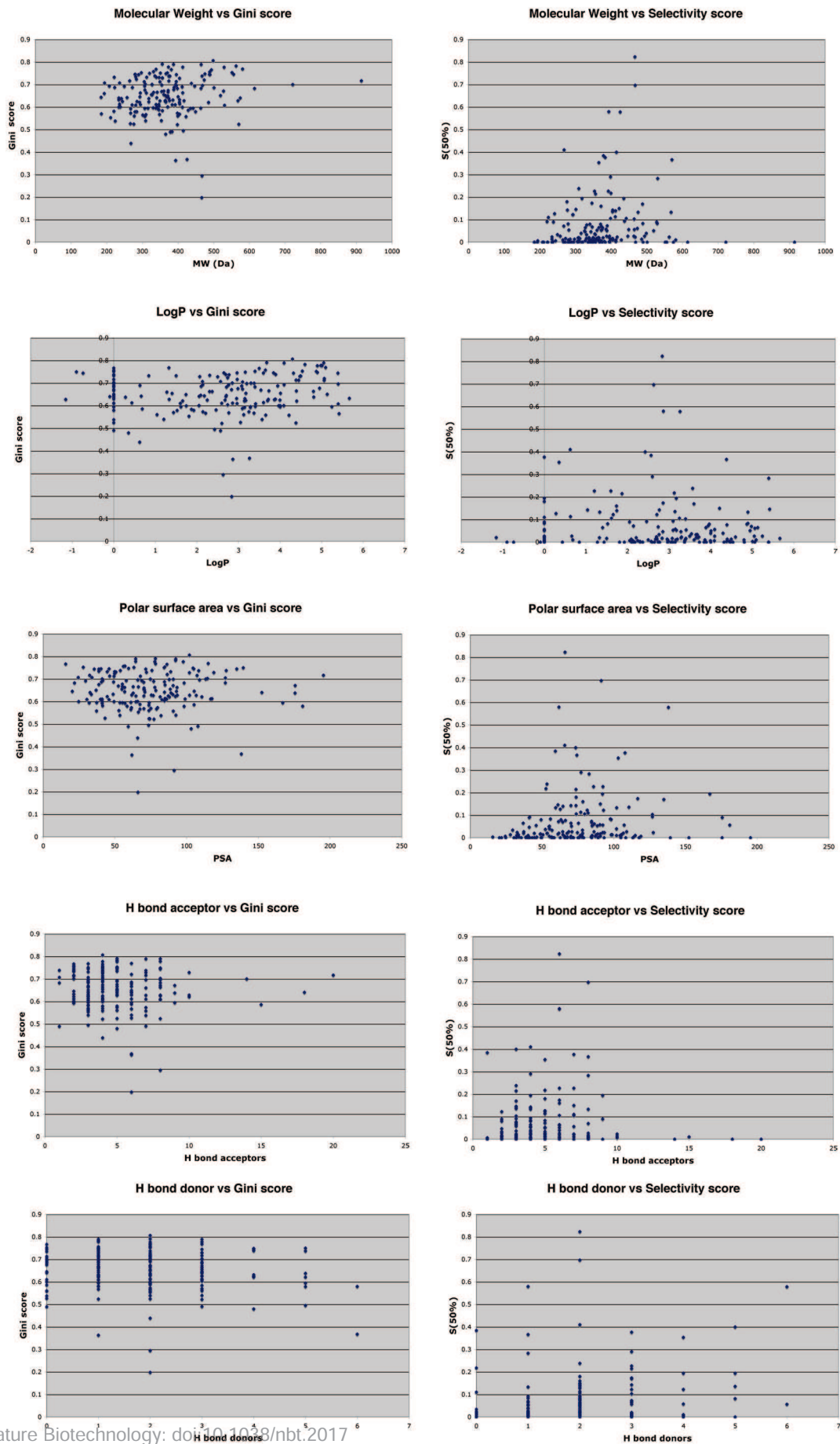
**Supplementary Figure 3.** Kinase inhibitors frequently inhibit kinases outside of the subfamily containing their intended targets. All compounds intended to target a kinase in the indicated specific subfamily of kinases were analyzed as to whether the kinases they inhibit fall within the subfamily of their intended target (blue) or outside of that family (red, percent of total shown). The final pie chart presents aggregate data for all of the subfamilies presented. “n” reports the number of compounds analyzed for each target subfamily. The following compound types were not included in this analysis: compounds intended to target lipid kinases, inactive control compounds, compounds intended to target kinases from multiple subfamilies, compounds that did not inhibit any kinases. For example, none of the four compounds intended to target STE subfamily kinases inhibited any kinases significantly.

### Supplementary Figure 3



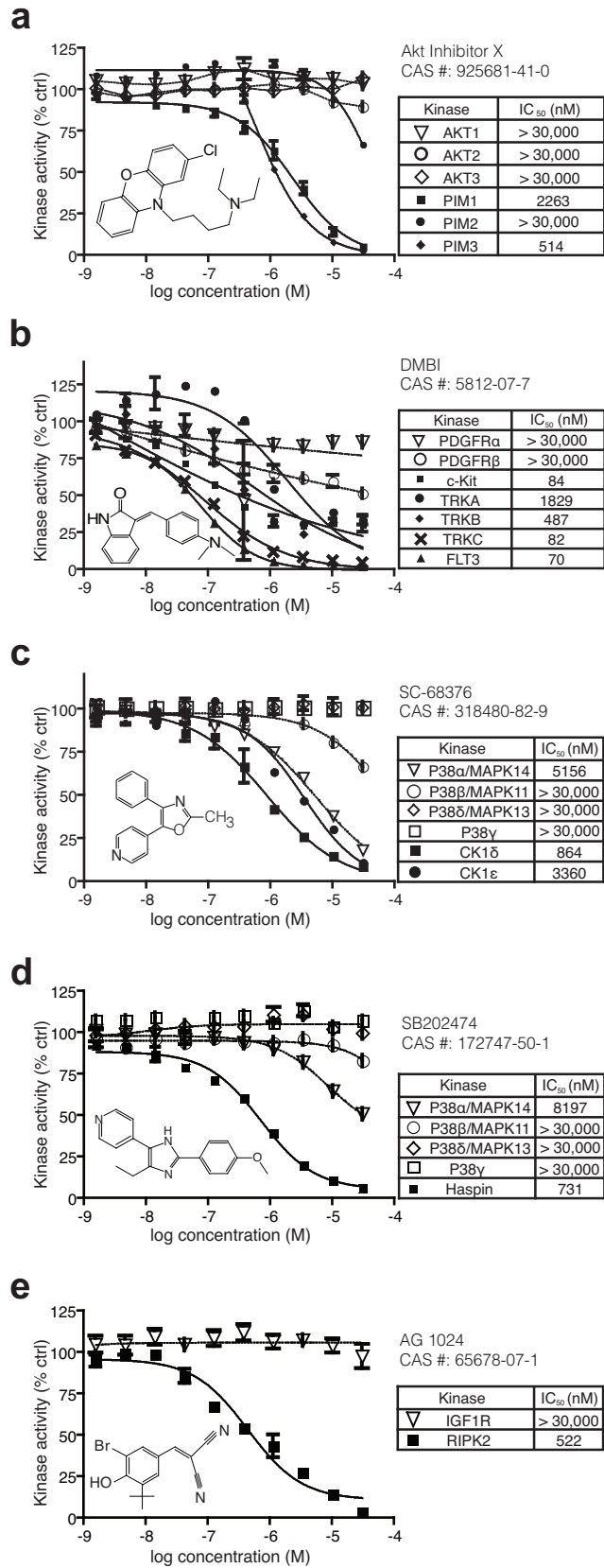
**Supplementary Figure 4.** No single physicochemical property correlates with inhibitor selectivity. All 178 test compounds were analyzed with regard to molecular weight, predicted LogP, polar surface area (PSA), number of hydrogen bond acceptors, and number of hydrogen bond donors. These features are plotted for each compound as a function of inhibitor selectivity from the screening data reported either as Gini score (from Supplementary Table 5) or as Selectivity score ( $S_{(50\%)}$ ). The Selectivity score of a compound corresponds to the number of kinases that it inhibited by at least 50% divided by the number of kinases against which the compound was tested. More selective inhibitors are associated with lower Selectivity scores and higher Gini scores.

# Supplementary Figure 4

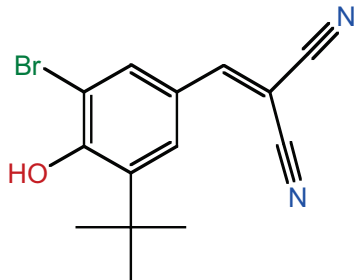
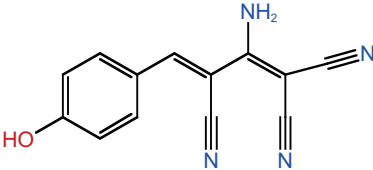
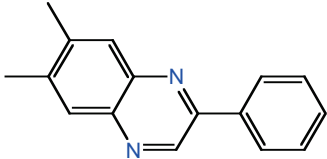
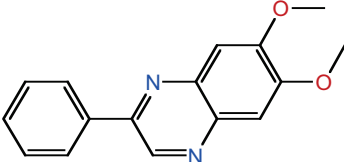
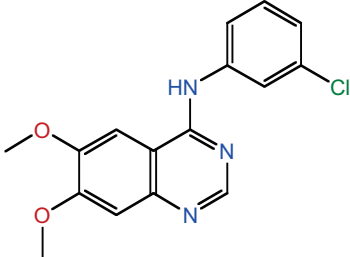
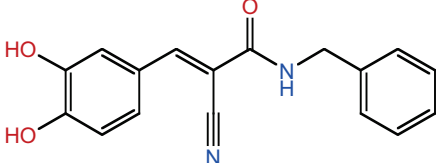


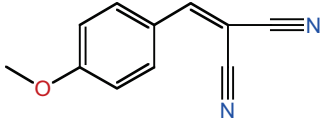
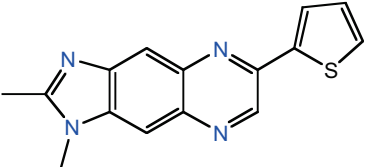
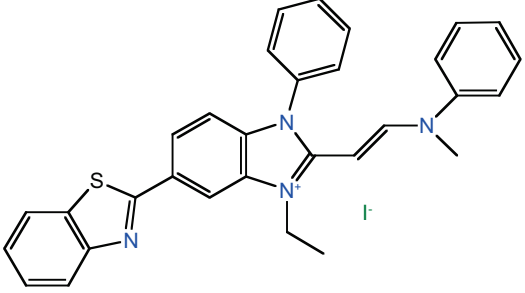
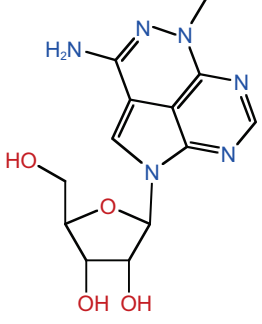
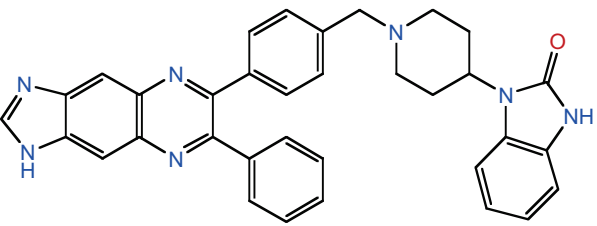
**Supplementary Figure 5.** Validation of novel uni-specific kinase inhibitors. Complete *in vitro* kinase assay dose-response results are shown for the five indicated uni-specific compounds (**a-e**) from **Figure 5** against both the intended targets of each inhibitor and their novel, more potently inhibited target(s). Data for intended kinase target(s) are shown with open symbols and novel target(s) with closed symbols. Data points represent averages of two independent replicates. Error bars denote standard error of the mean. Data exhibiting significant inhibition was fitted with a sigmoidal dose-response curve to derive IC<sub>50</sub> values.

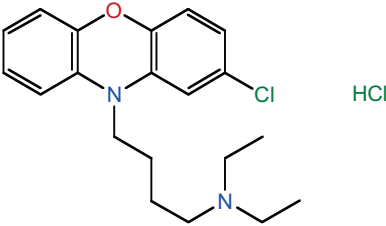
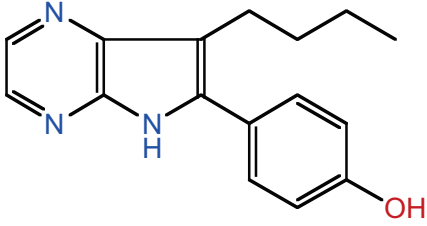
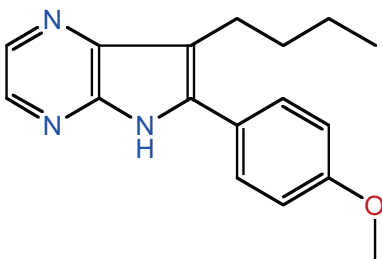
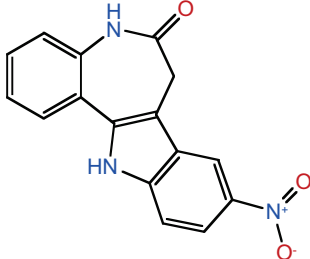
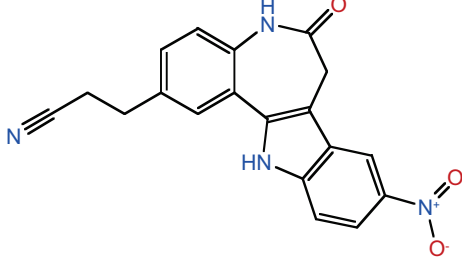
# Supplementary Figure 5

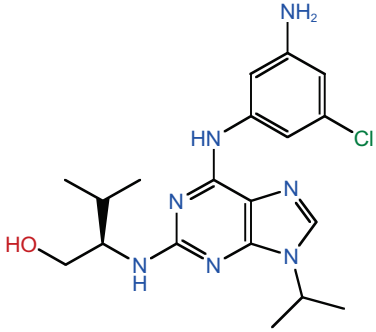
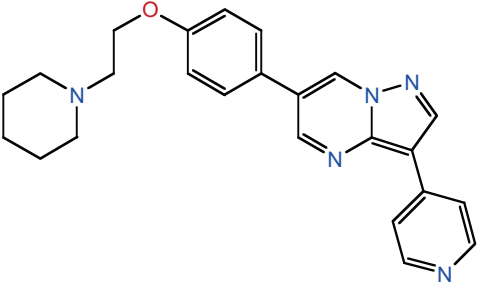
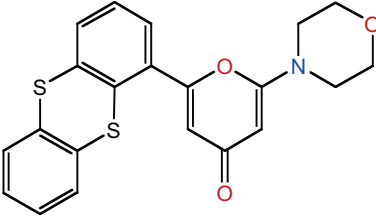
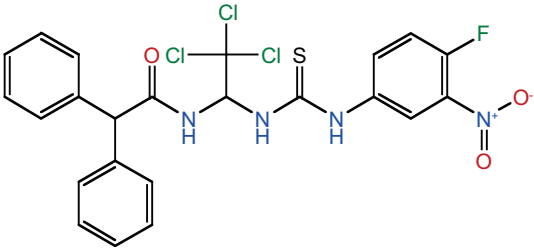
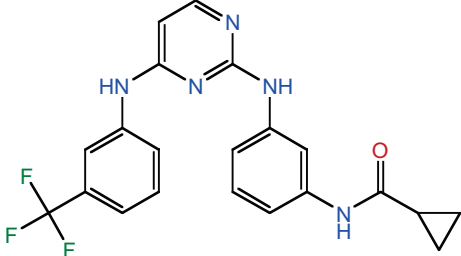


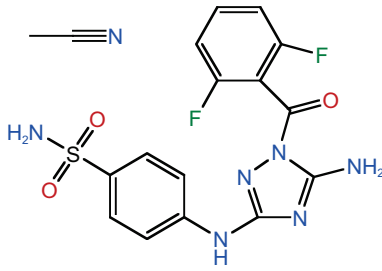
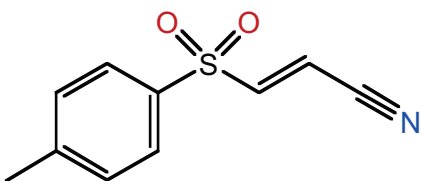
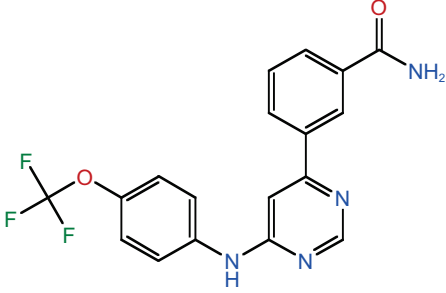
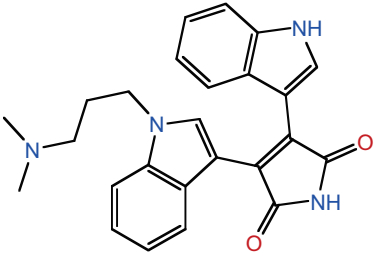
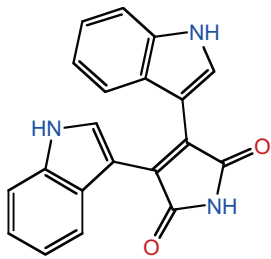
**Supplementary Table 1.** Compounds used in this study.

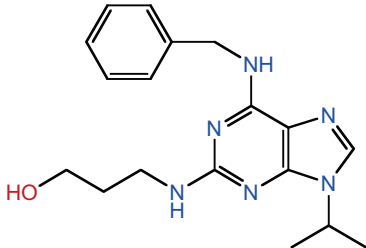
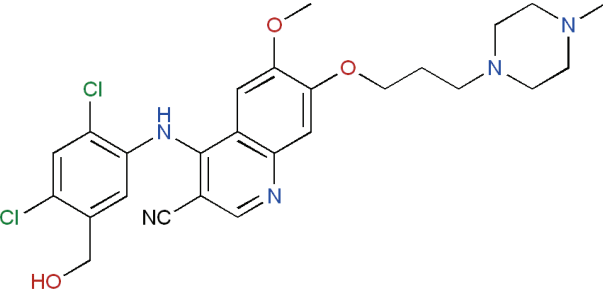
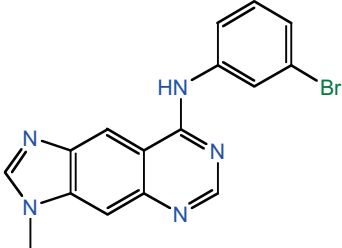
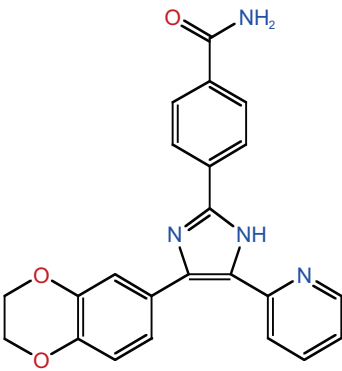
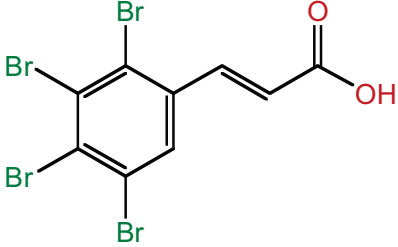
Name	CAS #	Structure	Target family
AG 1024	65678-07-1		TK
AG 112	144978-82-5		TK
AG 1295	71897-07-9		TK
AG 1296	146535-11-7		TK
AG 1478	175178-82-2		TK
AG 490	133550-30-8		TK

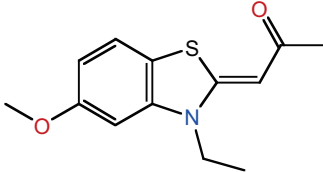
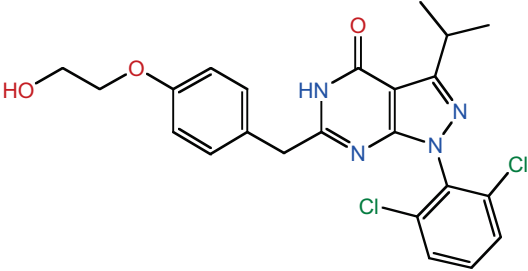
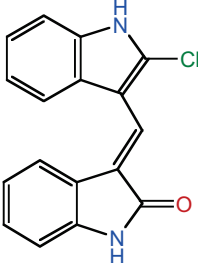
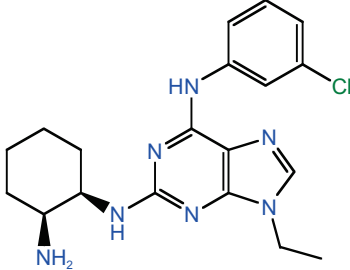
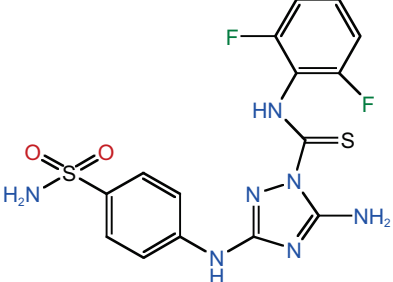
AG 9	2826-26-8		TK
AGL 2043	226717-28-8		TK
Akt Inhibitor IV	681281-88-9		AGC
Akt Inhibitor V, Triciribine	35943-35-2		AGC
Akt Inhibitor VIII, Isozyme-Selective, Akti-1/2	612847-09-3		AGC

Akt Inhibitor X	925681-41-0		AGC
Aloisine A, RP107	496864-16-5		CMGC
Aloisine, RP106	496864-15-4		CMGC
Alsterpaullone	237430-03-4		CMGC
Alsterpaullone, 2-Cyanoethyl	852527-97-0		CMGC

Aminopurvalanol A	220792-57-4		CMGC
AMPK Inhibitor, Compound C	866405-64-3		CAMK
ATM Kinase Inhibitor	587871-26-9		ATYPICAL
ATM/ATR Kinase Inhibitor	905973-89-9		ATYPICAL
Aurora Kinase Inhibitor III	879127-16-9		OTHER

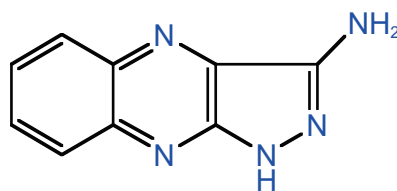
Aurora Kinase/ Cdk Inhibitor	443797-96-4	 <p>The structure features a central 1,2,4-triazole ring. One nitrogen is substituted with a 4-(aminosulfonyl)phenyl group. The other nitrogen is substituted with a 2-cyano-3-fluorophenyl group. The third nitrogen is part of a fused ring system, specifically a 2,3-dihydro-1,4-benzodiazepine derivative.</p>	OTHER, CMGC
BAY 11-7082	19542-67-7	 <p>The structure consists of a 4-methylphenyl ring connected to a sulfonyl group (-SO<sub>2</sub>-). This sulfonyl group is further connected to a trans-alkene, which is terminated by a nitrile group (-C≡N).</p>	OTHER
Bcr-abl Inhibitor	778270-11-4	 <p>The structure features a central pyrimidine ring. One nitrogen is substituted with a 4-(difluoromethoxy)phenyl group. The other nitrogen is substituted with a 4-aminophenyl group.</p>	TK
Bisindolylmaleimide I	133052-90-1	 <p>The structure is a bisindolylmaleimide derivative. It features a central maleimide ring system substituted with two indole rings. One indole ring is further substituted with a dimethylaminoethyl group.</p>	AGC
Bisindolylmaleimide IV	119139-23-0	 <p>The structure is a bisindolylmaleimide derivative, similar to the previous one, but with a different substitution pattern on the indole rings.</p>	AGC

Bohemine	189232-42-6		CMGC
Bosutinib	380843-75-4		TK
BPIQ-I	174709-30-9		TK
Casein Kinase I Inhibitor, D4476	301836-43-1		CK1, CMGC, TKL
Casein Kinase II Inhibitor III, TBCA	934358-00-6		CK1

Cdc2-Like Kinase Inhibitor, TG003	300801-52-9		CMGC
Cdk/Crk Inhibitor	784211-09-2		CMGC
Cdk1 Inhibitor	220749-41-7		CMGC
Cdk1 Inhibitor, CGP74514A	190654-01-4		CMGC
Cdk1/2 Inhibitor III	443798-55-8		CMGC

Cdk1/5 Inhibitor

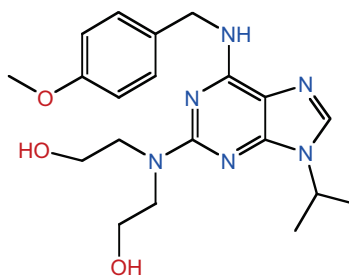
40254-90-8



CMGC

Cdk2 Inhibitor III

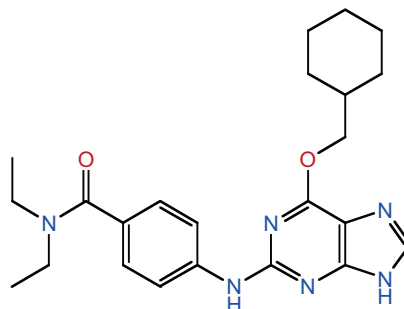
199986-75-9



CMGC

Cdk2 Inhibitor IV,  
NU6140

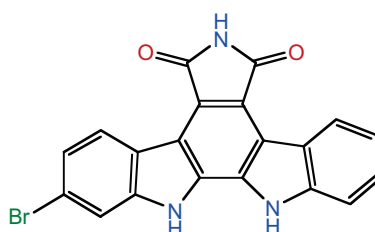
444723-13-1



CMGC

Cdk4 Inhibitor

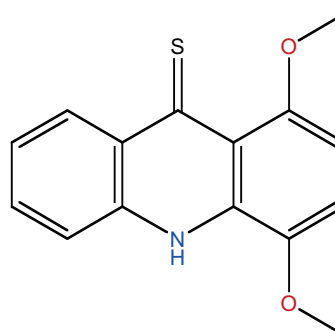
546102-60-7



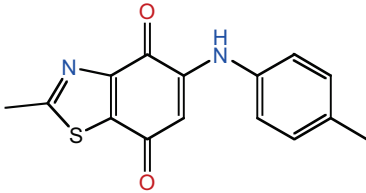
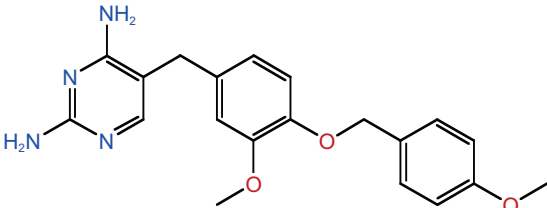
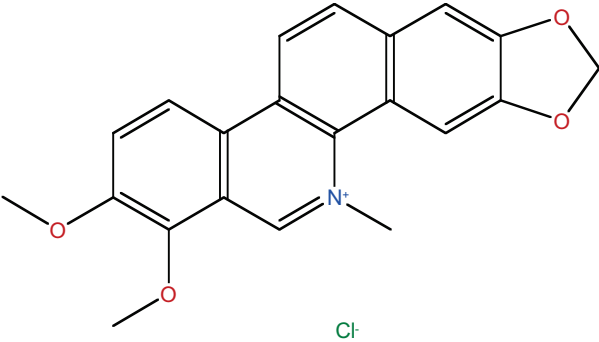
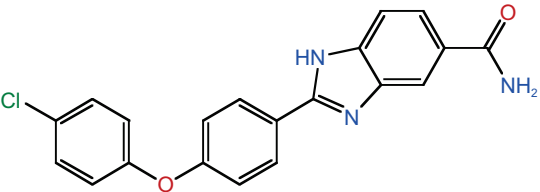
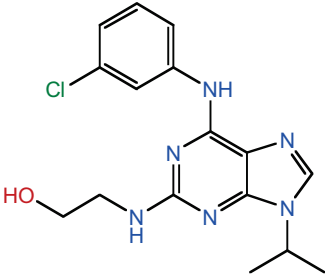
CMGC

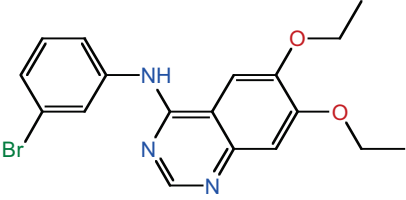
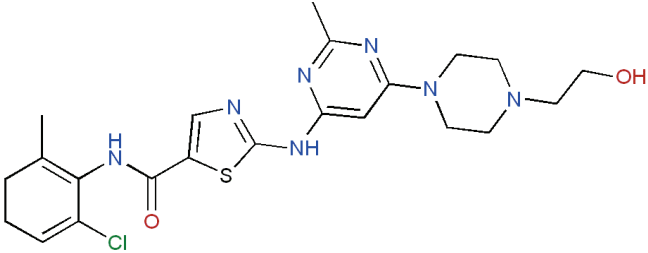
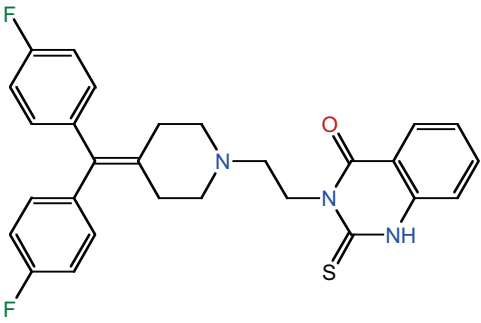
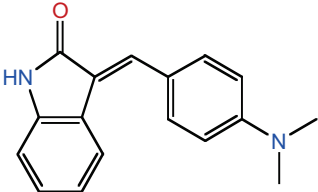
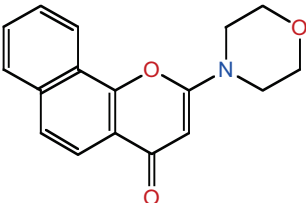
Cdk4 Inhibitor II,  
NSC 625987

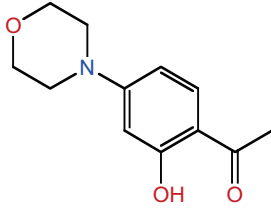
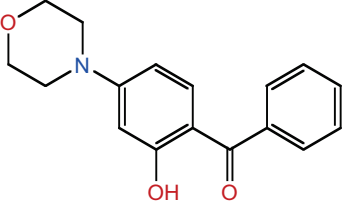
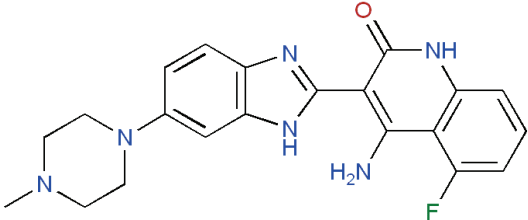
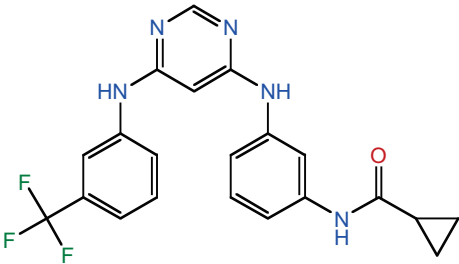
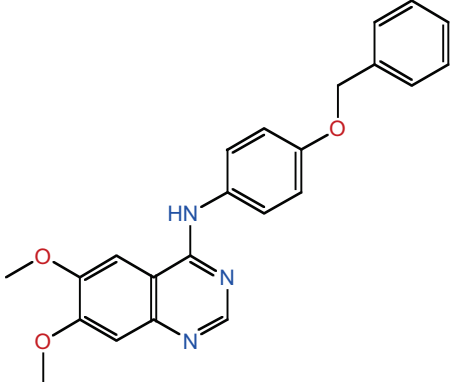
141992-47-4

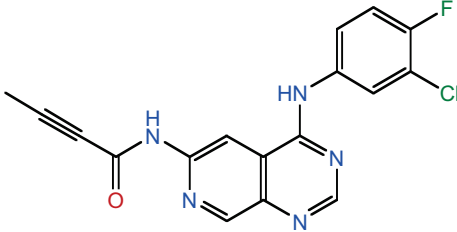
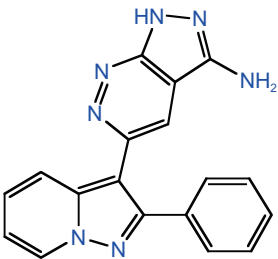
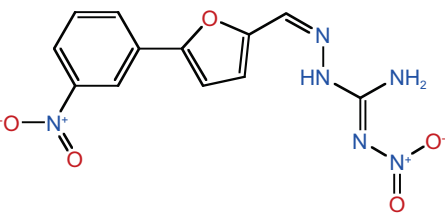
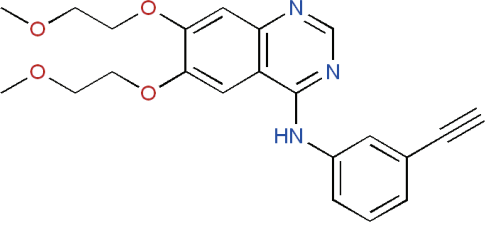
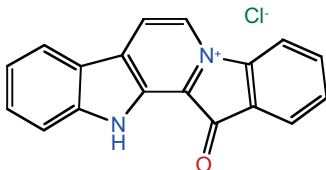


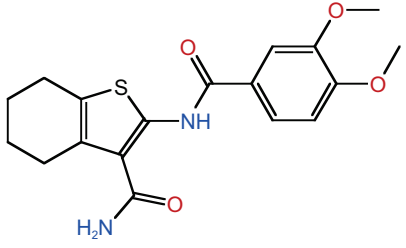
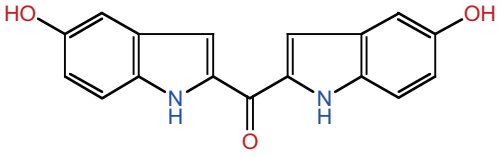
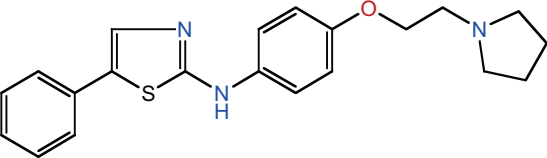
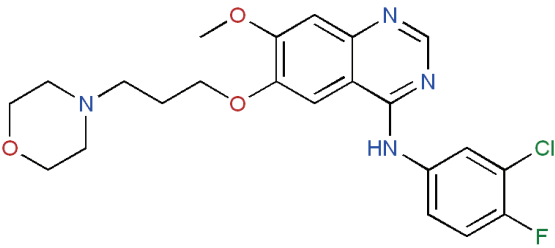
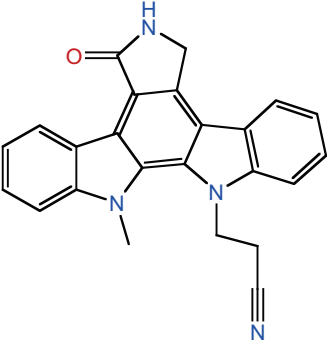
CMGC

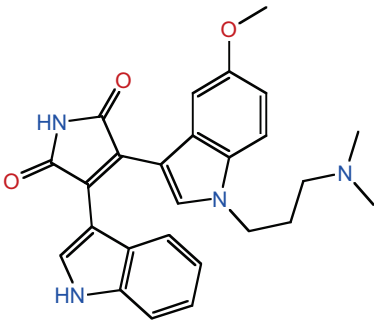
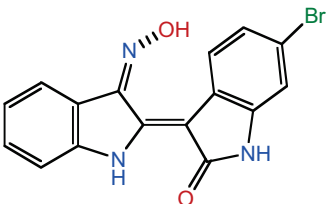
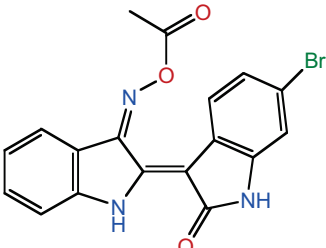
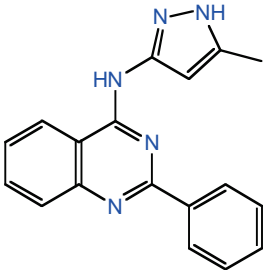
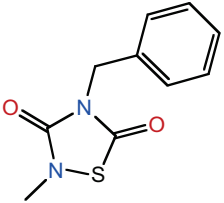
Cdk4 Inhibitor III	265312-55-8		CMGC
cFMS Receptor Tyrosine Kinase Inhibitor	870483-87-7		TK
Chelerythrine Chloride	3895-92-9		AGC
Chk2 Inhibitor II	516480-79-8		CAMK
Compound 52	212779-48-1		CMGC

Compound 56	171745-13-4		TK
Dasatinib	302962-49-8		TK
Diacylglycerol Kinase Inhibitor II	120166-69-0		LIPID
DMBI	5812-07-7		TK
DNA-PK Inhibitor II	154447-35-5		ATYPICAL

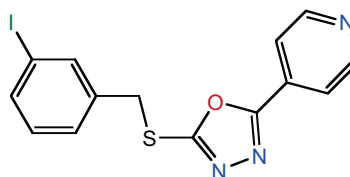
DNA-PK Inhibitor III	404009-40-1		ATYPICAL
DNA-PK Inhibitor V	404009-46-7		ATYPICAL
Dovitinib	405169-16-6		TK
EGFR Inhibitor	879127-07-8		TK
EGFR/ErbB-2 Inhibitor	179248-61-4		TK

EGFR/ErbB-2/ErbB-4 Inhibitor	881001-19-0		TK
ERK Inhibitor II, FR180204	865362-74-9		CMGC
ERK Inhibitor III	345616-52-6		CMGC
Erlotinib	183319-69-9		TK
Fascaplysin, Synthetic	114719-57-2		CMGC

Flt-3 Inhibitor	301305-73-7		TK
Flt-3 Inhibitor II	896138-40-2		TK
Flt-3 Inhibitor III	852045-46-6		TK
Gefitinib	184475-35-2		TK
Gö 6976	136194-77-9		AGC

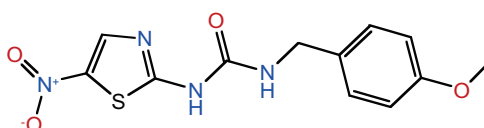
Gö 6983	133053-19-7		AGC
GSK-3 Inhibitor IX	667463-62-9		CMGC
GSK-3 Inhibitor X	740841-15-0		CMGC
GSK-3 Inhibitor XIII	404828-08-6		CMGC
GSK-3b Inhibitor I	327036-89-5		CMGC, AGC, TK

GSK-3b Inhibitor II 478482-75-6



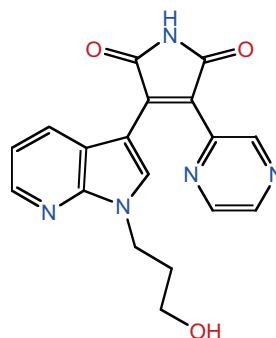
CMGC

GSK-3b Inhibitor VIII 487021-52-3

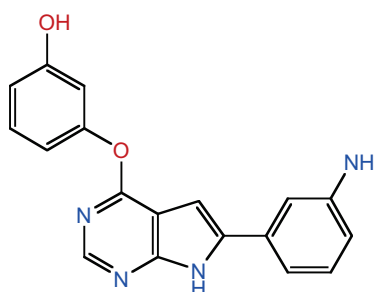


CMGC

GSK-3b Inhibitor XI 626604-39-5

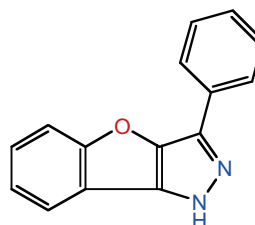


CMGC

GSK3b Inhibitor XII,  
TWS119 601514-19-6

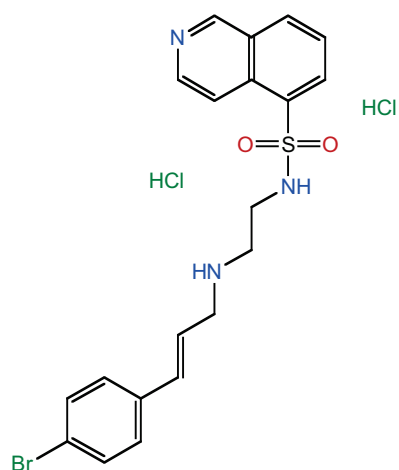
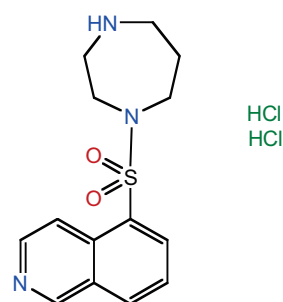
CMGC

GTP-14564 34823-86-4

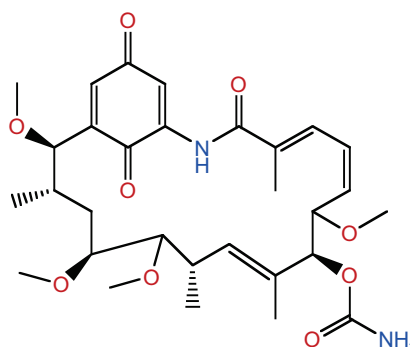


TK

H-89, Dihydrochloride 127243-85-0

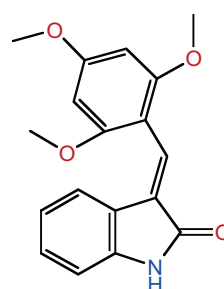
AGC, CK1,  
CAMKHA 1077,  
Dihydrochloride  
Fasudil 103745-39-7

AGC

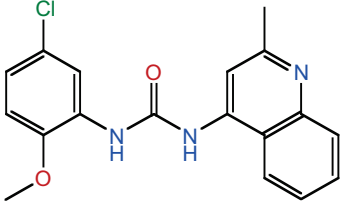
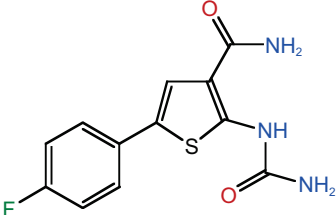
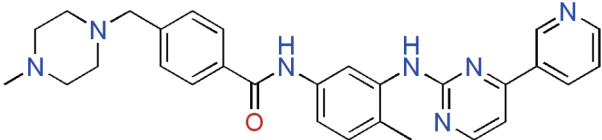
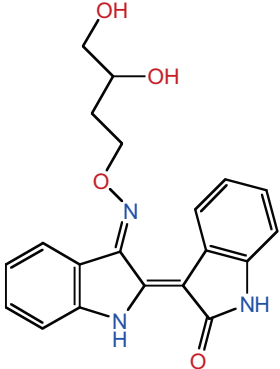
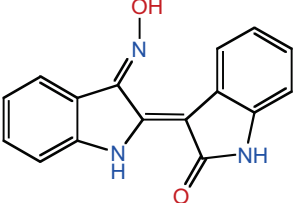
Herbimycin A,  
Streptomyces sp. 70563-58-5

TK

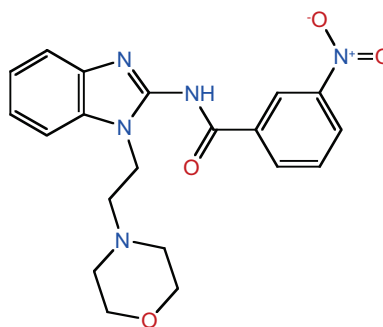
IC261 186611-52-9



CK1

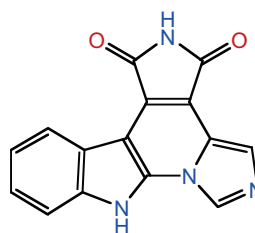
IGF-1R Inhibitor II	196868-63-0		TK
IKK-2 Inhibitor IV	507475-17-4		OTHER
Imatinib	220127-57-1		TK
Indirubin Derivative E804	854171-35-0		CMGC, TK
Indirubin-3'-monoxime	160807-49-8		CMGC

IRAK-1/4 Inhibitor 509093-47-4

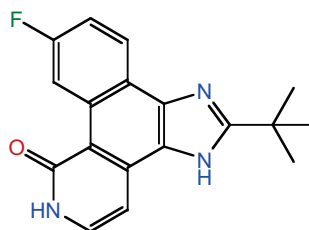


TKL

Isogranulatimide 244148-46-7

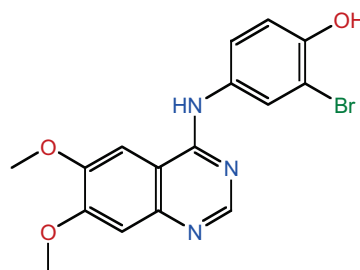
CAMK,  
CMGC,  
ATYPICAL

JAK Inhibitor I 457081-03-7



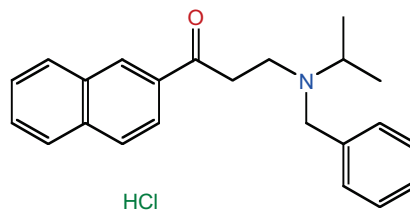
TK

JAK3 Inhibitor II 211555-04-3

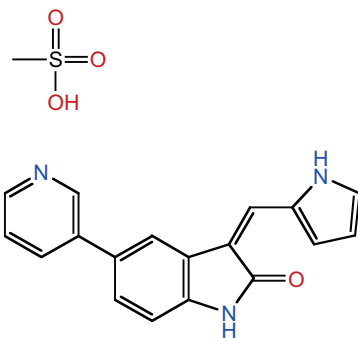
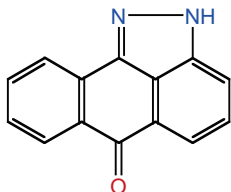
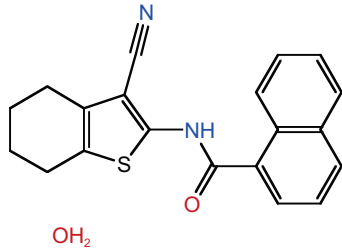
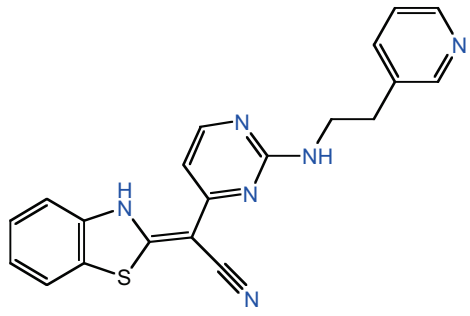
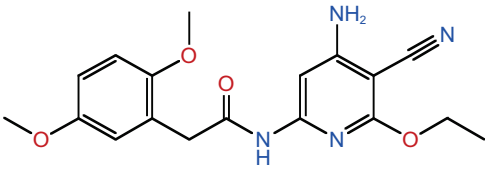


TK

JAK3 Inhibitor IV 58753-54-1

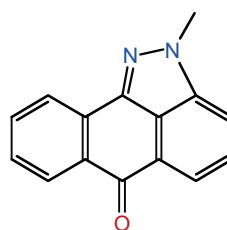


TK

JAK3 Inhibitor VI	856436-16-3		TK
JNK Inhibitor II	129-56-6		CMGC
JNK Inhibitor IX	312917-14-9		CMGC
JNK Inhibitor V	345987-15-7		CMGC
JNK Inhibitor VIII	894804-07-0		CMGC

JNK Inhibitor,  
Negative Control

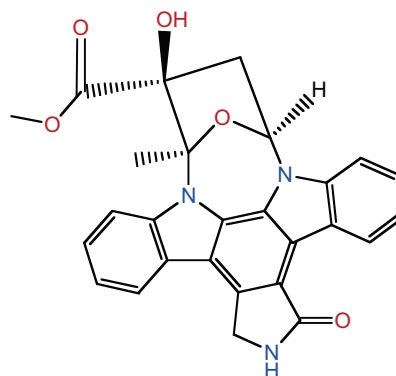
54642-23-8



INACTIVE

K-252a,  
Nocardioopsis sp.

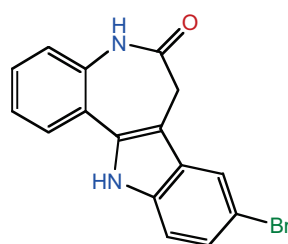
97161-97-2



AGC

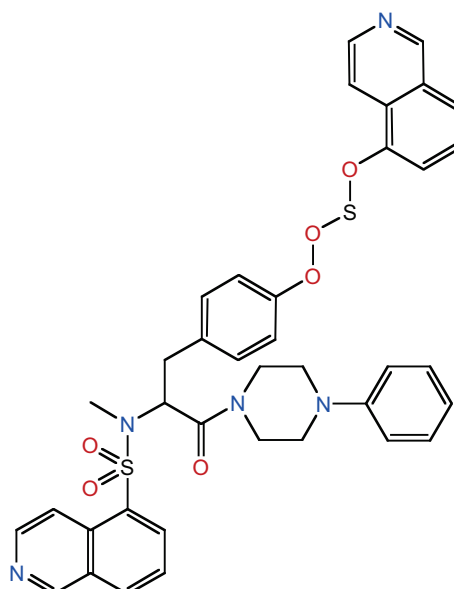
Kenpaullone

142273-20-9

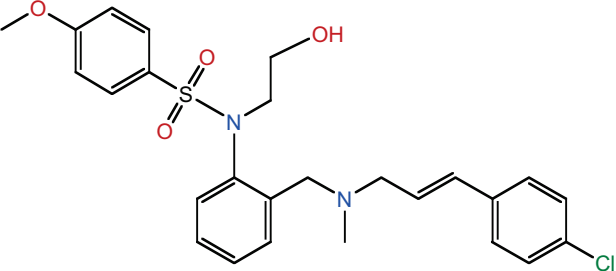
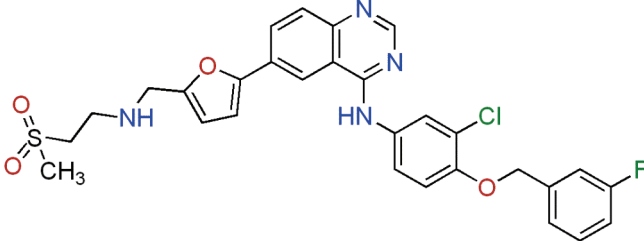
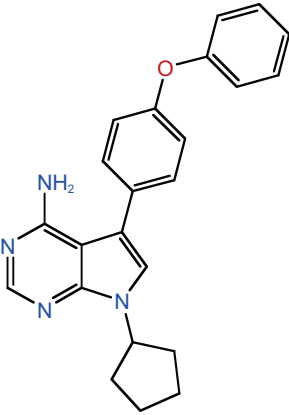
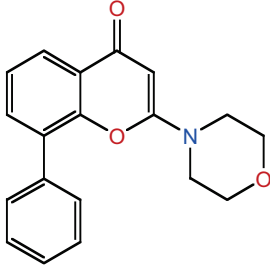
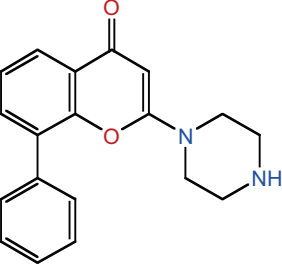
CMGC, CK1,  
TK

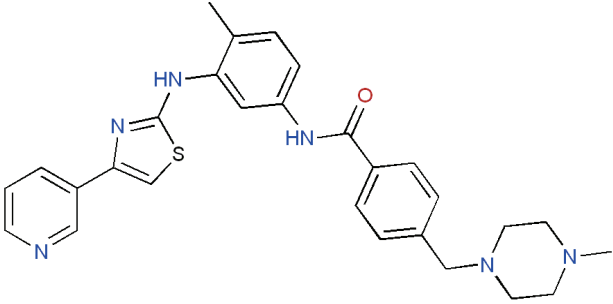
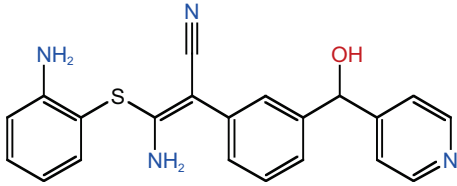
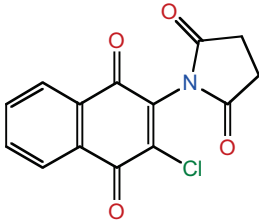
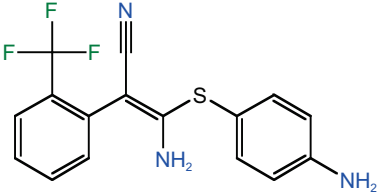
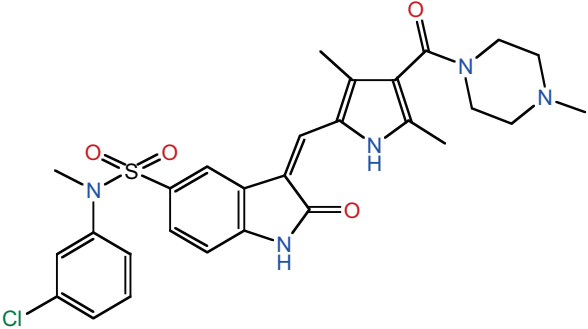
KN-62

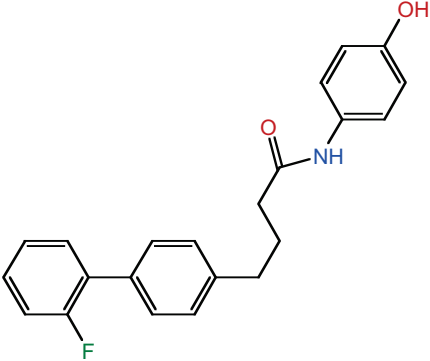
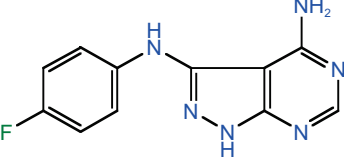
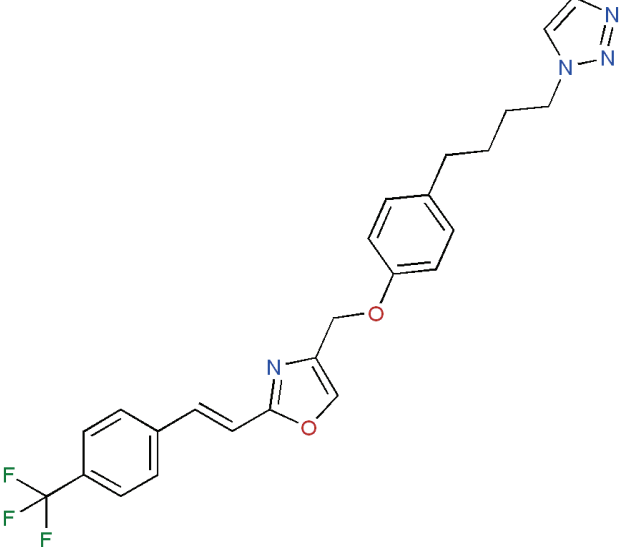
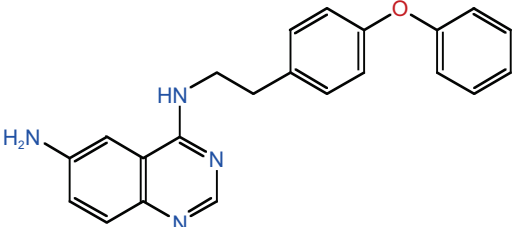
127191-97-3

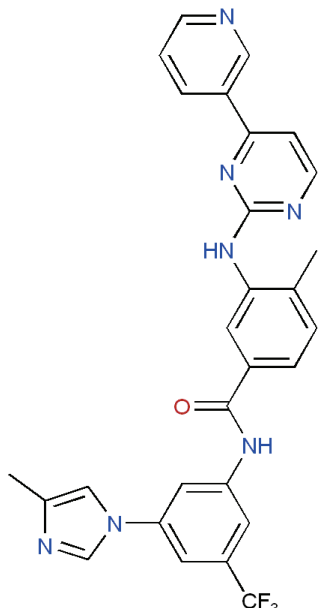
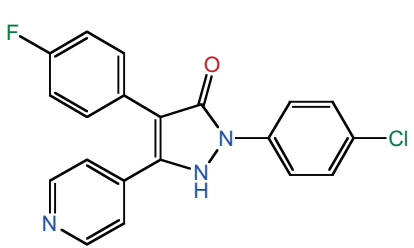
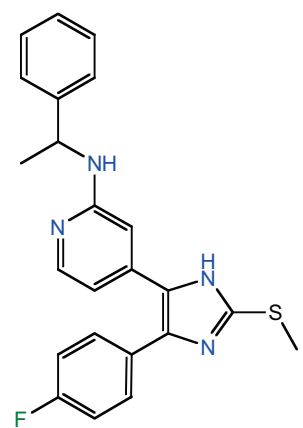
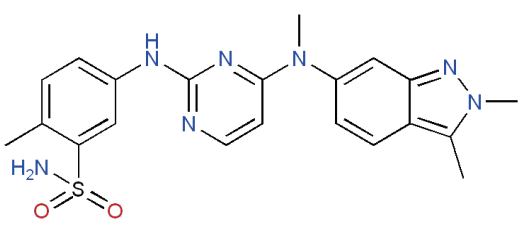


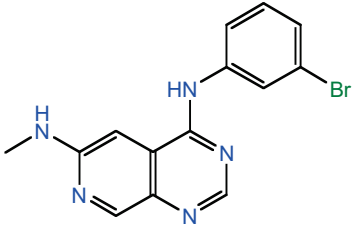
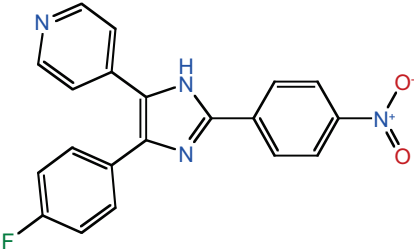
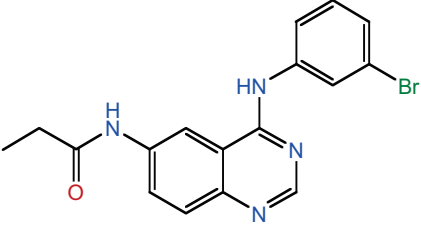
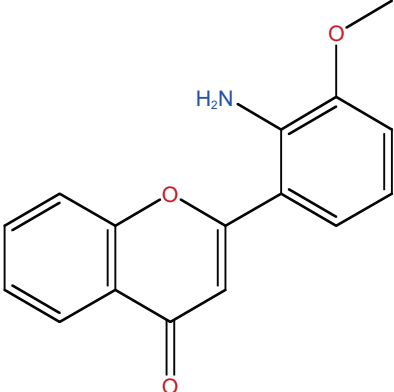
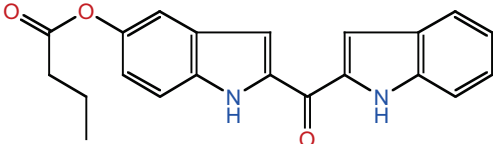
CAMKII

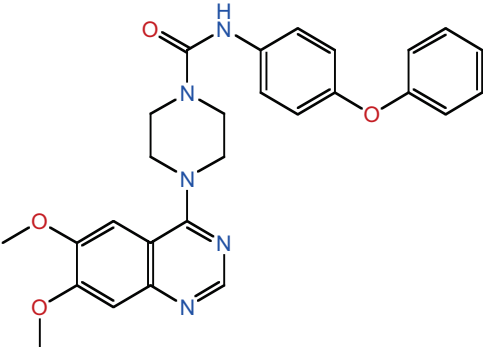
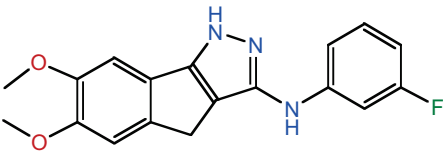
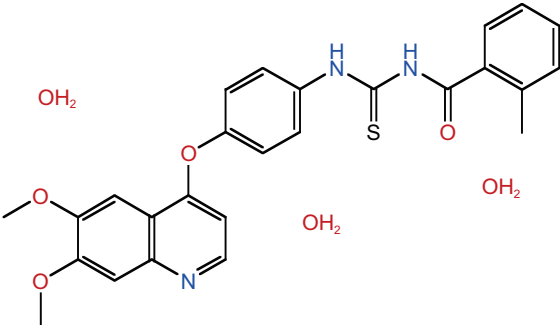
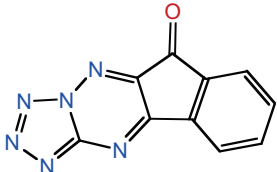
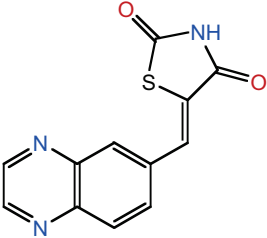
KN-93	139298-40-1		CAMK
Lapatinib	231277-92-2		TK
Lck Inhibitor	213743-31-8		TK
LY 294002	154447-36-6		LIPID
LY 303511- Negative control	154447-38-8		INACTIVE

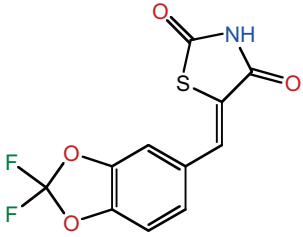
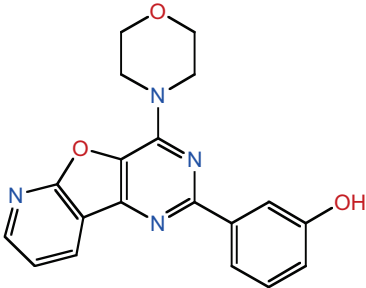
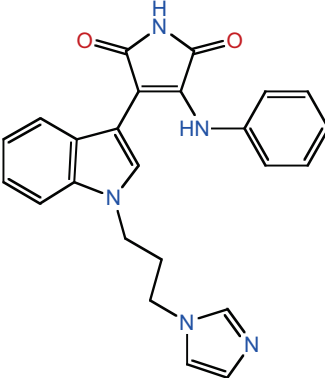
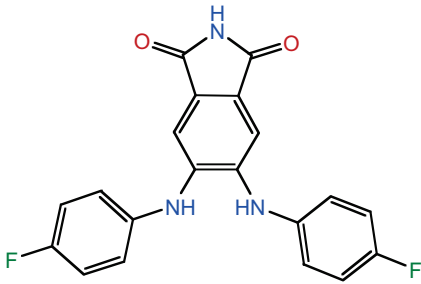
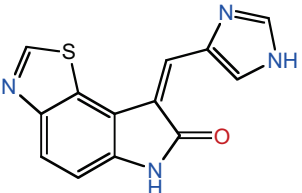
Masitinib	790299-79-5		TK
MEK Inhibitor I	297744-42-4		STE
MEK Inhibitor II	623163-52-0		STE
MEK1/2 Inhibitor	305350-87-2		STE
Met Kinase Inhibitor	658084-23-2		TK

MK2a Inhibitor	41179-33-3		CAMK
MNK1 Inhibitor	522629-08-9		CAMK
Mubritinib	366017-09-6		TK
NF-kB Activation Inhibitor	545380-34-5		OTHER

Nilotinib	641571-10-0	 <p>The chemical structure of Nilotinib consists of a central benzimidazole ring system. One of the benzimidazole nitrogens is substituted with a 4-(4-(4-(4-(trifluoromethyl)phenyl)amino)phenyl)pyridin-2-yl)phenyl group. The other benzimidazole nitrogen is substituted with a methyl group.</p>	TK
p38 MAP Kinase Inhibitor	219138-24-6	 <p>The chemical structure features a central imidazole ring. One imidazole nitrogen is substituted with a 4-chlorophenyl group. The 2-position of the imidazole ring is substituted with a 4-fluorophenyl group, and the 4-position is substituted with a 4-pyridinyl group.</p>	CMGC
p38 MAP Kinase Inhibitor III	581098-48-8	 <p>The chemical structure features a central imidazole ring. One imidazole nitrogen is substituted with a 4-(4-phenylphenyl)phenyl group. The 2-position of the imidazole ring is substituted with a 4-fluorophenyl group, and the 4-position is substituted with a 4-(methylamino)pyridin-2-yl group.</p>	CMGC
Pazopanib	444731-52-6	 <p>The chemical structure features a central pyridine ring. One pyridine nitrogen is substituted with a 4-(4-(4-(4-(sulfamoyl)phenyl)amino)phenyl)phenyl group. The other pyridine nitrogen is substituted with a 4-(4-(4-(4-(methylamino)phenyl)phenyl)phenyl)phenyl group.</p>	TK

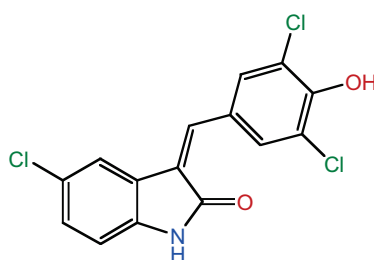
PD 158780	171179-06-9		TK
PD 169316	152121-53-4		CMGC
PD 174265	216163-53-0		TK
PD 98059	167869-21-8		STE
PDGF Receptor Tyrosine Kinase Inhibitor II	249762-74-1		TK

PDGF Receptor Tyrosine Kinase Inhibitor III	205254-94-0	 <chem>COc1cc(OC)c2nc3c(nc12)N(CCN3C(=O)Nc4ccc(Oc5ccccc5)cc4)C</chem>	TK
PDGF Receptor Tyrosine Kinase Inhibitor IV	627518-40-5	 <chem>COc1cc(OC)c2c(c1)c3c(nc23)N=C(Nc4ccc(F)cc4)N</chem>	TK
PDGF RTK Inhibitor	347155-76-4	 <chem>COc1cc(OC)c2nc3c(nc12)Oc4ccc(NC(=O)Nc5ccc(O)cc5)cc3O</chem>	TK
PDK1/Akt/Flt Dual Pathway Inhibitor	331253-86-2 and 329710-24-9	 <chem>O=C1C2=CC=CC=C2N3C(=O)N4C(=O)N5C(=O)N431</chem>	AGC, ATYPICAL, TK
PI 3-Kg Inhibitor	648450-29-7	 <chem>O=C1NC(=O)S1C=Cc2ccc3ncnc23</chem>	LIPID

PI 3-Kg Inhibitor II	648449-76-7		LIPID
PI-103	371935-74-9		LIPID
PKCb Inhibitor	257879-35-9		AGC
PKCbII/EGFR Inhibitor	145915-60-2		TK, AGC
PKR Inhibitor	608512-97-6		OTHER

PKR Inhibitor,  
Negative Control

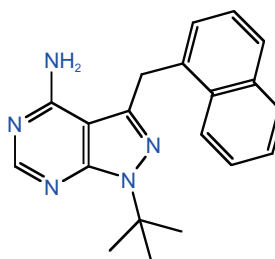
852547-30-9



INACTIVE

PP1 Analog II,  
1NM-PP1

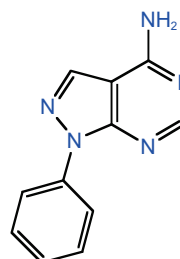
221244-14-0



TK

PP3

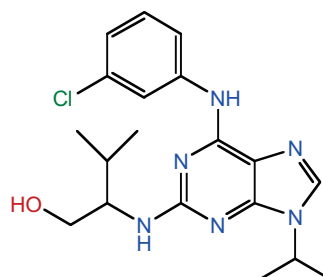
5334-30-5



TK

Purvalanol A

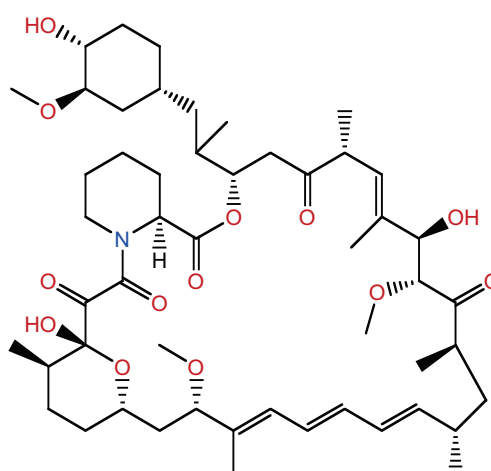
212844-53-6



CMGC

Rapamycin

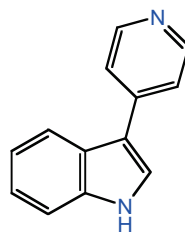
53123-88-9



AGC

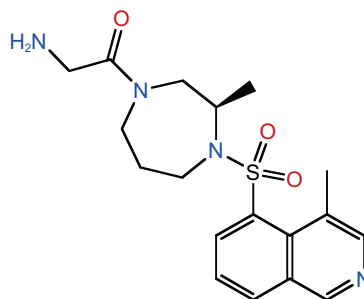
Rho Kinase Inhibitor III,  
Rockout

7272-84-6



AGC

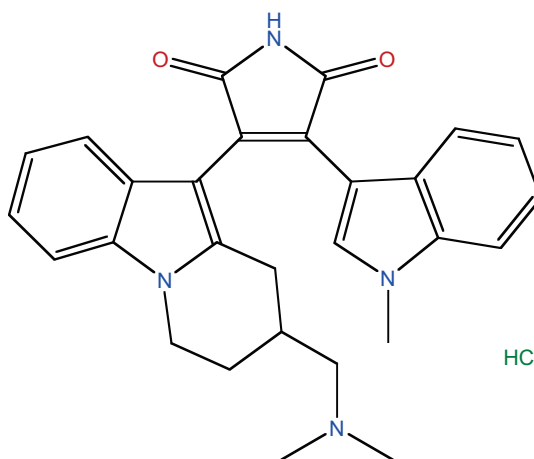
Rho Kinase Inhibitor IV 913844-45-8



AGC

Ro-32-0432

151342-35-7

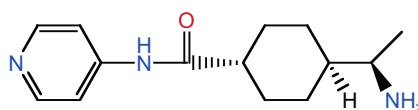


HCl

AGC

ROCK Inhibitor,  
Y-27632

146986-50-7

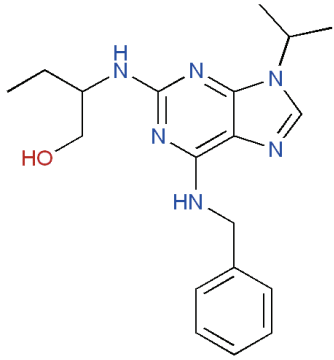
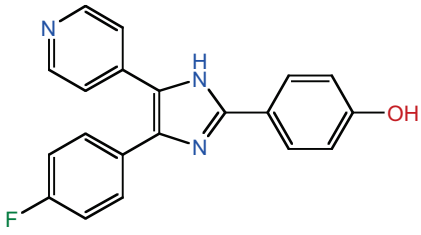
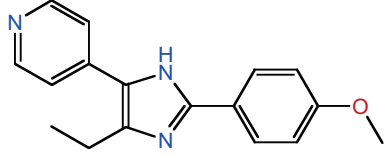
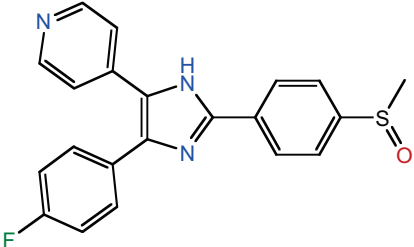
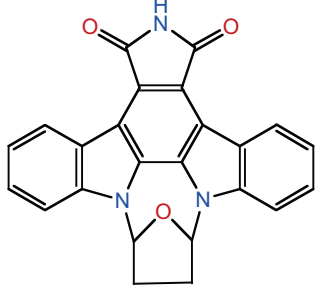


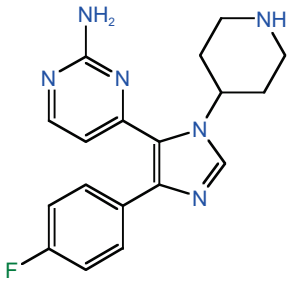
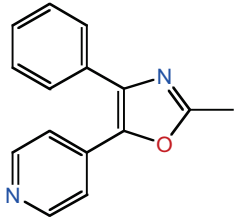
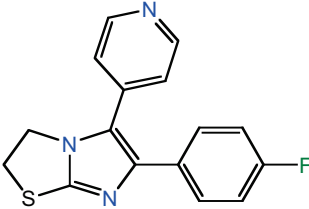
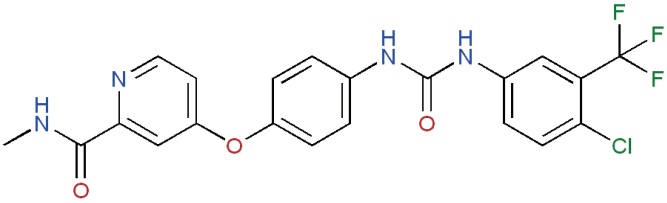
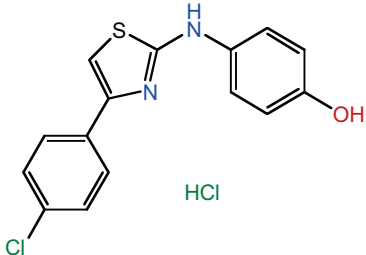
HCl

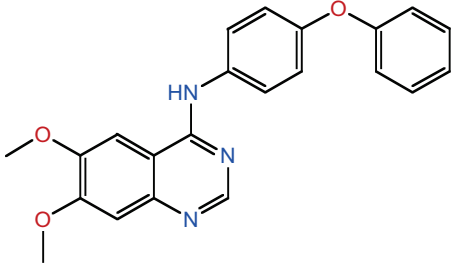
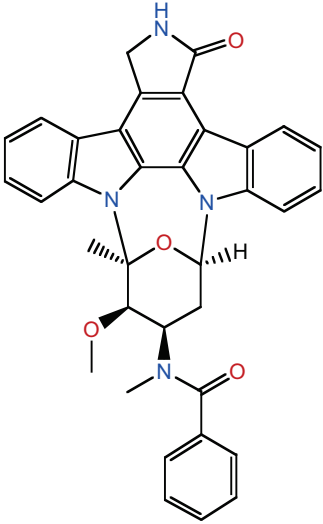
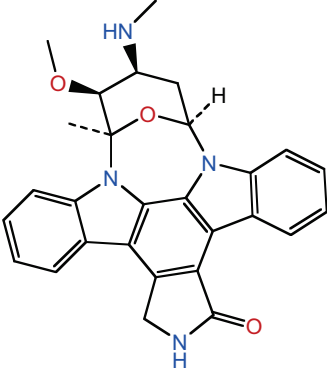
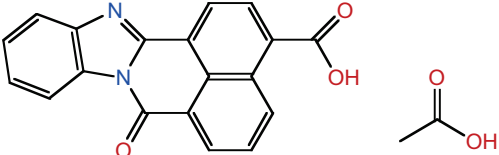
HCl

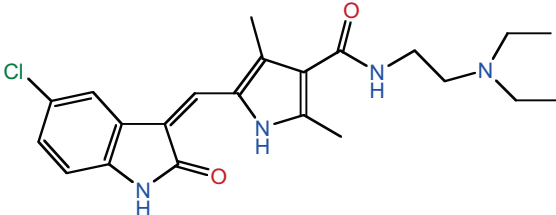
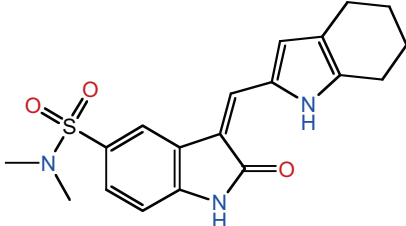
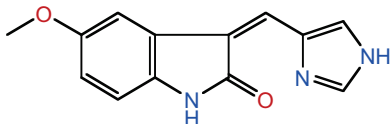
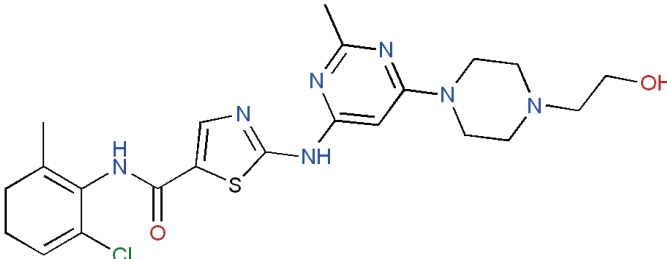
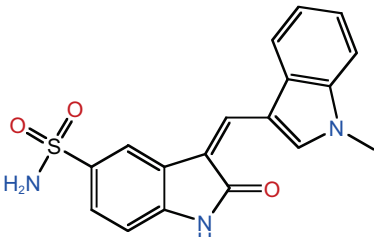
OH<sub>2</sub>

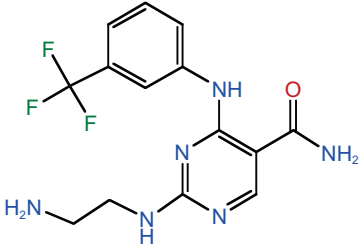
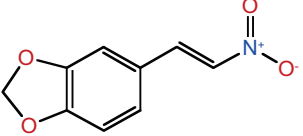
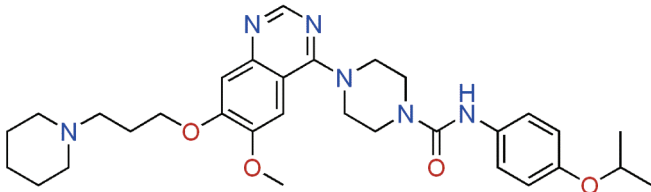
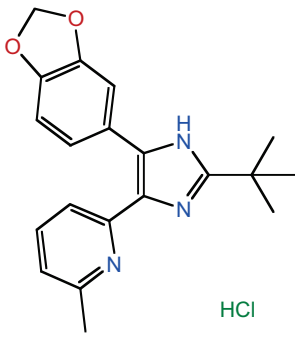
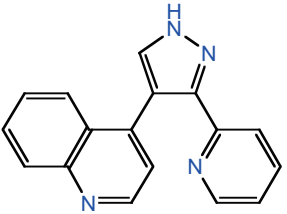
AGC

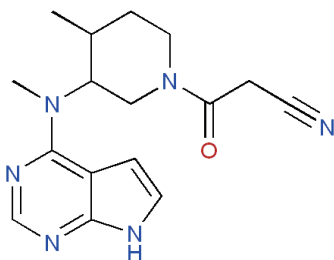
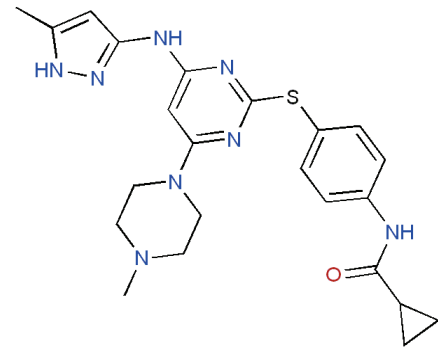
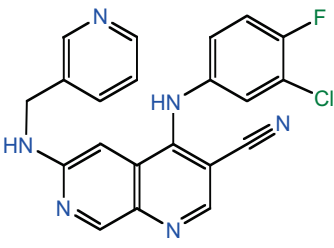
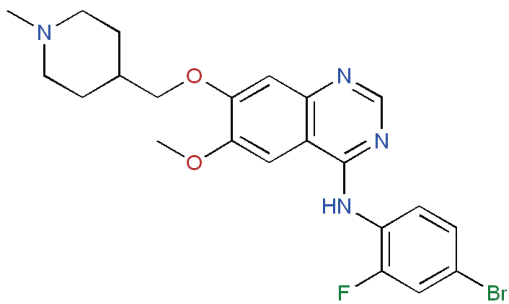
Roscovitine	186692-46-6		CMGC
SB 202190	152121-30-7		CMGC
SB 202474, Negative control for p38 MAPK inhibition studies	172747-50-1		INACTIVE
SB 203580	152121-47-6		CMGC
SB 218078	135897-06-2		CAMK

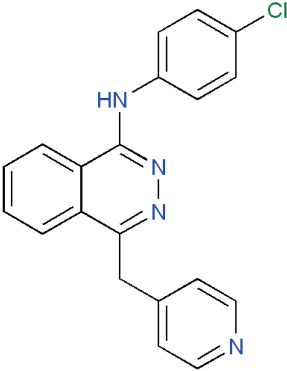
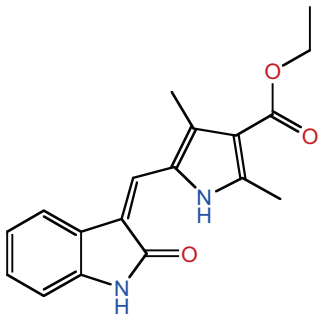
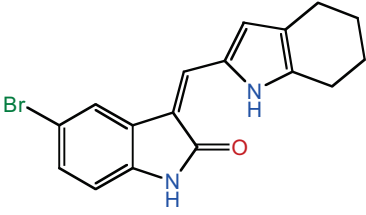
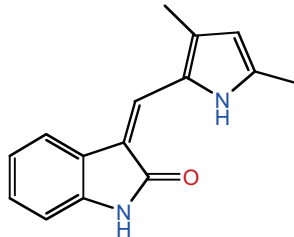
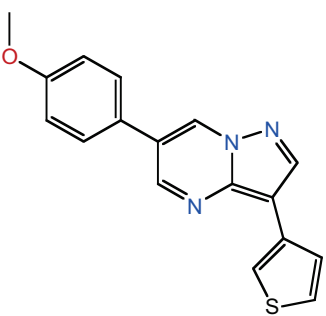
SB220025	165806-53-1		CMGC
SC-68376	318480-82-9		CMGC
SKF-86002	72873-74-6		CMGC
Sorafenib	284461-73-0		TK
Sphingosine Kinase Inhibitor	312636-16-1		LIPID

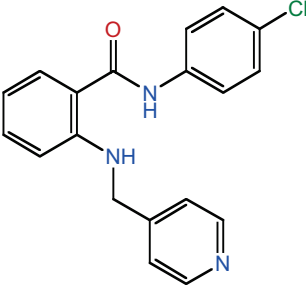
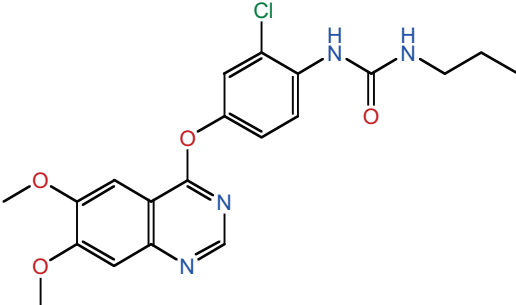
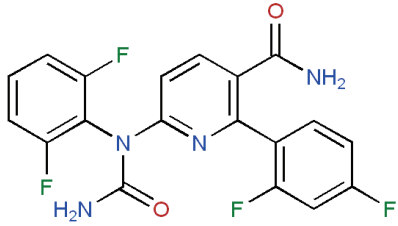
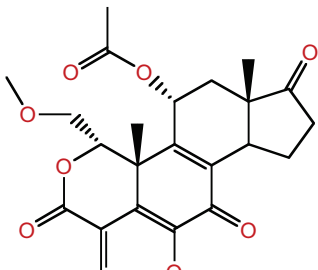
Src Kinase Inhibitor I	179248-59-0		TK
Staurosporine, N-benzoyl-	120685-11-2		AGC, CMGC, TK
Staurosporine, Streptomyces sp.	62996-74-1		AGC, CAMK, TK
STO-609	52029-86-4		CAMK

SU11652	326914-10-7		TK
SU6656	330161-87-0		TK
SU9516	666837-93-0		CMGC
Sunitinib	557795-19-4		TK
Syk Inhibitor	622387-85-3		TK

Syk Inhibitor II	227449-73-2		$\text{OH}_2$ $\text{OH}_2$ HCl HCl	TK
Syk Inhibitor III	1485-00-3			TK
Tandutinib	387867-13-2			TK
TGF- $\beta$ RI Inhibitor III	356559-13-2		HCl	TKL
TGF- $\beta$ RI Kinase Inhibitor	396129-53-6			TKL

Tofacitinib	477600-75-2	 <chem>CN1CCN(C1)C2=CN3C=CC=C3N2C(=O)CC#N</chem>	TK
Tozasertib	639089-54-6	 <chem>CN1CCN(C1)C2=CN3C=CC=C3N2S4=CC=C(C=C4)NC(=O)C5CC5</chem>	OTHER
Tpl2 Kinase Inhibitor	871307-18-5	 <chem>C#Nc1nc2c(ncn2C3=CC=C(C=C3)F)N(C3=CC=CC=C3Cl)CC4=CC=CC=N4</chem>	CMGC
Vandetanib	443913-73-3	 <chem>COC1=CC=C(C=C1OC2=CC=CC=C2N3=CC=CC=N3)C#N</chem>	TK

Vatalanib	212141-51-0		TK
VEGF Receptor 2 Kinase Inhibitor I	15966-93-5		TK
VEGF Receptor 2 Kinase Inhibitor II	288144-20-7		TK
VEGF Receptor 2 Kinase Inhibitor III	204005-46-9		TK
VEGF Receptor 2 Kinase Inhibitor IV	216661-57-3		TK

VEGF Receptor Tyrosine Kinase Inhibitor II	269390-69-4	 <chem>CC1=CC=C(C=C1)C(=O)NC2=CC=C(C=C2)NC3=CC=CC=N3</chem>	TK
VEGF Receptor Tyrosine Kinase Inhibitor III, KRN633	286370-15-8	 <chem>CCOC1=CC=C(C=C1)C2=CC(OC)=C(C=C2)N3=CC=CC=N3C4=CC=C(C=C4)OC5=CC=C(C=C5)NC(=O)NCC</chem>	TK
VX-702	745833-23-2	 <chem>NC(=O)C1=CC=C(C=C1)N2C(=O)C3=CC=C(C=C3)N(C2)C4=CC=C(C=C4)F</chem>	CMGC
Wortmannin	19545-26-7	 <chem>CC(=O)OC12C3C(C1)OC(=O)C4=C(C(=O)O)C(=O)C5=C(C(=O)O)C(=O)C6=C(C(=O)O)C(=O)C7=C(C(=O)O)C(=O)C8=C(C(=O)O)C(=O)C9=C(C(=O)O)C(=O)C10=C(C(=O)O)C(=O)C11=C(C(=O)O)C(=O)C12</chem>	ATYPICAL

**Supplementary Table 2.** Kinase constructs and substrates used in this study.

RBC Enzyme Name	HUGO symbol	Substrate	Genbank Accession #	Protein Accession #	Clone	Mutation	Expression	Tag
ABL1	ABL1	Abltide	NP_005148.2	P00519	full-length	-	baculovirus in Sf21 insect cells	C-terminal His
ABL2/ARG	ABL2	Abltide	NP_009298	P42684	full-length	-	baculovirus in Sf21 insect cells	C-terminal His
ACK1	TNK2	Abltide	NP_005772.3	Q07912	aa 110-476	-	baculovirus in Sf21 insect cells	N-terminal GST
AKT1	AKT1	Crosstide	NP_005154	P31749	full-length		baculovirus in Sf21 insect cells	N-terminal His
AKT2	AKT2	Crosstide	NP_001617	P31751	full-length		baculovirus in Sf21 insect cells, activated by PDK1	N-terminal His
AKT3	AKT3	Crosstide	NP_005456	Q9Y243	full-length		baculovirus in Sf21 insect cells	N-terminal His
ALK	ALK	pEY	NP_004295.2	Q9UM73	cytoplasmic	-	Insect	N-terminal GST
ALK1/ACVRL1	ACVRL1	Casein	NP_000011.2	P37023	cytoplasmic aa139-503	-	Insect	N-terminal GST
ALK2/ACVR1	ACVR1	Casein	NP_001096.1	Q04771	cytoplasmic aa145-509	-	Insect	N-terminal GST
ALK4/ACVR1B	ACVR1B	Casein	NP_004293	P36896	aa 150-505	-	Baculovirus infected insect cells	N-terminal GST
ALK5/TGFBR1	TGFBR1	Casein	NM_004612	P36897	aa200-503	-	Sf9 cells	GST-HIS fusion
ARAF	ARAF	MEK1 (K97R)	NM_001654	P10398	aa 282-end	YY301-302DD	Baculovirus infected Sf9 cells	N-terminal GST-tag
ARK5/NUAK1	NUAK1	CHKtide	NP_055655	O60285	full-length	-	Insect	N-terminal His
ASK1/MAP3K5	MAP3K5	MBP	NP_005914	O99683	full-length	-	Insect	N-terminal GST
Aurora A	AURKA	Kemptide	NP_940839	O14965	full length	-	baculovirus in Sf21 insect cells	N-terminal His6-tag
Aurora B	AURKB	Kemptide	NP_004208.2	Q96GD4	full-length	-	Insect	N-terminal His
Aurora C	AURKC	Kemptide	AAH75064, NP_003151	Q9UQB9	full-length	-	Insect	N-terminal His

RBC Enzyme Name	HUGO symbol	Substrate	Genbank Accession #	Protein Accession #	Clone	Mutation	Expression	Tag
AXL	AXL	Abltide + Mn	NP_068713	P30530	aa 473-894	-	Baculovirus infected Sf9 cells	C-terminal His
BLK	BLK	pEY	NP_001706	P51451	full-length	-	Insect	N-terminal His
BMX/ETK	BMX	pEY	NP_001712	P51813	full length	-	baculovirus in Sf21 insect cells	C-terminal His
BRAF	BRAF	MEK1 (K97R)	NP_004324.2	P15056	full-length	-	Insect	N-terminal GST
BRK	PTK6	pEY + Mn	NP_005966	Q13882	full-length	-	Insect	C-terminal His
BRSK1	BRSK1	CHKtide	NP_115806	Q8TDC3	full-length	-	Insect	N-terminal GST-tag
BRSK2	BRSK2	ZIPTide	GenBank NM_003957	Q8IWQ3	full-length	-	baculovirus in Sf21 insect cells	N-terminal His6-tag
BTK	BTK	pEY	NP_000052	Q06187	full-length	-	Insect	N-terminal His6-tagged
CAMK1a	CAMK1	Autocamtide 2 + Ca-CaM	NP_003647.1	Q14012	full length	-	baculovirus insect cell	N-terminal His-tag
CAMK1b	PNCK	Autocamtide 2 + Ca-CaM	GenBank NM_012040	Q6P2M8	full length	-	baculovirus insect cell	N-terminal GST-tag
CAMK1d	CAMK1D	Autocamtide 2 + Ca-CaM	NP_705718.1	Q8IU85	full length	-	baculovirus insect cell	N-terminal His-tag
CAMK1g	CAMK1G	Autocamtide 2 + Ca-CaM	GenBank NM_020439	Q96NX5	C-terminal truncation	-	baculovirus insect cell	N-terminal GST-tag
CAMK2a	CAMK2A	Autocamtide 2 + Ca-CaM	NP_741960	Q9UQM7	full length	-	baculovirus insect cell	C-terminal His-tag
CAMK2b	CAMK2B	Autocamtide 2 + Ca-CaM	NP_742078.1	Q13554	full length	-	baculovirus insect cell	N-terminal His6-tag
CAMK2d	CAMK2D	ZIPTide + Ca-CaM*	NP_742113	Q13557	full length	-	baculovirus insect cell	C-terminal His6-tag
CAMK2g	CAMK2G	ZIPTide + Ca-CaM*	GenBank NM_172169	Q13555	C-terminal truncation	-	baculovirus in Sf9 insect cells	N-terminal GST-tag
CAMK4	CAMK4	ZIPTide + Ca-CaM*	NP_001735	Q9UQM7	full length	-	E. coli	N-terminal GST-tag
CAMKK1	CAMKK1	MBP + Ca-CaM	GenBank NM_032294	Q8N5S9	full-length	-	baculovirus in Sf9 insect cells	N-terminal GST

RBC Enzyme Name	HUGO symbol	Substrate	Genbank Accession #	Protein Accession #	Clone	Mutation	Expression	Tag
CAMKK2	CAMKK2	MBP + Ca-CaM	NP_757380.1	Q96RR4	full-length	-	Baculovirus infected insect cells	N-terminal GST
CDK1/cyclin A	CDK1/CCNA <sub>2</sub>	Histone H1	NM_001786/ NM_001237	CDK1: P06493; cyclin A: P20248	full length / full length	-	baculovirus in Sf9 insect cells	N-terminal GST-tag / N-terminal GST-tag
CDK1/cyclin B	CDK1/CCNB <sub>1</sub>	Histone H1	NP_001777/B P_114172	CDK1: P06493; cyclin B: P14635	full length / full length	-	baculovirus insect cell	C-terminal His6-tag / N-terminal His6-tag
CDK2/cyclin A	CDK2/CCNA <sub>2</sub>	Histone H1	NP_001789, NP_001228	CDK2: P24941; cyclin A: P20248	full-length	-	Insect	N-terminal His6-tag / N-terminal His6-tag
CDK2/cyclin E	CDK2/CCNE <sub>1</sub>	Histone H1	EMBL M68520, GenBank NM_001238	CDK2: P24941; cyclin E: P24864	full length / full length	-	baculovirus in Sf21 insect cells	C-terminal His6-tag / N-terminal GST-tag
CDK3/cyclin E	CDK3/CCNE <sub>1</sub>	Histone H1	NM_001258, NM_001238	CDK3: Q00526; cyclin E: P24864	full length / full length	-	baculovirus in Sf9 insect cells	N-terminal GST-tag
CDK4/cyclin D1	CDK4/CCND <sub>1</sub>	RB-CTF	NP_000066, NP_444284	CDK4: P11802; Cyclin D1: P24385	full length	-	baculovirus insect cell	N-terminal GST-tag
CDK4/cyclin D3	CDK4/CCND <sub>3</sub>	RB-CTF	NM_000075, NM_001760	CDK4: P11802; Cyclin D3: P30281	full length	-	baculovirus in Sf9 insect cells	N-terminal GST-tag
CDK5/p25	CDK5/CDK5R1	Histone H1	NP_004926.1, NP_003876	CDK5: Q00535; p25: Q15078	full length / full length	-	baculovirus insect cell	N-terminal His6-tag / N-terminal GST-tag

RBC Enzyme Name	HUGO symbol	Substrate	Genbank Accession #	Protein Accession #	Clone	Mutation	Expression	Tag
CDK5/p35	CDK5/CDK5 R1	Histone H1	NP_004926.1, NP_003876	CDK5: Q00535; p35: Q15078	full length / full length	-	baculovirus insect cell	N-terminal His6- tag / N-terminal His6-tag
CDK6/cyclin D1	CDK6/CCND 1	RB-CTF	NP_001250, NP_444284	CDK6: Q00534; Cyclin D1: P24385	full-length	-	Baculovirus infected insect cells	N-terminal GST
CDK6/cyclin D3	CDK6/CCND 3	RB-CTF	X66365, M90814	CDK6: Q00534; Cyclin D3: P30281	full length / full length	-	baculovirus in Sf9 insect cells	N-terminal His6- tag / N-terminal GST-tag
CDK7/cyclin H	CDK7/CCNH/ MNAT1	Histone H1	NP_001790, NP_001230, NP_002422.1	CDK7: P50613; Cyclin H: P51946; MNAT1: Q61CQ7	full-length	-	Insect	N-terminal His
CDK9/cyclin K	CDK9/CCNK	PDKtide	NP_001252, NP_003849	CDK9: P50750; Cyclin K: O75909	full length / full length	-	Insect	N-terminal His6- tag / N-terminal His6-tag
CDK9/cyclin T1	CDK9/CCNT 1	PDKtide	NP_001252, NP_001231	CDK9: P50750; Cyclin T1: O60563	full-length	-	Insect	N-terminal His
CHK1	CHEK1	CHKtide	GenBank NM_001274	O14757	full length	-	baculovirus in Sf9 insect cells	N-terminal His
CHK2	CHEK2	CHKtide	NP_009125	O96017	full-length	-	baculovirus in Sf21 insect cells	C-terminal His
CK1a1	CSNK1A1	CK1tide	NP_001883.4	P48729	full length	-	baculovirus insect cell	GST-tag
CK1d	CSNK1D	CK1tide	NP_620693	P48730	full length	-	baculovirus insect cell	N-terminal GST- tag
CK1epsilon	CSNK1E	CK1tide	NP_001885	P49674	full length	-	baculovirus insect cell	C-terminal His-tag
CK1g1	CSNK1G1	CK1tide	NP_071331	Q9HCPO	full-length	-	Insect	N-terminal GST

RBC Enzyme Name	HUGO symbol	Substrate	Genbank Accession #	Protein Accession #	Clone	Mutation	Expression	Tag
CK1g2	CSNK1G2	CK1tide	NP_001310	P78368	full length	-	baculovirus insect cell	C-terminal His-tag
CK1g3	CSNK1G3	CK1tide	NP_004375.1, NP_004375.2	Q9Y6M4	full-length	-	Insect	N-terminal GST
CK2a	CSNK2A1	CK2 sub	NP_001886	P68400	full length	-	baculovirus insect cell	C-terminal GST-tag
CK2a2	CSNK2A2	CK2 sub	NP_001887	P19784	full length	-	baculovirus insect cell	N-terminal GST-tag
c-Kit	KIT	pEY + Mn	NP_000213	P10721	aa 544-976	-	Insect	His6-tag
CLK1	CLK1	MBP	NP_004062	P49759	full catalytic domain	-	E. coli	N-terminal GST
CLK2	CLK2	MBP	NP_003984	P49760	catalytic domain aa137-498	-	baculovirus insect cell	N-terminal GST
CLK3	CLK3	MBP	NP_003983	P49761	full-length	-	Insect	N-terminal GST
CLK4	CLK4	MBP	NP_065717	Q9HAZ1	full-length	-	Insect	N-terminal GST
c-MER	MERTK	pEY	NP_006334.2	Q12866	aa 578-872	-	baculovirus insect cell	N-terminal GST
c-MET	MET	MBP	NP_000236.2	P10721	aa 956-1390	-	baculovirus insect cell	N-terminal His
COT1/MAP3K8	MAP3K8	MEK1 (K97R)	NP_005195	P41279	aa 30-397	-	Baculovirus infected insect cells	N-terminal GST
CSK	CSK	pEY	NP_004374	P41240	full-length	-	E. coli	C-terminal His
c-Src	SRC	pEY	NP_005408	P12931	full-length	-	Insect	C-terminal His
CTK/MATK	MATK	pEY	NP_647611	P42679	full-length	-	Insect	C-terminal His
DAPK1	DAPK1	ZIPtide	NP_004929	P53355	full catalytic	-	Insect	N-terminal GST
DAPK2	DAPK2	ZIPtide + Ca-CaM	NP_055141	Q9UIK4	full catalytic	-	Insect	N-terminal GST
DCAMKL2	DCLK2	Autocamtide 2 + Ca-CaM	NP_689832	Q8N568	full-length	-	Baculovirus infected insect cells	N-terminal GST
DDR2	DDR2	AXLtide + Mn	NP_006173.2	Q16832	aa 424-855	-	baculovirus in insect cells	N-terminal GST

RBC Enzyme Name	HUGO symbol	Substrate	Genbank Accession #	Protein Accession #	Clone	Mutation	Expression	Tag
DMPK	DMPK	AXLtide	NP_004400	Q09013	full-length	-	Insect	N-terminal GST
DRAK1/STK17A	STK17A	ZIPtide	NP_004751	Q9UEE5	full-length	-	Insect	N-terminal GST
DYRK1/DYRK1A	DYRK1A	Casein	NP_001387	Q13627	full-length	-	Insect	N-terminal GST
DYRK1B	DYRK1B	Casein	NP_004705	Q9Y463	full-length	-	Insect	N-terminal GST
DYRK2	DYRK2	Casein	GenBank NM_003583	Q92630	full length	-	baculovirus in Sf21 insect cells	His6-tag
DYRK3	DYRK3	Casein	NP_003573	O43781	full length	-	Insect	N-terminal GST
DYRK4	DYRK4	Casein	NP_003836.1	Q9NR20	full length	-	Insect	N-terminal GST
EGFR	EGFR	pEY + Mn	NP_005219.2	P00533	cytoplasmic	-	Insect	N-terminal GST
EPHA1	EPHA1	pEY + Mn	NP_005223.2	P21709	cytoplasmic	-	Insect	N-terminal GST
EPHA2	EPHA2	pEY	NP_004422.2	P29317	cytoplasmic	-	Insect	N-terminal GST
EPHA3	EPHA3	pEY + Mn	NP_005224	P29320	cytoplasmic	-	Insect	C-terminal His
EPHA4	EPHA4	pEY + Mn	NP_004429.1	P54764	aa 616-887	-	baculovirus in insect cells	N-terminal GST
EPHA5	EPHA5	pEY + Mn	NP_004430.1	P54756	aa 595-1037	-	baculovirus in insect cells	N-terminal GST
EPHA6	EPHA6	pEY	NM_001080448	Q9UF33	Catalytic (561-end)	-	Insect	N-terminal GST
EPHA7	EPHA7	pEY	NP_004431.1	Q15375	catalytic domain (aa 579-998)	-	baculovirus insect cell	N-terminal GST-tag
EPHA8	EPHA8	pEY	NP_065387	P29322	catalytic domain (aa 565-1005)	-	baculovirus insect cell	N-terminal GST-tag
EPHB1	EPHB1	pEY	NP_004432	P54762	cytoplasmic	-	Insect	N-terminal GST
EPHB2	EPHB2	pEY + Mn	NP_004433	P29323	aa 616-889	-	Insect	GST
EPHB3	EPHB3	pEY	NP_004434	P54753	cytoplasmic	-	Insect	N-terminal GST
EPHB4	EPHB4	pEY	NP_004435	P54760	cytoplasmic	-	Insect	C-terminal His
ERBB2/HER2	ERBB2	pEY + Mn	GenBank X03363	P04626	aa679-1255	-	Insect	N-terminal GST
ERBB4/HER4	ERBB4	pEY + Mn	NP_005226	Q15303	aa 708-993	-	baculovirus insect cell	N-terminal GST
ERK1/MAPK3	MAPK3	MBP	NP_002737	P27361	full-length	-	Insect	N-terminal GST

RBC Enzyme Name	HUGO symbol	Substrate	Genbank Accession #	Protein Accession #	Clone	Mutation	Expression	Tag
ERK2/MAPK1	MAPK1	MBP	NP_620407	P28482	full-length	-	E. coli	N-terminal GST
FAK/PTK2	PTK2	pEY	NP_722560	Q05397	full-length	-	Insect	N-terminal GST
FER	FER	pEY	NP_005237	P16591	aa540-822	-	baculovirus insect cell	N-terminal GST
FES/FPS	FES	pEY	NP_001996	P07332	full-length	-	Insect	C-terminal His
FGFR1	FGFR1	pEY + Mn	NP_000595	P11362	cytoplasmic	-	Insect	C-terminal His
FGFR2	FGFR2	pEY + Mn	NP_075261	P21802	cytoplasmic	-	Insect	C-terminal His
FGFR3	FGFR3	pEY + Mn	NP_000133	P22607	cytoplasmic	-	Insect	N-terminal His
FGFR4	FGFR4	pEY + Mn	NP_002002	P22455	aa 460-802	-	baculovirus insect cell	N-terminal His6-tag
FGR	FGR	pEY	NP_005239	P09769	full-length	-	baculovirus insect cell	C-terminal His6-tag
FLT1/VEGFR <sub>1</sub>	FLT1	pEY + Mn	NP_002010	P17948	aa 781-1338	-	baculovirus insect cell	N-terminal GST tagged
FLT3	FLT3	Abltide	NP_004110	P36888	aa 564-958	-	baculovirus insect cell	C-terminal His6-tag
FLT4/VEGFR <sub>3</sub>	FLT4	pEY + Mn	NP_891555.1, AAA85215	P35916	aa 800-1297	Q890H	Insect	N-terminal GST
FMS	CSF1R	pEY + Mn	NP_005202	P07333	cytoplasmic	-	Insect	C-terminal His
FRK/PTK5	FRK	pEY + Mn	NP_002022	P42685	full-length	-	Insect	N-terminal GST
FYN	FYN	pEY	NP_694592	P06241	full-length	-	Insect	C-terminal His
GCK/MAP4K2	MAP4K2	MBP	NP_004570.2	Q12851	full-length	-	Insect	N-terminal His6-tagged
GRK2	ADRBK1	Casein	AAH37963	P25098	full length	-	baculovirus insect cell	C-terminal His-tag
GRK3	ADRBK2	Casein	NP_005151	P35626	full-length	-	Insect	N-terminal GST
GRK4	GRK4	Casein	NP_892027	P32298	full-length	-	Insect	N-terminal GST
GRK5	GRK5	Casein	NP_005299	P34947	full-length	-	Insect	N-terminal GST
GRK6	GRK6	Casein	NP_00100410 <sub>6</sub>	P43250	full-length	-	Insect	N-terminal GST
GRK7	GRK7	Casein	NP_631948	Q8WTQ7	full-length	-	Insect	N-terminal GST
GSK3a	GSK3A	Phospho-Glycogen Synthase peptide	NP_063937.2	P49840	full length	-	baculovirus insect cell	C-terminal His-tag

RBC Enzyme Name	HUGO symbol	Substrate	Genbank Accession #	Protein Accession #	Clone	Mutation	Expression	Tag
GSK3b	GSK3B	Phospho-Glycogen Synthase peptide	NP_002084	P49841	full-length		baculovirus insect cell	C-terminal His6-tag
Haspin	GSG2	Histone H3	NP_114171.1	Q8TF76	aa471-798	-	Insect	C-terminal His
HCK	HCK	Src Substrate peptide	NP_002101	P08631	full-length	-	Insect	C-terminal His
HGK/MAP4K4	MAP4K4	MBP	NP_004825	O95819	full catalytic	-	Insect	N-terminal GST
HIPK1	HIPK1	MBP	NP_689909	Q86Z02	aa 158-555	-	baculovirus insect cell	N-terminal GST
HIPK2	HIPK2	MBP	NP_073577.3	Q9H2X6	aa 165-564	-	baculovirus insect cell	N-terminal GST
HIPK3	HIPK3	MBP	NP_005725.2	Q9H422	aa 163-562	-	baculovirus insect cell	N-terminal His6-tag
HIPK4	HIPK4	MBP	NP_653286	Q8NE63	full-length	-	baculovirus insect cell	N-terminal GST
IGF1R	IGF1R	pEY + Mn	NP_000866	P08069	aa 960-1367	-	baculovirus insect cell	C-terminal His
IKKa/CHUK	CHUK	IKKtide	NP_001269	O15111	full-length	-	Baculovirus infected insect cells	N-terminal 6X-His tag
IKKb/IKKB	IKKB	IKKtide	NP_001547	O14920	full-length	-	Insect	N-terminal GST
IKKe/IKBKE	IKBKE	Casein	NP_054721.1	Q14164	full-length	-	Insect	N-terminal GST
IR	INSR	pEY + Mn		P06213	cytoplasmic domain of the $\beta$ -subunit (aa 941-1343)	-	baculovirus expression system	GST-tag
IRAK1	IRAK1	MBP	NP_001560	P51617	aa 197-721	-	Baculovirus infected insect cells	N-terminal GST
IRAK4	IRAK4	MBP	NP_057207, AAH13316	Q9NWX3	full-length	-	baculovirus insect cell	N-terminal His6-tag
IRR/INSRR	INSRR	AXLtide	NP_055030	P14616	cytoplasmic	-	Insect	N-terminal GST

RBC Enzyme Name	HUGO symbol	Substrate	Genbank Accession #	Protein Accession #	Clone	Mutation	Expression	Tag
ITK	ITK	MBP	NP_005537	Q08881	full-length	-	Insect	N-terminal GST
JAK1	JAK1	pEY	NP_002218.2	P23458	aa 866-1154	-	Insect	N-terminal GST
JAK2	JAK2	pEY	NP_004963	O60674	aa 809-1132 <sup>+g</sup>	-	Insect	N-terminal GST
JAK3	JAK3	JAK3tide	NP_000206	P52333	aa 781-1124	-	Insect	N-terminal GST
JNK1	MAPK8	ATF2	NP_002741.1	P45983-2	full length	-	baculovirus in insect cell, activated by MAP2K7	N-terminal His-tag
JNK2	MAPK9	ATF2	NP_002743	P45984-1	full length	-	baculovirus in insect cell, activated by MAP2K7	N-terminal His-tag
JNK3	MAPK10	ATF2	NP_002744	P53779	full length	-	baculovirus in insect cell	N-terminal GST
KDR/VEGFR2	KDR	pEY + Mn	NP_002244	P35968	aa 789-1356	-	baculovirus in insect cell, activated by autophosphorylation	C-terminal His6-tagged
KHS/MAP4K5	MAP4K5	MBP	NP_942089	Q9Y4K4	full length	-	baculovirus in insect cell	N-terminal GST
LCK	LCK	pEY + Mn	NP_005347	P06239	full-length	-	baculovirus in insect cells	C-terminal His6-tagged
LIMK1	LIMK1	Cofilin 1	NP_002305	P53667	catalytic domain (aa 285-638)	-	baculovirus in insect cells, activated by co-expression with ROCK1	N-terminal His6-tag
LKB1	STK11/STRADA/CAB39	LKB1tide	NM000455/A F308302/NM_016289	STK11:Q15831; STRADA:Q7RTN6; CAB39:Q9Y376	full length	-	baculovirus in Sf21 cells	

RBC Enzyme Name	HUGO symbol	Substrate	Genbank Accession #	Protein Accession #	Clone	Mutation	Expression	Tag
LOK/STK10	STK10	Axltide	GenBank NM_005990	O94804	aa 1-348	-	baculovirus in Sf21 insect cells	N-terminal His6-tag
LRRK2	LRRK2	LRRKtide	NP_940980.2	Q5S007	aa 970-2527	-	baculovirus in insect cells	N-terminal GST
LYN	LYN	pEY	NP_002341	P07948-1	full length	-	baculovirus in insect cells	C-terminal His6-tag
LYN B	LYN	pEY + Mn	NP_002341	P07948-2	full-length	-	Insect	C-terminal His
MAPKAPK2	MAPKAPK2	Glycogen Synthase-derived peptide	NP_116584	P49137	ful length		E. coli, activated by MAPK14	N-terminal His-tag
MAPKAPK3	MAPKAPK3	Glycogen Synthase-derived peptide	NP_004626	Q16644	full length	-	Insect cell, activated by MAPK14	N-terminal His-tag
MAPKAPK5/IPRAK	MAPKAPK5	Glycogen Synthase-derived peptide	NP_003659	Q8IW41	full length	-	baculovirus in insect cells	N-terminal His6-tag
MARK1	MARK1	CHKtide	NP_061120.1	Q9P0L2	full length	-	baculovirus in insect cells	N-terminal GST-tag
MARK2/PAR-1Ba	MARK2	CHKtide	NP_059672.2	Q7KZI7-4	full length	-	baculovirus in insect cells	N-terminal GST-tag
MARK3	MARK3	CHKtide	NP_002367.3	P27448	full length	-	baculovirus in insect cells	N-terminal GST-tag
MARK4	MARK4	CHKtide	NP_113605	Q96L34	full length	-	baculovirus in insect cells	N-terminal GST-tag
MEK1	MAP2K1	ERK(K52R)	NP_002746	Q02750	full length	-	baculovirus in insect cell, activated by RAF1 in vivo	N-terminal His6-tag
MEK2	MAP2K2	ERK(K52R)	NP_109587	P36507	full length	-	baculovirus in insect cells, activated by co-expression with RAF1	C-terminal His6-tag

RBC Enzyme Name	HUGO symbol	Substrate	Genbank Accession #	Protein Accession #	Clone	Mutation	Expression	Tag
MEKK2	MAP3K2	MBP	NM_006609	Q9Y2U5	full length	-	baculovirus in Sf9 insect cells	N-terminal GST-tag
MEKK3	MAP3K3	MBP	NM_002401	Q99759	full length	-	baculovirus in Sf9 insect cells	N-terminal GST-tag
MELK	MELK	ZIPtide	NP_055606.1	Q14680	aa 1-340	-	Insect cell	N-terminal GST-tag
MINK/MINK1	MINK1	MBP	NP_056531	Q8N4C8	full catalytic	-	Insect	N-terminal GST
MKK4	MAP2K4	JNK(K55M)	NM_003010	P45985	aa 33-end		baculovirus in Sf9 insect cells	N-terminal His-tag
MKK6	MAP2K6	MBP	NP_002749	P52564	full length	S207E, T211E	E. coli	N-terminal His-tag
MLCK/MYLK	MYLK	ZIPtide + Ca-CaM	NP_444253	Q15746	Catalytic (aa 1428-1771)		Insect	N-terminal GST
MLCK2/MYLK <sub>2</sub>	MYLK <sub>2</sub>	ZIPtide + Ca-CaM	NP_149109	Q9H1R3	full length		Insect	N-terminal GST
MLK1/MAP3K <sub>9</sub>	MAP3K9	Casein	NP_149132.1	P80192	full catalytic	-	Insect	N-terminal GST
MLK2/MAP3K <sub>10</sub>	MAP3K10	MBP	NP_002437	Q02779	full catalytic	-	Insect	N-terminal GST
MLK3/MAP3K <sub>11</sub>	MAP3K11	MBP	NP_002410.1	Q16584	full catalytic	-	Insect	N-terminal GST
MNK1	MKNK1	MBP	GenBank NM_003684	Q9BUB5	aa2-end (deletion aa165-205)	T385D	baculovirus in Sf9 insect cells	N-terminal GST
MNK2	MKNK2	MBP	NP_060042.2	Q9HBH9	full length	-	Baculovirus infected insect cells	N-terminal GST
MRCKa/CDC42BPA	CDC42BPA	Long S6 Kinase substrate peptide	NP_055641	Q5VT25	aa 1-473	-	Baculovirus infected insect cells	C-terminal 6X-His tag
MRCKb/CDC42BPB	CDC42BPB	Long S6 Kinase substrate peptide	NP_006026.2	Q9Y5S2	aa 1-473	-	Baculovirus infected insect cells	C-terminal 6X-His tag

RBC Enzyme Name	HUGO symbol	Substrate	Genbank Accession #	Protein Accession #	Clone	Mutation	Expression	Tag
MSK1/RPS6K A5	RPS6KA5	Crosstide	NP_004746.2	O75582	full-length	-	Insect	N-terminal GST
MSK2/RPS6K A4	RPS6KA4	Crosstide	NP_003933	O75676	full-length	-	Insect	N-terminal GST
MSSK1/STK23	SRPK3	RS peptide	NP_055185	Q9UPE1	full-length	-	Insect	N-terminal GST
MST1/STK4	STK4	Axifide	NP_006273	Q13043	full-length	-	Insect	N-terminal GST
MST2/STK3	STK3	MBP	NP_006272.2	Q13188	full length	-	Insect	N-terminal GST
MST3/STK24	STK24	MBP	NP_003567	Q9Y6E0	full length	-	Insect	N-terminal GST
MST4	MST4	MBP	NP_057626.2	Q9P289	full-length	-	Insect	N-terminal GST
MUSK	MUSK	MBP	NP_005583.1	O15146	cytoplasmic	-	Insect	N-terminal GST
MYLK3	MYLK3	MYLK3	ZlPptide + Ca-CaM	BC109097	Q32MK0	full-length	Insect	N-terminal GST
MYO3B	MYO3B	MYO3B	MBP	NM_138995	Q8WXR4	Catalytic (1-326)	Insect	N-terminal GST
NEK1	NEK1	MBP	NP_036356	Q96PY6	aa 1-505	-	Insect	N-terminal GST
NEK11	NEK11	MBP	NP_079076	Q8NG66	full-length	-	Baculovirus infected insect cells	N-terminal GST
NEK2	NEK2	MBP	NP_002488	P51955	full-length	-	Insect	C-terminal His6-tagged
NEK3	NEK3	MBP	NP_689933	Q8WUN5	full-length	-	Insect	N-terminal GST
NEK4	NEK4	MBP	NP_003148	P51957	full-length	-	Insect	N-terminal GST
NEK6	NEK6	MBP	NP_055212	Q9HC98	aa 7-313	-	baculovirus insect cell	C-terminal His-tag
NEK7	NEK7	MBP	NP_598001.1	Q8TDX7	full length	-	Insect	N-terminal GST tag
NEK9	NEK9	MBP	NP_149107.2	Q8TD19	Catalytic (aa 347-732)	-	Insect	N-terminal GST tag
NIK/MAP3K14	MAP3K14	MBP	NP_003945.2	Q99558	Catalytic (aa 318-947)	-	Insect	N-terminal GST tag
NLK	NLK	MBP	NP_057315.1	Q9UBE8	full length	-	Insect	N-terminal GST
OSR1/OXSR1	OXSR1	CATCHtide	NP_005100.1	O95747	full length	-	Baculovirus infected insect cells	N-terminal GST

RBC Enzyme Name	HUGO symbol	Substrate	Genbank Accession #	Protein Accession #	Clone	Mutation	Expression	Tag
P38a/MAPK1 <sub>4</sub>	MAPK14	MBP	NP_620581	Q16539	full-length	-	E. coli	N-terminal GST
P38b/MAPK1 <sub>1</sub>	MAPK11	MBP	NP_002742	Q15759	full-length	-	Insect	N-terminal His
P38d/MAPK1 <sub>3</sub>	MAPK13	MBP	NP_002745	O15264	full-length	-	Insect	N-terminal His
P38g/MAPK1 <sub>2</sub>	MAPK12	MBP	NP_002960	P53778	full-length	-	Insect	N-terminal His
p70S6K/RPS6KB1	RPS6KB1	S6K/Rsk2 peptide 2	NP_003152, T412E	P23443	Catalytic (aa 1-421)	-	Insect	N-terminal GST
p70S6Kb/RPS6KB2	RPS6KB2	S6K/Rsk2 peptide 2	NP_003943	Q9UBS0	full length	-	Insect	N-terminal GST
PAK1	PAK1	Long S6 Kinase substrate peptide	NP_002567	Q13153	full length	-	Insect	N-terminal GST
PAK2	PAK2	Long S6 Kinase substrate peptide	NP_002568.2	Q13177	full length	-	Insect	N-terminal GST
PAK3	PAK3	ZIPtide	NP_002569	O75914	full length	-	Insect	N-terminal His6-tag
PAK4	PAK4	MBP	NP_005875	O96013	Catalytic (aa 295-591)	-	Insect	N-terminal GST
PAK5	PAK7	ZIPtide	NP_065074	Q9P286	aa 425-719	-	Baculovirus infected insect cells	N-terminal 6X-His tag
PAK6	PAK6	ZIPtide	NP_064553	Q9NQU5	full-length	-	Insect	C-terminal His
PASK	PASK	ZIPtide	NP_055963	Q96RG2	full catalytic	-	Insect	N-terminal GST
PBK/TOPK	PBK	MBP	NP_060962	Q96KB5	full catalytic	-	Insect	C-terminal His
PDGFRA	PDGFRA	pEY + Mn	NP_006197	Q9DE49	Cytoplasmic (550-1089)		Insect	N-terminal GST
PDGFRb	PDGFRB	pEY + Mn	NP_002600	P09619	Cytoplasmic (558-1106)		Insect	N-terminal His6-tagged

RBC Enzyme Name	HUGO symbol	Substrate	Genbank Accession #	Protein Accession #	Clone	Mutation	Expression	Tag
PDK1/PDPK1	PDPK1	PDKtide	NP_002604	O15530	full length	-	Insect	N-terminal His6-tag
PHKg1	PHKG1	ZIPtide	NP_006204	Q16816	full length	-	Insect	N-terminal GST-tag
PHKg2	PHKG2	ZIPtide	NP_000285	P15735	full length	-	Insect	N-terminal GST-tag
PIM1	PIM1	S6K/Rsk2 peptide 2	NP_002639	P11309	full length	-	Insect	C-terminal His tagged
PIM2	PIM2	Pim2tide	NP_006866	Q9P1W9	full-length	-	Insect	N-terminal GST
PIM3	PIM3	Pim2tide	GenBank AB114795	Q86V86	aa 2-end	-	Baculovirus in Sf21 insect cells	N-terminal His6-tag
PKA	PRKACA	PKA sub	NP_002721.1	P17612	Catalytic (1-351)	-	E. coli	N-terminal His6-tag
PKAca	KAPCA	Long S6 Kinase substrate peptide	NM_002730	P17612	full-length	-	baculovirus in Sf9 cells	N-terminal GST
PKAcb	KAPCB	Long S6 Kinase substrate peptide	NM_002730	P22694	full-length	-	baculovirus in Sf9 cells	N-terminal GST
PKAcg	KAPCG	Long S6 Kinase substrate peptide	NM_002732	P22612	full-length	-	Insect	N-terminal GST
PKCa	PRKCA	Histone H1 + Lipid Activator	NP_002728	P17252	full length	-	Insect	none
PKCb1	PRKCB1	Histone H1 + Lipid Activator	NP_991100.1	P05771	full length	-	baculovirus in Sf21 insect cells	none
PKCb2	PRKCB2	Histone H1 + Lipid Activator	NP_002729	P05771	full length	-	insect	none

RBC Enzyme Name	HUGO symbol	Substrate	Genbank Accession #	Protein Accession #	Clone	Mutation	Expression	Tag
PKCd	PRKCD	PKCe Pep + Lipid Activator	NP_006245	Q05655	full length	-	insect	none
PKCepsilon	PRKCE	S25 PKC Peptide	NP_005391.1	Q02156	full-length	-	Insect	none
PKCeta	PRKCH	PKCe Pep + Lipid Activator	NM_006255	P24723	full length	-	baculovirus in Sf9 insect cells	N-terminal GST
PKCg	PRKCG	Histone H1 + Lipid Activator	NP_002730	P05129	-	-	baculovirus in insect cells	none
PKCiota	PRKCI	PKCepsilon Peptide	NP_002731	P41743	full length	-	baculovirus insect cell	N-terminal His-tag
PKCmu/PRKD1	PRKD1	Glycogen Synthase-derived peptide	NP_002733	Q15139	full length	-	Insect	N-terminal GST
PKCnu/PRKD3	PRKD3	Glycogen Synthase-derived peptide	NP_005804	O94806	full-length	-	Insect	N-terminal GST
PKCtheta	PRKCQ	Histone H1 + Lipid Activator	NP_006248	Q04759	full length	P330L	baculovirus in insect cells	C-terminal His6-tag
PKCzeta	PRKCZ	PKCepsilon Peptide	NP_002735	Q05513	full-length	-	Insect	none
PKD2/PRKD2	PRKD2	Glycogen Synthase-derived peptide	NP_057541	Q9BZL6	full-length	-	Insect	N-terminal GST
PKG1a	PRKG1	Kemptide	NM_001098512	Q13976	full length	-	baculovirus in Sf9 cells	N-terminal His6-tag
PKG1b	PRKG1	Kemptide	GenBank NM_006258	P14619	full length	-	baculovirus in Sf21 insect cells	N-terminal His6-tag
PKG2/PRKG2	PRKG2	Kemptide	NP_006250	Q13237	full length	-	Insect	N-terminal GST

RBC Enzyme Name	HUGO symbol	Substrate	Genbank Accession #	Protein Accession #	Clone	Mutation	Expression	Tag
PKN1/PRK1	PKN1	Glycogen Synthase-derived peptide	NP_998725	Q16512	full length	-	Insect	N-terminal GST
PKN2/PRK2	PKN2	Glycogen Synthase-derived peptide	NP_006247	Q16513	full length	-	Insect	N-terminal GST
PLK1	PLK1	Casein	NP_005021	P53350	full length	-	Insect	C-terminal His6-tag
PLK2	PLK2	Casein	NP_006613	Q9NYY3	full length	-	Insect	N-terminal GST-His6 tag
PLK3	PLK3	Casein	NP_004064	Q9H4B4	Catalytic (58-340)	-	Insect	N-terminal GST
PRKX	PRKX	Kemptide	NP_722560	P51817	full length	-	Insect	N-terminal GST
PYK2	PTK2B	pEY + Mn	NP_004094	Q14289	full-length	-	Insect	N-terminal GST
RAF1	RAF1	MEK1 (K97R)	NP_002871	P04049	full catalytic	-	Insect	N-terminal GST
RET	RET	CHKtide	NP_066124	P07949	cytoplasmic	-	Insect	N-terminal GST
RIPK2	RIPK2	MBP	NP_003812	O43353	aa 1-299	-	Baculovirus infected insect cells	N-terminal 6X-His tag
RIPK5	DSTYK	MBP	NP_056190.1	Q6XUX3	full length	-	Insect	N-terminal GST
ROCK1	ROCK1	Long S6 Kinase substrate peptide	NP_005397	Q13464	aa 1-535	-	Insect	N-terminal GST
ROCK2	ROCK2	Long S6 Kinase substrate peptide	NM_004850	O75116	aa 5-554	-	baculovirus in Sf9 insect cells	N-terminal GST
RON/MST1R	MST1R	Axltide + Mn	NP_002438	Q04912	aa 983-1400	-	Baculovirus infected insect cells	N-terminal GST
ROS/ROS1	ROS1	IGF-1Rtide	NP_002935	P08922	cytoplasmic	-	Insect	N-terminal GST

RBC Enzyme Name	HUGO symbol	Substrate	Genbank Accession #	Protein Accession #	Clone	Mutation	Expression	Tag
RSK1	RPS6KA1	Glycogen Synthase-derived peptide	NP_002944	Q15418	full length	-	Insect	N-terminal His6-tag
RSK2	RPS6KA3	Glycogen Synthase-derived peptide	NP_004577	P51812	full length	-	baculovirus insect cell	C-terminal His-tag
RSK3	RPS6KA2	Glycogen Synthase-derived peptide	NP_066958	Q15349	full length	-	Insect	N-terminal His6-tag
RSK4	RPS6KA6	Long S6 Kinase substrate peptide	NP_055311	Q9UK32	full-length	-	Insect	N-terminal GST
SGK1	SGK1	Crosstide	NP_005618, S589D	O00141	Catalytic (60-431)	S422D	Insect	N-terminal GST
SGK2	SGK2	Crosstide		Q9HBY8	full length (Met1-Cys367)	-	baculovirus expression system	GST-tag
SGK3/SGKL	SGK3	Crosstide	NP_037389, S487D	Q96BR1	Catalytic (87-496)	-	Insect	N-terminal GST-tag
SIK2	SIK2	Kemptide	NP_056006.1	Q9H0K1	full length	-	Insect	N-terminal GST-tag
SLK/STK2	SLK	Histone H3	NP_055535.1	Q9H2G2	full length	-	Insect	N-terminal GST-tag
SNARK/NUAK2	NUAK2	MBP	NM_030952	Q9H093	aa M1 - T628	-	baculovirus in Sf9 insect cells	N-terminally fused to GST-His6
SRMS	SRMS	pEY + Mn	NP_543013	Q9H3Y6	full length	-	Insect	N-terminal GST
SRPK1	SRPK1	RS peptide	NP_003128	Q96SB4	full length	-	Insect	N-terminal His-tag
SRPK2	SRPK2	RS peptide	NP_872633	P78362	full length	-	Insect	N-terminal GST-tag
STK16	STK16	MBP	NP_003682	O75716	full length	-	Insect	N-terminal His-tag

RBC Enzyme Name	HUGO symbol	Substrate	Genbank Accession #	Protein Accession #	Clone	Mutation	Expression	Tag
STK22D/TSSK1	TSSK1B	CHKtide	NP_114417	Q9BXA7	full length	-	Insect	C-terminal His-tag
STK25/YSK1	STK25	MBP	NP_006365	O00506	full length	-	Insect	N-terminal GST
STK33	STK33	MBP	NP_112168	Q9BYT3	full length	-	Insect	N-terminal His-tag
STK38/NDR1	STK38/NDR1	STK38	Modified PKA Substrate	NM_007271	Q15208	full-length	Insect	N-terminal GST
STK39/STLK3	STK39	CATCHtide	NP_037365.2	Q9UEW8	full length	-	Insect	N-terminal GST
SYK	SYK	pEY	NP_003168	P43405	full-length	-	Insect	N-terminal GST
TAK1	MAP3K7/MA P3K7IP1	Casein	NP_663306, NP_006107	MAP3K7:O43 318; TAB1:Q15750	full-length MAP3K7; aa 437-504 MAP3K7IP1	-	Baculovirus infected insect cells	N-terminal 6X-His tag
TAOK1	TAOK1	MBP	NM_020791	Q7L7X3	aa1-314	-	baculovirus in Sf9 insect cells	N-terminal GST
TAOK2	TAOK2	MBP	NP_004774	Q9UL54	full catalytic	-	Insect	N-terminal GST
TAOK3/JIK	TAOK3	MBP	NP_057365	Q9H2K8	full-length	-	Insect	N-terminal GST
TBK1	TBK1	CK1tide	NP_037386	Q9UHD2	full-length	-	Insect	N-terminal GST
TEC	TEC	pEY + Mn	NP_003206	P42680	full length	-	baculovirus insect cell	C-terminal His-tag
TGFBR2	TGFBR2	MBP	NM_003242	P37173	190-end	-	baculovirus in Sf9 insect cells	N-terminal GST
TIE2/TEK	TEK	pEY + Mn	NP_000450	Q02763	Cytoplasmic (817-1101)	-	Insect	N-terminal GST- tag
TLK2	TLK2	TLK2	Casein	NM_006852	Q86UE8	Catalytic (388-end)	Insect	N-terminal GST
TRKA	NTRK1	pEY + Mn	NP_002520	P04629	Cytoplasmic (441-796)	-	insect	C-terminal His-tag
TRKB	NTRK2	pEY + Mn	NP_006171	Q16620	Cytoplasmic (526-838)	-	Insect	C-terminal His-tag
TRKC	NTRK3	pEY	NP_002521.2	Q16288	catalytic domain (aa 510-825)	-	baculovirus insect cell	C-terminal His-tag
TSSK2	TSSK2	CHKtide	NP_443732	Q96PF2	full length	-	Insect	N-terminal His6- tag

RBC Enzyme Name	HUGO symbol	Substrate	Genbank Accession #	Protein Accession #	Clone	Mutation	Expression	Tag
TTK	TTK	MBP	NP_003309	P33981	full-length	-	Insect	N-terminal
TXK	TXK	ABLtide	NP_003319.2	P42681	full length	-	Insect	N-terminal GST-tag
TYK1/LTK	LTK	ABLtide	NP_002335.2	P29376	Cytoplasmic (450-864)	-	Insect	N-terminal GST-tag
TYK2	TYK2	AXLtide	NP_003322.2	P29597	aa 833-1187	-	Insect	N-terminal GST
TYRO3/SKY	TYRO3	pEY + Mn	NP_006284	Q06418	Cytoplasmic (451-890)	-	Insect	N-terminal GST-tag
ULK1	ULK1	MBP	BC111603	O75385	aa 1-649	-	baculovirus in Sf9 insect cells	N-terminal GST-tag
ULK2	ULK2	MBP	NM_014683	Q81YT8	aa 1-631	-	baculovirus in Sf9 insect cells	N-terminal GST-tag
ULK3	ULK3	ULK3	Casein	BC157884	Q6PHR2	full-length	Insect	N-terminal His6-tag
VRK1	VRK1	Casein	NM_003384	Q99986	full length, Met1-Lys396	-	Sf9 cells	GST-HIS fusion
WEE1	WEE1	MBP	NP_003381.1	P30291	full-length	-	Insect	N-terminal
WNK2	WNK2	MBP	NP_006639.3	Q9Y3S1	Catalytic (166-489)	-	Insect	N-terminal GST
WNK3	WNK3	MBP	NP_065973	Q9BYP7	Catalytic (1-434)	-	Insect	N-terminal His6-tag
YES/YES1	YES1	pEY	NP_005424	P07947	full length	-	Insect	C-terminal His-tag
ZAK/MLTK	ZAK	MBP	NP_598407.1	Q9NYL2	full length	-	Insect	N-terminal GST
ZAP70	ZAP70	pEY	NP_001070	P43403	full length	-	Insect	C-terminal His6-tag
ZIPK/DAPK3	DAPK3	ZIPtide	NP_001339	O43293	full-length	-	Insect	N-terminal GST

**Supplementary Table 4.** A ranked table of kinases sorted by Selectivity score, the fraction of all tested inhibitors that inhibited the catalytic activity of the test kinase by >50%.

Kinase	Selectivity Score
COT1/MAP3K8	0.000
CTK MATK	0.000
DYRK4	0.000
GRK2	0.000
GRK3	0.000
HIPK1	0.000
JNK3	0.000
MAPKAPK3	0.000
NEK6	0.000
NEK7	0.000
P38d/MAPK13	0.000
P38g	0.000
VRK1	0.000
WNK3	0.000
ALK2/ACVR1	0.006
CAMK1b	0.006
CAMK4	0.006
DMPK	0.006
GRK5	0.006
NEK2	0.006
NEK3	0.006
OSR1/OXSR1	0.006
PLK2	0.006
RON/MST1R	0.006
SGK3/SGKL	0.006
STK39/STLK3	0.006
WNK2	0.006
MRCKa/CDC42BPA	0.006
AKT2	0.011
ALK4/ACVR1B	0.011
CDK7/cyclin H	0.011
DCAMKL2	0.011
ERK1	0.011
ERK2 MAPK1	0.011
HIPK4	0.011
IKKa/CHUK	0.011
JNK1	0.011
MAPKAPK2	0.011
MRCKb/CDC42BPB	0.011
NEK11	0.011
PKCzeta	0.011
SRPK1	0.011
TSSK2	0.011
WEE1	0.011
ZAP70	0.011
AKT1	0.011
ALK5/TGFBR1	0.011
CAMK1a	0.011
MAPKAPK5/PRAK	0.011
NIK/MAP3K14	0.011
ALK1/ACVRL1	0.017
BRAF	0.017
c-MET	0.017
FGFR4	0.017

Kinase	Selectivity Score
GRK4	0.017
HIPK2	0.017
HIPK3	0.017
IKKb/IKBKB	0.017
PKCiota	0.017
PAK6	0.017
CK1g1	0.022
MEK1	0.022
MKK6	0.022
MSSK1/STK23	0.022
p70S6Kb/RPS6KB2	0.022
PAK4	0.022
SRMS	0.022
TEC	0.022
AKT3	0.023
CAMK1g	0.023
DAPK2	0.023
PBK/TOPK	0.023
TIE2/TEK	0.023
SRPK2	0.023
EPHB3	0.023
ASK1/MAP3K5	0.028
EPHA8	0.028
NEK9	0.028
PAK2	0.028
PAK3	0.028
RIPK5	0.028
TGFBR2	0.028
TTK	0.028
ZIPK/DAPK3	0.028
CK1g2	0.028
DYRK3	0.028
CAMK1d	0.028
PKAcg	0.031
EPHA3	0.034
EPHA5	0.034
EPHA7	0.034
GRK6	0.034
GRK7	0.034
MEK2	0.034
P38b/MAPK11	0.034
PAK5	0.034
PIM2	0.034
PKCg	0.034
PKG1b	0.034
PKN2/PRK2	0.034
PLK1	0.034
STK25/YSK1	0.034
PKA	0.034
SGK2	0.034
CK1g3	0.039
EPHA1	0.039
IGF1R	0.039
NEK4	0.039

Kinase	Selectivity Score	Kinase	Selectivity Score
PAK1	0.039	MEKK2	0.067
PASK	0.039	PKCb2	0.067
PLK3	0.039	PKG2/PRKG2	0.067
PRKX	0.039	CAMKK1	0.068
ARAF	0.040	CDK1/cyclin A	0.068
PDK1/PDPK1	0.040	MST4	0.068
CK1a1	0.040	PKCepsilon	0.068
STK38/NDR1	0.040	PKCa	0.068
CAMK2b	0.045	IRAK1	0.073
DAPK1	0.045	MEKK3	0.073
DDR2	0.045	PYK2	0.073
EPHA4	0.045	SYK	0.073
EPHB2	0.045	ALK	0.073
PHKq2	0.045	DYRK1/DYRK1A	0.073
RAF1	0.045	ERBB4/HER4	0.073
TLK2	0.050	MARK3	0.073
FAK/PTK2	0.051	NLK	0.073
IR	0.051	CLK1	0.074
PKCtheta	0.051	AXL	0.079
SGK1	0.051	CAMK2a	0.079
SNARK/NUAK2	0.051	CAMK2d	0.079
NEK1	0.051	CDK3/cyclin E	0.079
PKG1a	0.051	c-MER	0.079
TAOK2/TAO1	0.051	ERBB2/HER2	0.079
ZAK/MLTK	0.051	FGFR3	0.079
CK2a	0.051	Haspin	0.079
EPHB4	0.052	MLK2/MAP3K10	0.079
CAMK2g	0.056	MUSK	0.079
CSK	0.056	PKCeta	0.079
ITK	0.056	ROCK2	0.079
ROCK1	0.056	STK16	0.079
TYRO3 SKY	0.056	ULK1	0.079
ULK2	0.056	MSK2/RPS6KA4	0.079
EPHB1	0.056	MYO3b	0.080
FES/FPS	0.056	ULK3	0.080
IRR/INSRR	0.056	CAMKK2	0.084
TAOK1	0.056	CDK9/cyclin T1	0.084
TAOK3/JIK	0.056	DYRK1B	0.084
CDK4/cyclin D1	0.062	JAK2	0.084
CLK3	0.062	LKB1	0.084
DYRK2	0.062	MARK1	0.084
EPHA2	0.062	PKCmu/PRKD1	0.084
FRK/PTK5	0.062	TYK1/LTK	0.084
JAK1	0.062	STK22D/TSSK1	0.085
MNK1	0.062	FER	0.090
MSK1/RPS6KA5	0.062	FGFR1	0.090
PKCb1	0.062	FLT1/VEGFR1	0.090
JNK2	0.062	LIMK1	0.090
P38a/MAPK14	0.062	MARK2/PAR-1Ba	0.090
CK2a2	0.067	MST3/STK24	0.090
CDK4/cyclin D3	0.067	STK33	0.090
FGFR2	0.067	PKD2/PRKD2	0.090
IKKe/IKBKE	0.067	TAK1	0.090
IRAK4	0.067	TBK1	0.090

Kinase	Selectivity Score
BMX/ETK	0.096
MLCK/MYLK	0.096
PKCd	0.096
ROS/ROS1	0.096
SIK2	0.096
CHK1	0.096
p70S6K/RPS6KB1	0.096
CDK6/cyclin D1	0.101
LYN B	0.101
MNK2	0.101
DRAK1/STK17A	0.107
PIM1	0.107
SLK/STK2	0.107
TXK	0.107
BRSK2	0.112
EGFR	0.112
MARK4	0.114
ABL1	0.118
Aurora C	0.118
CDK9 cyclin K	0.118
CK1d	0.118
CK1epsilon	0.118
JAK3	0.118
KDR/VEGFR2	0.118
PIM3	0.118
PKCnu/PRKD3	0.118
PKN1/PRK1	0.119
BLK	0.124
BRK	0.124
CDK1/cyclin B	0.124
PDGFRa	0.124
TRKA	0.124
HCK	0.124
BTK	0.129
RIPK2	0.129
BRSK1	0.130
CDK6/cyclin D3	0.130
CLK2	0.135
MELK	0.135
MLCK2/MYLK2	0.135
ABL2/ARG	0.140
Aurora A	0.140
CDK2/cyclin A	0.140
CDK2/cyclin E	0.140
CDK5/p25	0.140
c-SRC	0.140
MINK/MINK1	0.140
PHKg1	0.140
CDK5/p35	0.146
GCK MAP4K2	0.146
LRRK2	0.146
RSK2	0.146
RSK1	0.147
FYN	0.152

Kinase	Selectivity Score
MST2/STK3	0.153
CHK2	0.157
GSK3b	0.157
TYK2	0.157
CLK4	0.163
FLT4/VEGFR3	0.163
PDGFRb	0.164
GSK3a	0.169
LCK	0.169
LYN	0.174
MST1/STK4	0.174
RSK4	0.174
Aurora B	0.180
EPHA6	0.180
ACK1	0.191
FGR	0.191
RSK3	0.191
TRKB	0.191
LOK/STK10	0.198
FMS	0.202
MLK1/MAP3K9	0.202
MLK3/MAP3K11	0.202
c-Kit	0.208
YES/YES1	0.242
ARK5/NUAK1	0.249
RET	0.253
KHS MAP4K5	0.254
HGK MAP4K4	0.264
TRKC	0.271
FLT3	0.410

**Supplementary Table 5.** A ranked table of compounds sorted by Gini score.

CAS #	Inhibitor name	Gini score	CAS #	Inhibitor name	Gini score
62996-74-1	Staurosporine, Streptomyces sp.	0.20	404828-08-6	GSK-3 Inhibitor XIII	0.57
97161-97-2	K-252a, Nocardiosis sp.	0.29	15966-93-5	VEGF Receptor 2 Kinase Inhibitor I	0.57
135897-06-2	SB 218078	0.36	371935-74-9	PI-103	0.57
443798-55-8	Cdk1/2 Inhibitor III	0.37	546102-60-7	Cdk4 Inhibitor	0.57
608512-97-6	PKR Inhibitor	0.44	40254-90-8	Cdk1/5 Inhibitor	0.57
854171-35-0	Indirubin Derivative E804	0.48	496864-16-5	Aloisine A, RP107	0.57
136194-77-9	Gö 6976	0.49	740841-15-0	GSK-3 Inhibitor X	0.57
856436-16-3	JAK3 Inhibitor VI	0.49	507475-17-4	IKK-2 Inhibitor IV	0.58
326914-10-7	SU11652	0.50	227449-73-2	Syk Inhibitor II	0.58
557795-19-4	Sunitinib	0.52	265312-55-8	Cdk4 Inhibitor III	0.58
120685-11-2	Staurosporine, N-benzoyl-	0.52	129-56-6	JNK Inhibitor II	0.58
244148-46-7	Isogranulatimide	0.52	667463-62-9	GSK-3 Inhibitor IX	0.58
146535-11-7	AG 1296	0.53	19545-26-7	Wortmannin	0.59
331253-86-2	PDK1/Akt/Flt Dual Pathway Inhibitor	0.54	249762-74-1	PDGF Receptor Tyrosine Kinase Inhibitor II	0.59
457081-03-7	JAK Inhibitor I	0.54	167869-21-8	PD 98059	0.59
622387-85-3	Syk Inhibitor	0.54	288144-20-7	VEGF Receptor 2 Kinase Inhibitor II	0.59
5334-30-5	PP3	0.55	114719-57-2	Fascaplysin, Synthetic	0.59
444723-13-1	Cdk2 Inhibitor IV, NU6140	0.56	443797-96-4	Aurora Kinase/Cdk Inhibitor	0.59
216661-57-3	VEGF Receptor 2 Kinase Inhibitor IV	0.56	133053-19-7	Gö 6983	0.59
160807-49-8	Indirubin-3'-monoxime	0.56	175178-82-2	AG 1478	0.60
866405-64-3	AMPK Inhibitor, Compound C	0.56	934358-00-6	Casein Kinase II Inhibitor III, TBCA	0.60

CAS #	Inhibitor name	Gini score	CAS #	Inhibitor name	Gini score
269390-69-4	VEGF Receptor Tyrosine Kinase Inhibitor II	0.60	219138-24-6	p38 MAP Kinase Inhibitor	0.62
171179-06-9	PD 158780	0.60	601514-19-6	GSK3b Inhibitor XII, TWS119	0.62
133052-90-1	Bisindolylmaleimide I	0.60	145915-60-2	PKCbII/EGFR Inhibitor	0.62
71897-07-9	AG 1295	0.60	522629-08-9	MNK1 Inhibitor	0.63
852547-30-9	PKR Inhibitor, Negative Control	0.60	648449-76-7	PI 3-Kg Inhibitor II	0.63
216163-53-0	PD 174265	0.60	516480-79-8	Chk2 Inhibitor II	0.63
204005-46-9	VEGF Receptor 2 Kinase Inhibitor III	0.60	626604-39-5	GSK-3b Inhibitor XI	0.63
212779-48-1	Compound 52	0.60	658084-23-2	Met Kinase Inhibitor	0.63
380843-75-4	Bosutinib	0.61	286370-15-8	VEGF Receptor Tyrosine Kinase Inhibitor III, KRN633	0.63
496864-15-4	Aloisine, RP106	0.61	211555-04-3	JAK3 Inhibitor II	0.63
141992-47-4	Cdk4 Inhibitor II, NSC 625987	0.61	103745-39-7	HA 1077, Dihydrochloride Fasudil	0.63
405169-16-6	Dovitinib	0.61	190654-01-4	Cdk1 Inhibitor, CGP74514A	0.63
3895-92-9	Chelerythrine Chloride	0.61	54642-23-8	JNK Inhibitor, Negative Control	0.63
220749-41-7	Cdk1 Inhibitor	0.61	581098-48-8	p38 MAP Kinase Inhibitor III	0.63
852527-97-0	Alsterpaullone, 2-Cyanoethyl	0.61	666837-93-0	SU9516	0.64
146986-50-7	ROCK Inhibitor, Y-27632	0.61	345616-52-6	ERK Inhibitor III	0.64
144978-82-5	AG 112	0.61	778270-11-4	Bcr-abl Inhibitor	0.64
871307-18-5	Tpl2 Kinase Inhibitor	0.61	70563-58-5	Herbimycin A, Streptomyces sp.	0.64
205254-94-0	PDGF Receptor Tyrosine Kinase Inhibitor III	0.62	34823-86-4	GTP-14564	0.64
896138-40-2	FIt-3 Inhibitor II	0.62	189232-42-6	Bohemine	0.64
220792-57-4	Aminopurvalanol A	0.62	648450-29-7	PI 3-Kg Inhibitor	0.64

CAS #	Inhibitor name	Gini score	CAS #	Inhibitor name	Gini score
2826-26-8	AG 9	0.64	154447-36-6	LY 294002	0.68
58753-54-1	JAK3 Inhibitor IV	0.65	171745-13-4	Compound 56	0.68
237430-03-4	Alsterpaullone	0.65	681281-88-9	Akt Inhibitor IV	0.68
199986-75-9	Cdk2 Inhibitor III	0.65	301836-43-1	Casein Kinase I Inhibitor, D4476	0.68
330161-87-0	SU6656	0.65	639089-54-6	Tozasertib	0.68
852045-46-6	Flt-3 Inhibitor III	0.65	139298-40-1	KN-93	0.69
127243-85-0	H-89, Dihydrochloride	0.65	396129-53-6	TGF- $\beta$ RI Kinase Inhibitor	0.69
119139-23-0	Bisindolylmaleimide IV	0.65	327036-89-5	GSK-3 $\beta$ Inhibitor I	0.69
627518-40-5	PDGF Receptor Tyrosine Kinase Inhibitor IV	0.66	212844-53-6	Purvalanol A	0.69
152121-53-4	PD 169316	0.66	257879-35-9	PKC $\beta$ Inhibitor	0.69
1485-00-3	Syk Inhibitor III	0.66	300801-52-9	Cdc2-Like Kinase Inhibitor, TG003	0.69
186611-52-9	IC261	0.66	154447-38-8	LY 303511- Negative control	0.69
133550-30-8	AG 490	0.66	184475-35-2	Gefitinib	0.69
879127-16-9	Aurora Kinase Inhibitor III	0.66	19542-67-7	BAY 11-7082	0.69
221244-14-0	PP1 Analog II, 1NM-PP1	0.67	366017-09-6	Mubritinib	0.70
196868-63-0	IGF-1R Inhibitor II	0.67	509093-47-4	IRAK-1/4 Inhibitor	0.70
356559-13-2	TGF- $\beta$ RI Inhibitor III	0.67	186692-46-6	Roscovitine	0.70
174709-30-9	BPIQ-I	0.67	865362-74-9	ERK Inhibitor II, FR180204	0.70
347155-76-4	PDGF RTK Inhibitor	0.67	127191-97-3	KN-62	0.70
301305-73-7	Flt-3 Inhibitor	0.67	183319-69-9	Erlotinib	0.70
345987-15-7	JNK Inhibitor V	0.67	142273-20-9	Kenpaullone	0.70

CAS #	Inhibitor name	Gini score	CAS #	Inhibitor name	Gini score
487021-52-3	GSK-3b Inhibitor VIII	0.70	913844-45-8	Rho Kinase Inhibitor IV	0.74
444731-52-6	Pazopanib	0.71	152121-47-6	SB 203580	0.74
7272-84-6	Rho Kinase Inhibitor III, Rockout	0.71	305350-87-2	MEK1/2 Inhibitor	0.74
318480-82-9	SC-68376	0.71	623163-52-0	MEK Inhibitor II	0.74
41179-33-3	MK2a Inhibitor	0.71	587871-26-9	ATM Kinase Inhibitor	0.74
65678-07-1	AG 1024	0.71	120166-69-0	Diacylglycerol Kinase Inhibitor II	0.74
478482-75-6	GSK-3b Inhibitor II	0.71	302962-49-8	Dasatinib	0.74
52029-86-4	STO-609	0.72	226717-28-8	AGL 2043	0.75
53123-88-9	Rapamycin	0.72	172747-50-1	SB 202474, Negative control for p38 MAPK	0.75
5812-07-7	DMBI	0.72	905973-89-9	ATM/ATR Kinase Inhibitor	0.75
784211-09-2	Cdk/Crk Inhibitor	0.72	443913-73-3	Vandetanib	0.75
404009-46-7	DNA-PK Inhibitor V	0.72	870483-87-7	cFMS Receptor Tyrosine Kinase Inhibitor	0.75
745833-23-2	VX-702	0.73	35943-35-2	Akt Inhibitor V, Triciribine	0.75
894804-07-0	JNK Inhibitor VIII	0.73	312917-14-9	JNK Inhibitor IX	0.75
545380-34-5	NF-kB Activation Inhibitor	0.73	213743-31-8	Lck Inhibitor	0.75
212141-51-0	Vatalanib	0.73	72873-74-6	SKF-86002	0.75
312636-16-1	Sphingosine Kinase Inhibitor	0.73	612847-09-3	Akt Inhibitor VIII, Isozyme-Selective, Akti-1/2	0.75
404009-40-1	DNA-PK Inhibitor III	0.73	151342-35-7	Ro-32-0432	0.76
477600-75-2	Tofacitinib	0.73	152121-30-7	SB 202190	0.76
154447-35-5	DNA-PK Inhibitor II	0.73	220127-57-1	Imatinib	0.77
297744-42-4	MEK Inhibitor I	0.74	925681-41-0	Akt Inhibitor X	0.77

CAS #	Inhibitor name	Gini score
165806-53-1	SB220025	0.77
231277-92-2	Lapatinib	0.77
641571-10-0	Nilotinib	0.78
879127-07-8	EGFR Inhibitor	0.78
179248-59-0	Src Kinase Inhibitor I	0.78
387867-13-2	Tandutinib	0.78
284461-73-0	Sorafenib	0.79
179248-61-4	EGFR/ErbB-2 Inhibitor	0.79
881001-19-0	EGFR/ErbB-2/ErbB-4 Inhibitor	0.79
790299-79-5	Masitinib	0.81